

DRAFT

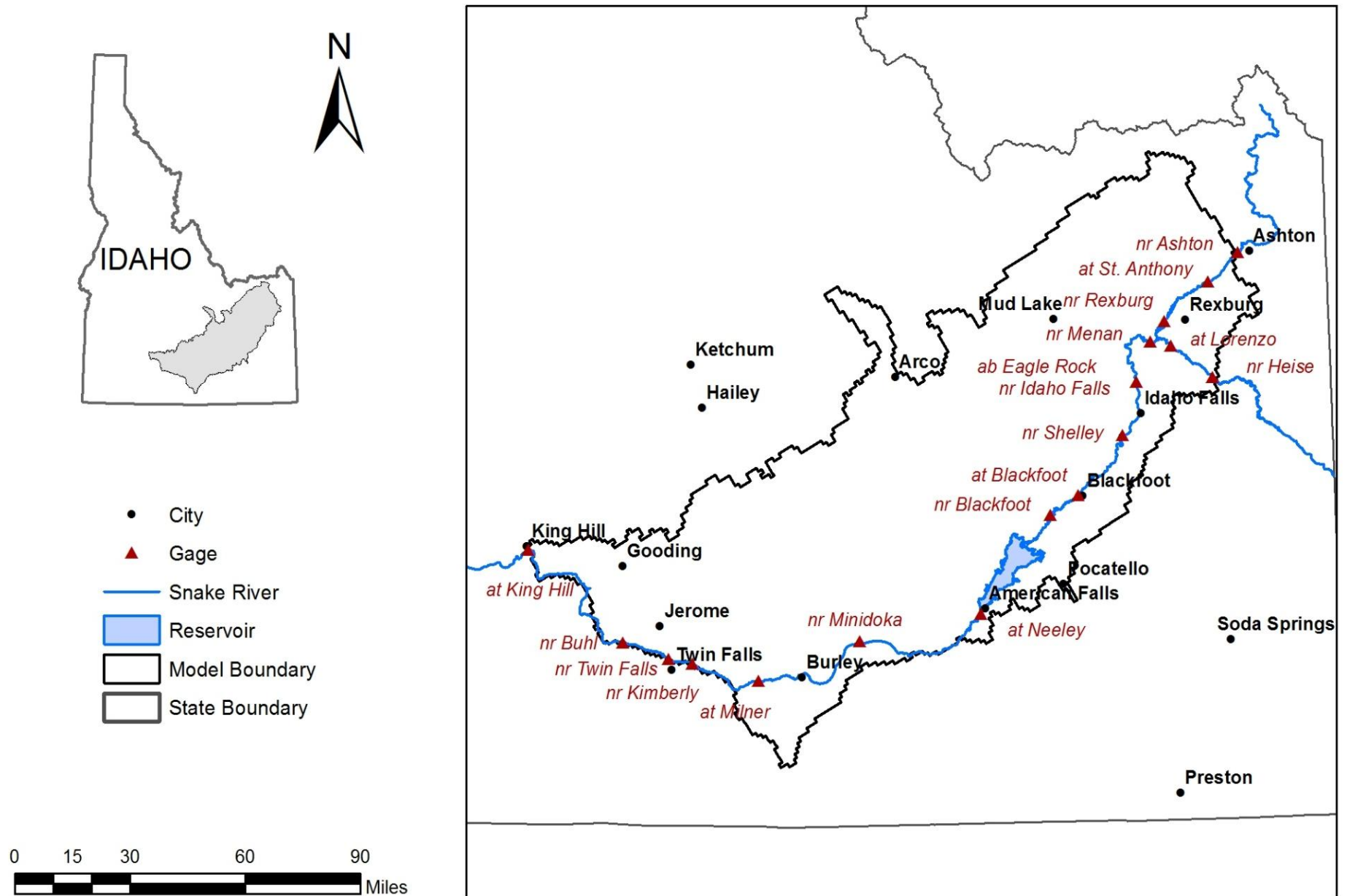


Figure 1. Study area and the Enhanced Snake Plain Aquifer Model version 2.1 (ESPAM2.1) boundary.

DRAFT

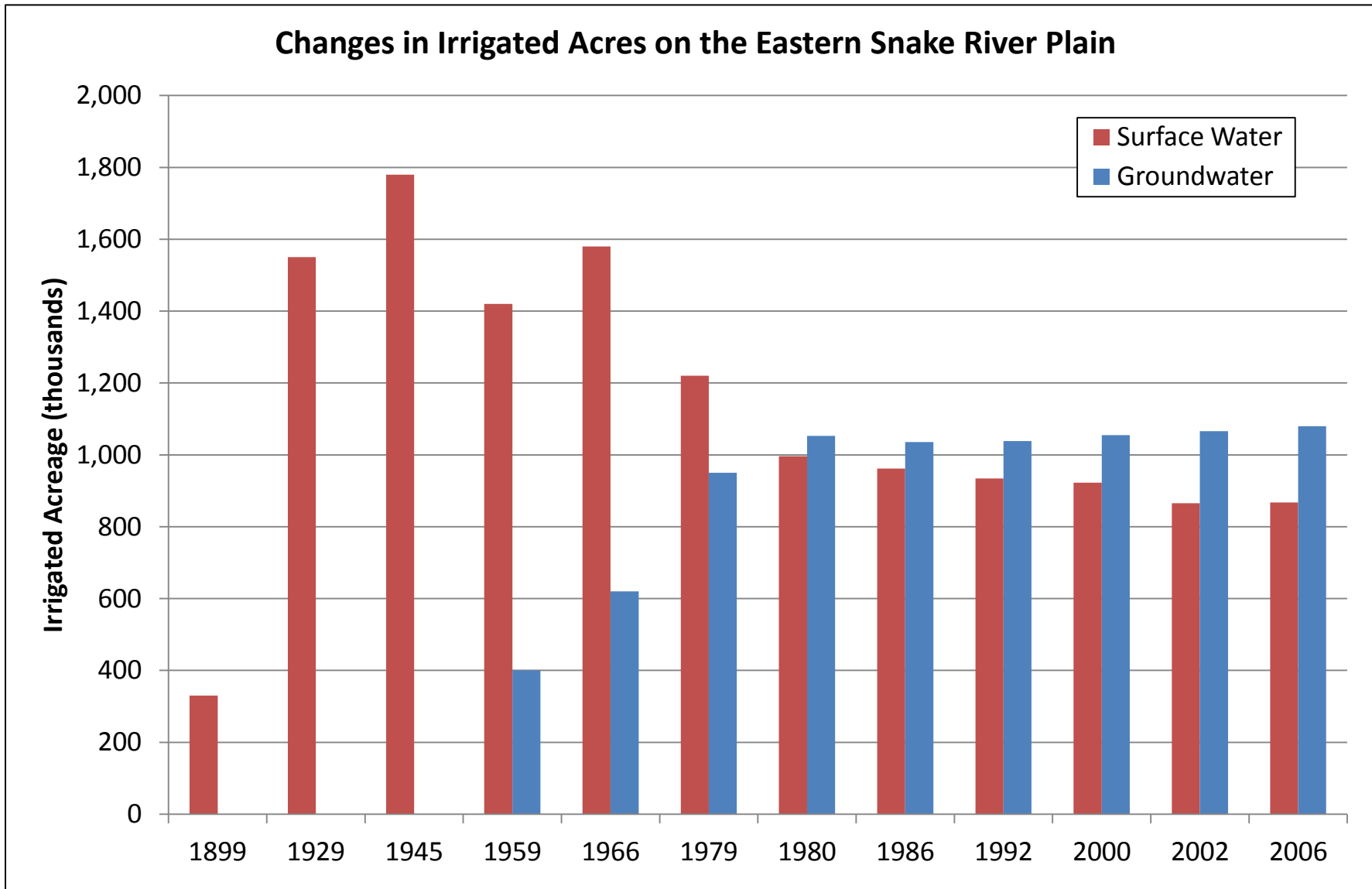


Figure 2. Surface-water and groundwater irrigated acres on the eastern Snake Plain (after Garabedian, 1992 and IDWR GIS shapefiles). The years 1899 through 1979 are represented in Garabedian (1992). The years 1980 – 2006 were acquired from IDWR GIS shapefiles.

DRAFT



Figure 3. Conceptual illustration of variation in average annual flow of the Snake River (after the US Bureau of Reclamation, 1996). Average annual flow values updated using 1980-2008 gage data.

DRAFT

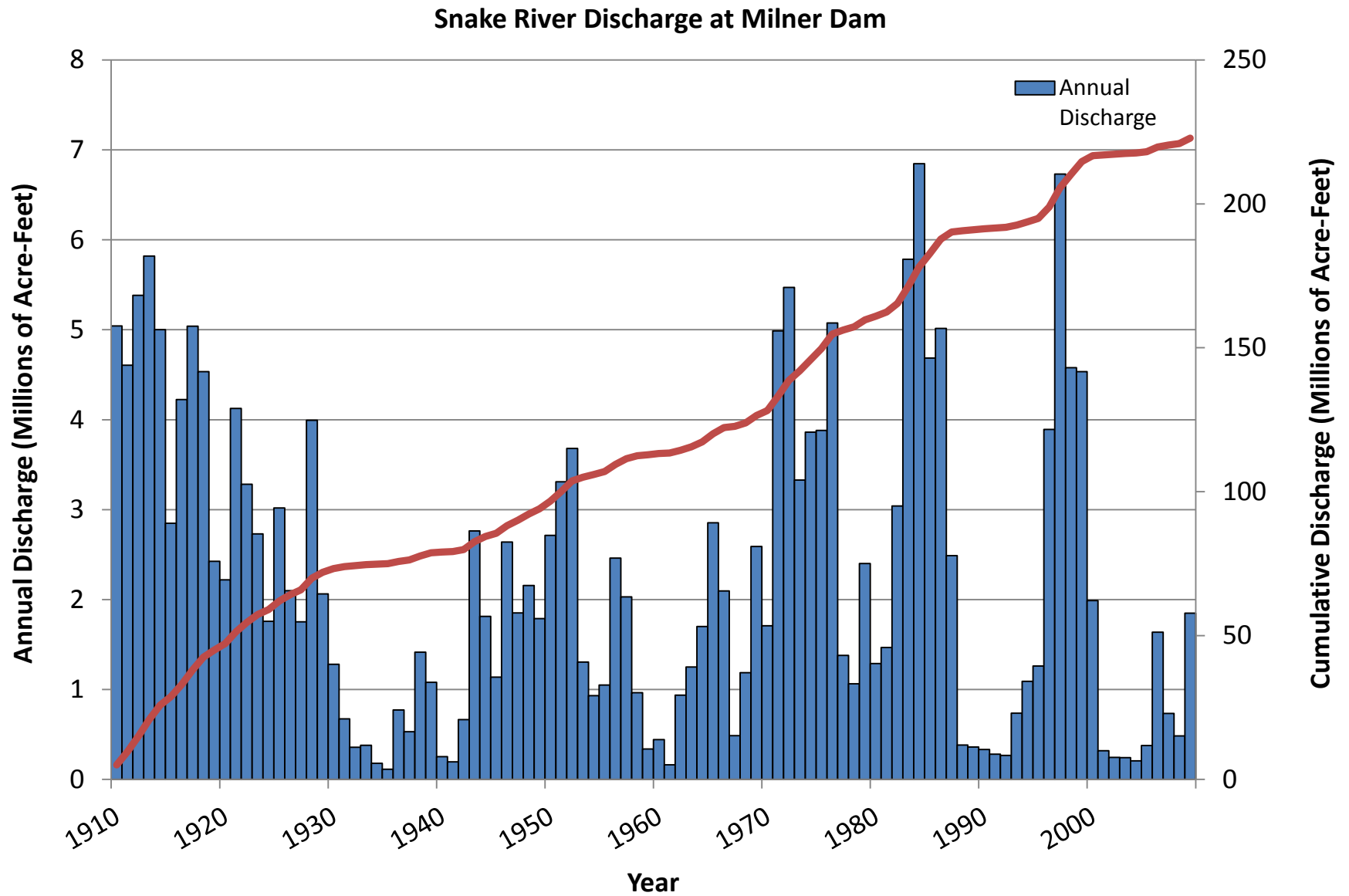


Figure 4. Annual and cumulative discharge of the Snake River at Milner Dam (US Geological Survey data).

DRAFT

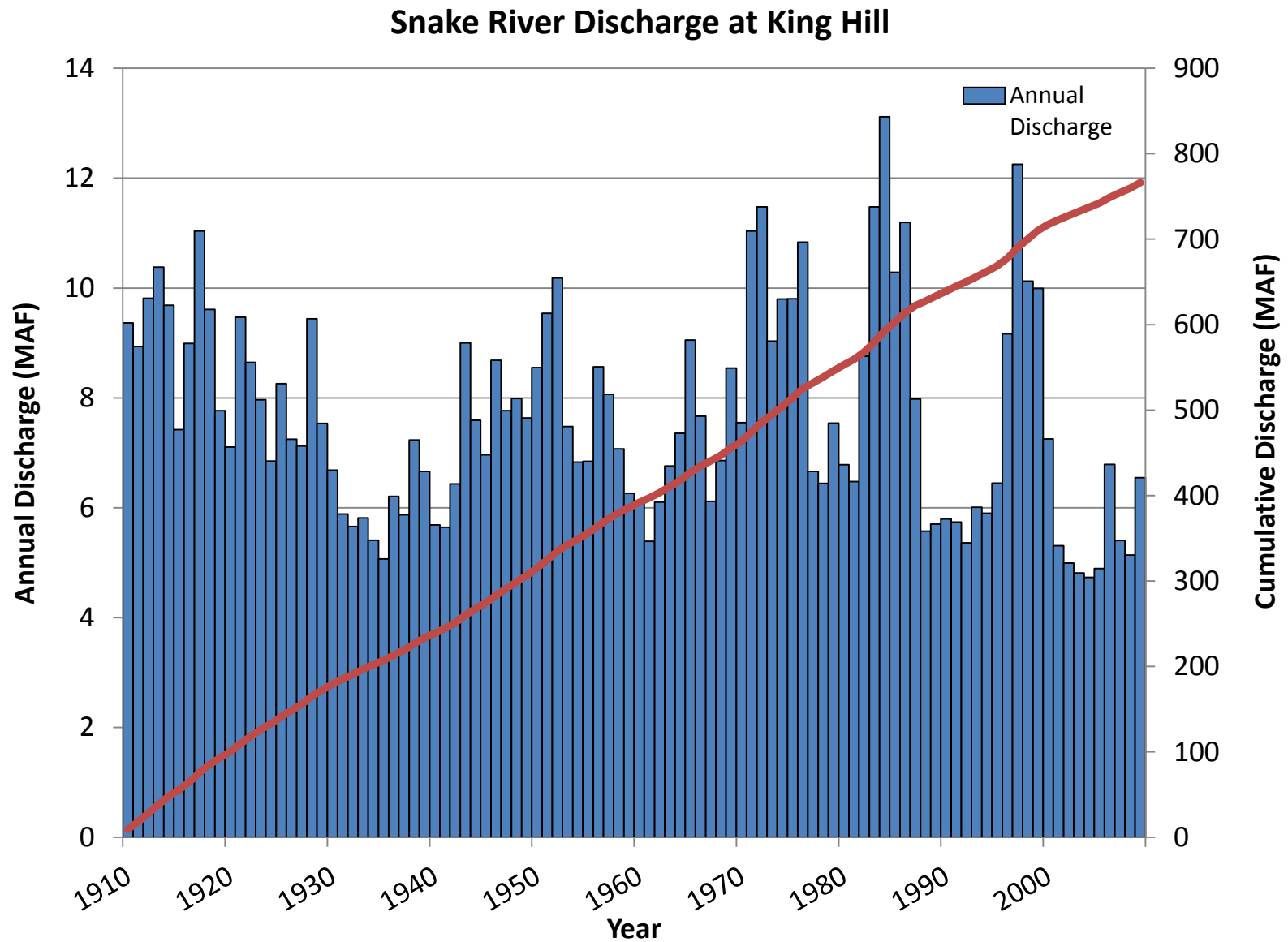


Figure 5. Annual and cumulative discharge of the Snake River at King Hill (US Geological Survey data).

DRAFT

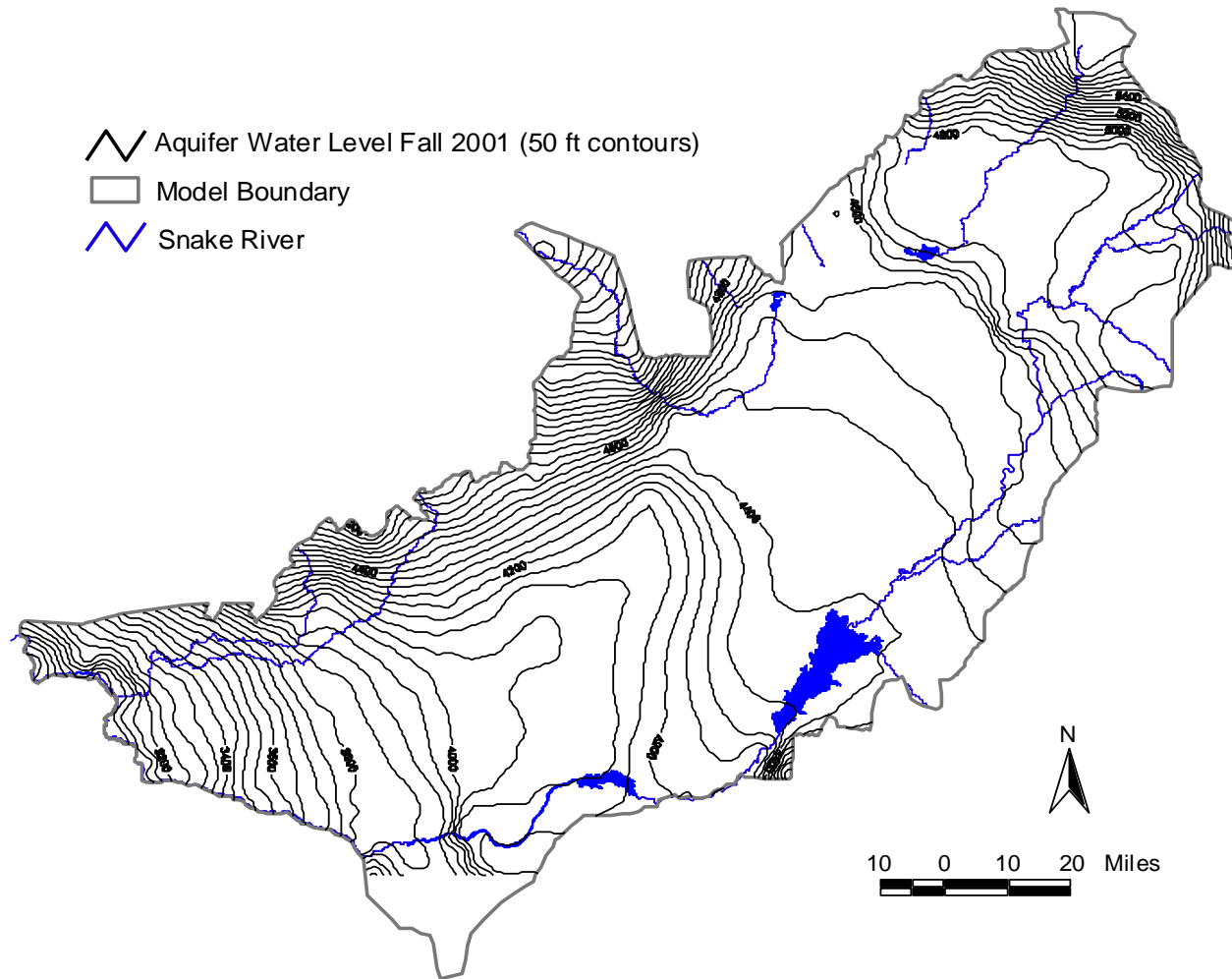


Figure 6. Contours of the Fall 2001 potentiometric surface of the eastern Snake River Plain aquifer.

DRAFT

Water Budget Conceptual Model

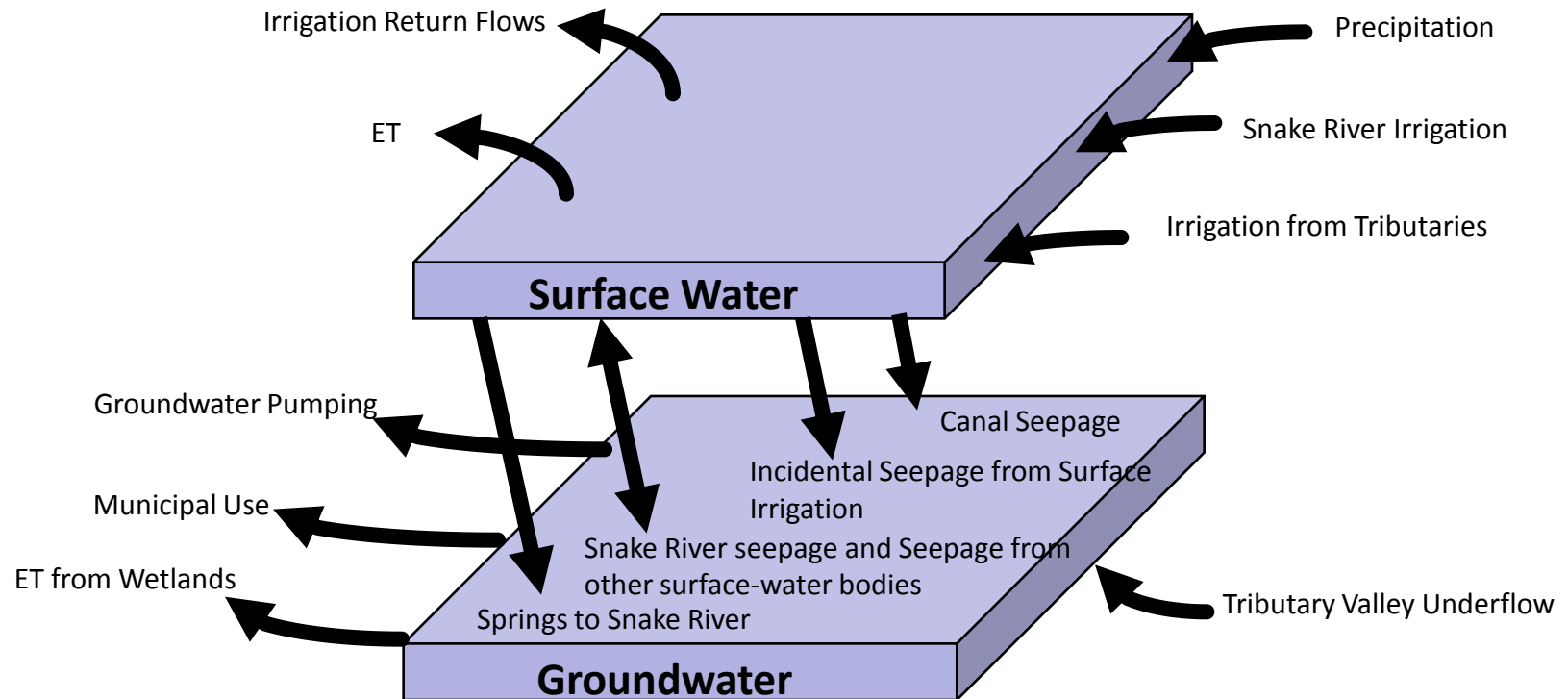


Figure 7. Conceptual water budget for the eastern Snake Plain aquifer. Adapted from ESPAM1.1 report.

DRAFT

Modeled Annual Average Aquifer Water Budget for Water Years 1981-2008

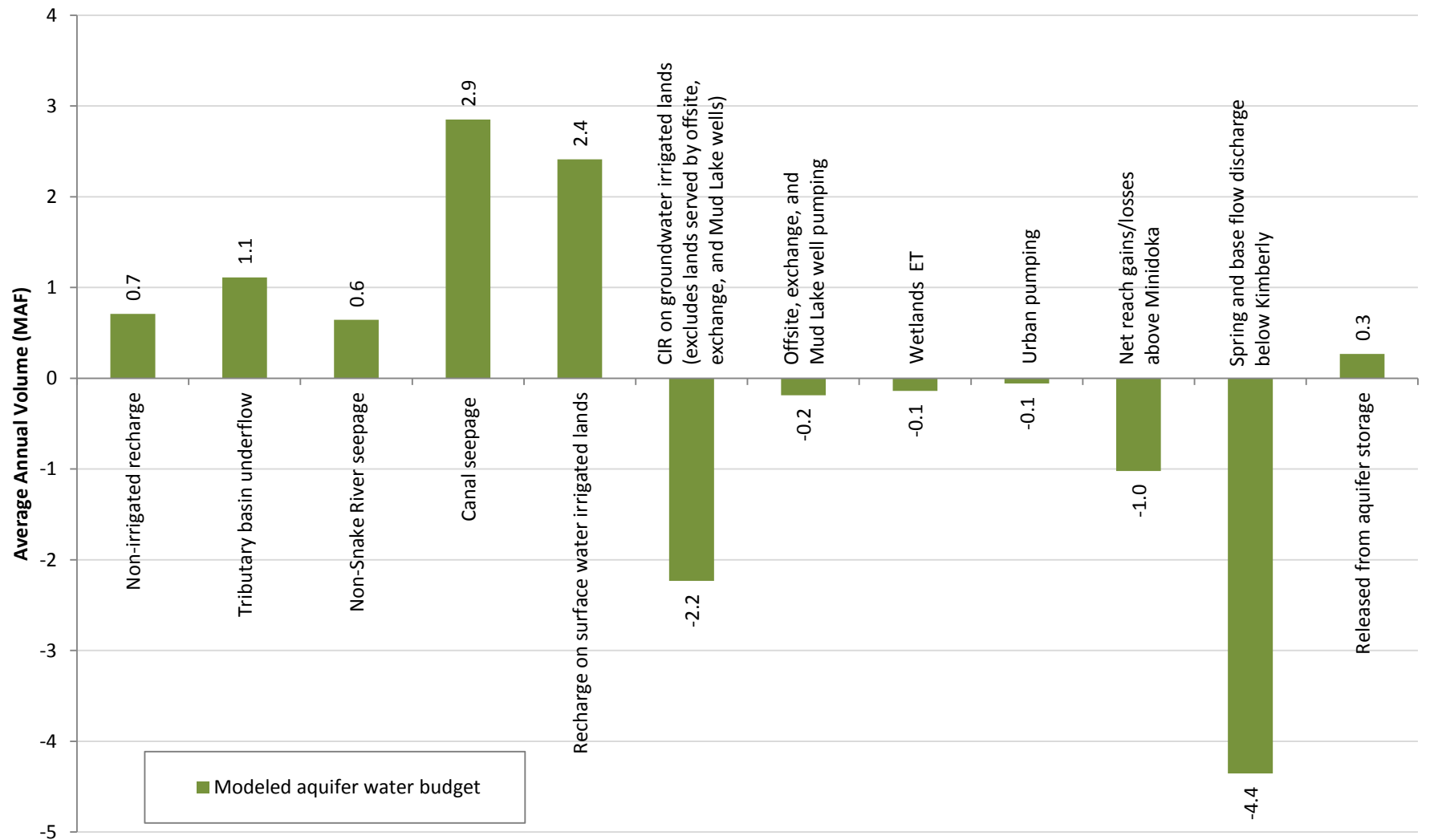


Figure 8. Enhanced Snake Plain Aquifer Model 2.1 average annual aquifer water budget. Positive values of aquifer storage represent water released from storage into the aquifer flow system. Negative values of aquifer storage represent water placed into storage.

DRAFT

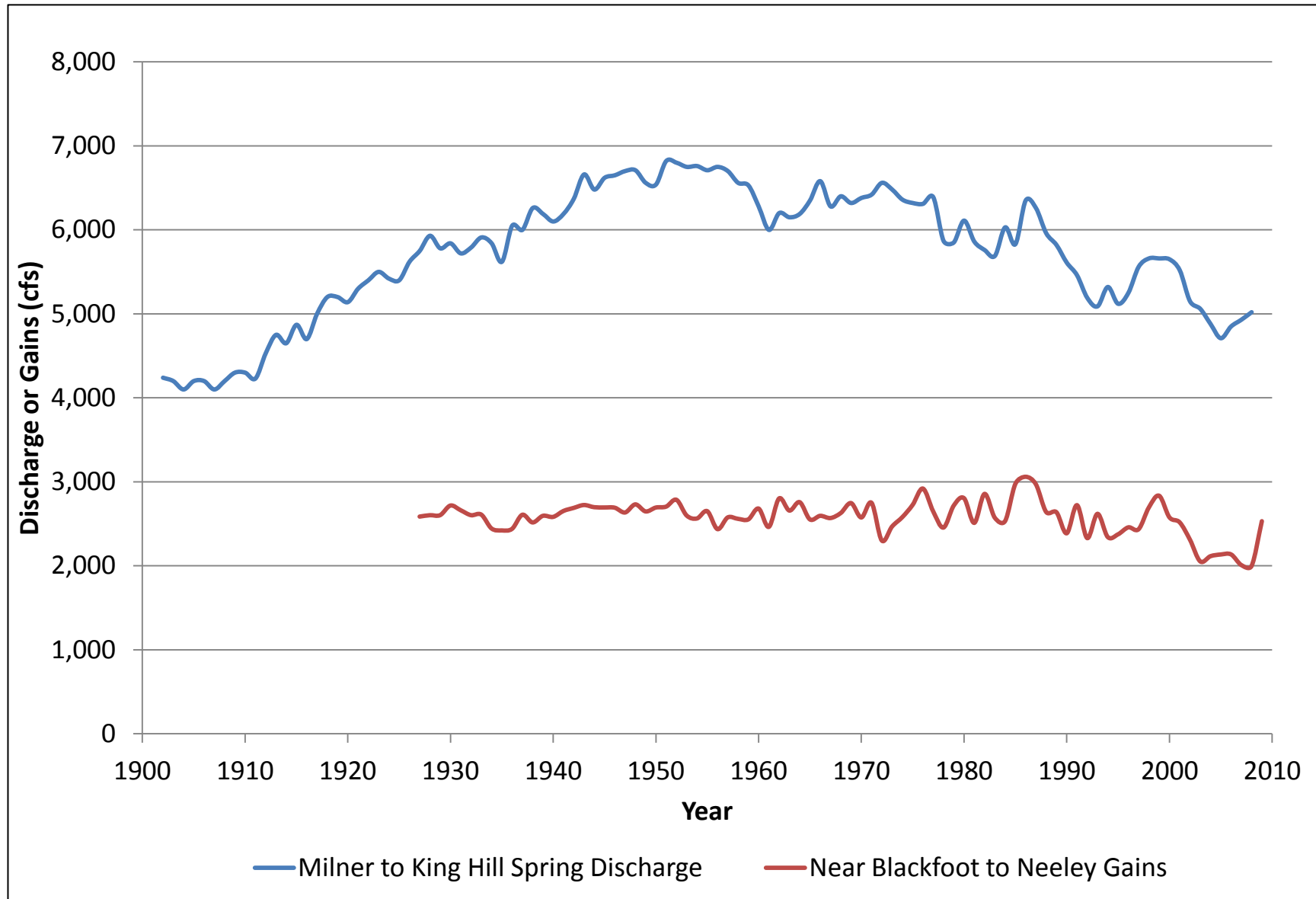


Figure 9. Average annual spring discharge for Milner-to-King Hill and near Blackfoot-to-Neeley river gains (from IDWR data).

DRAFT

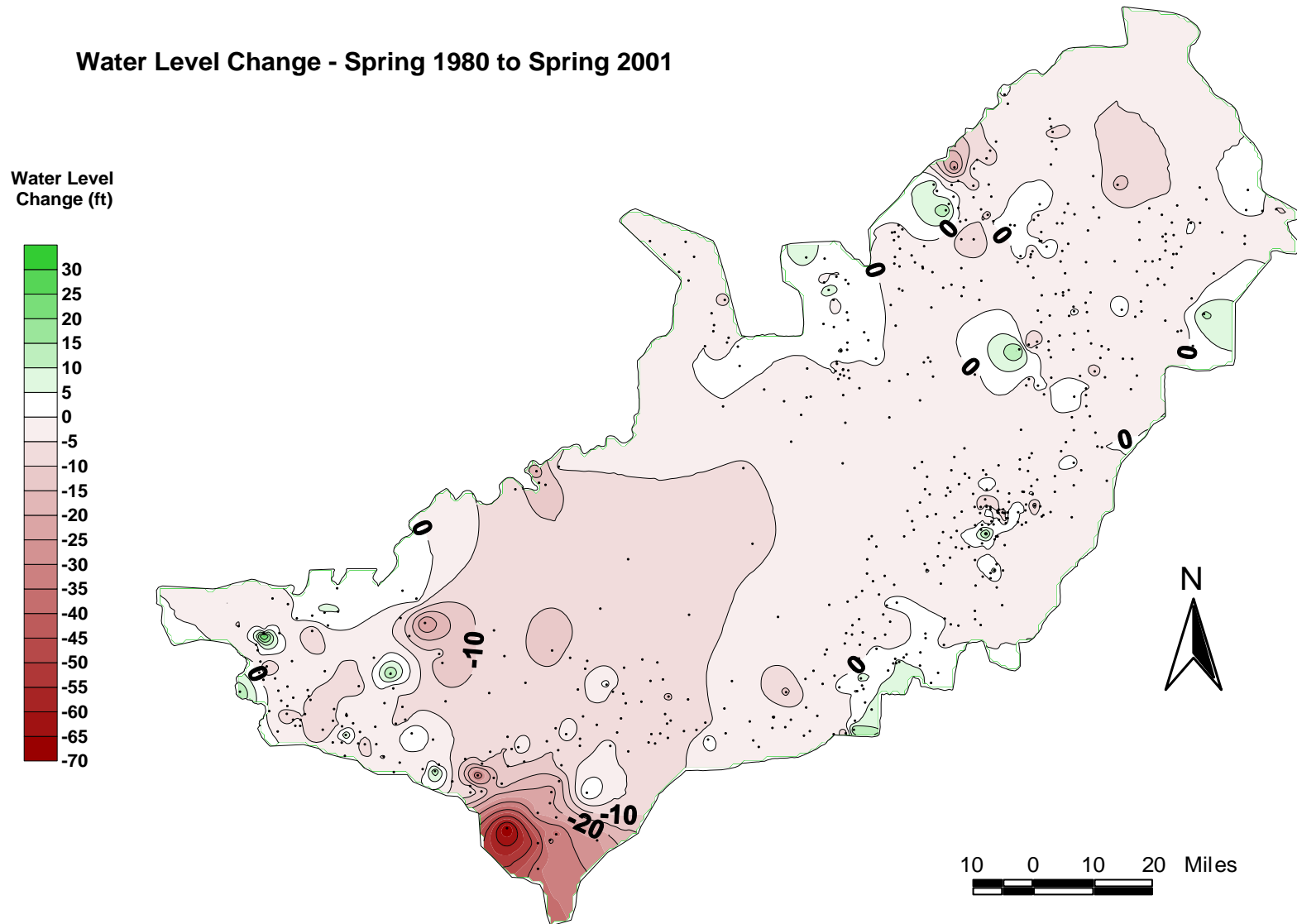


Figure 10. Water level change map, Spring 1980 – Spring 2001.

DRAFT

Water Level Change - Spring 2002 to Spring 2008

Water Level
Change (ft)

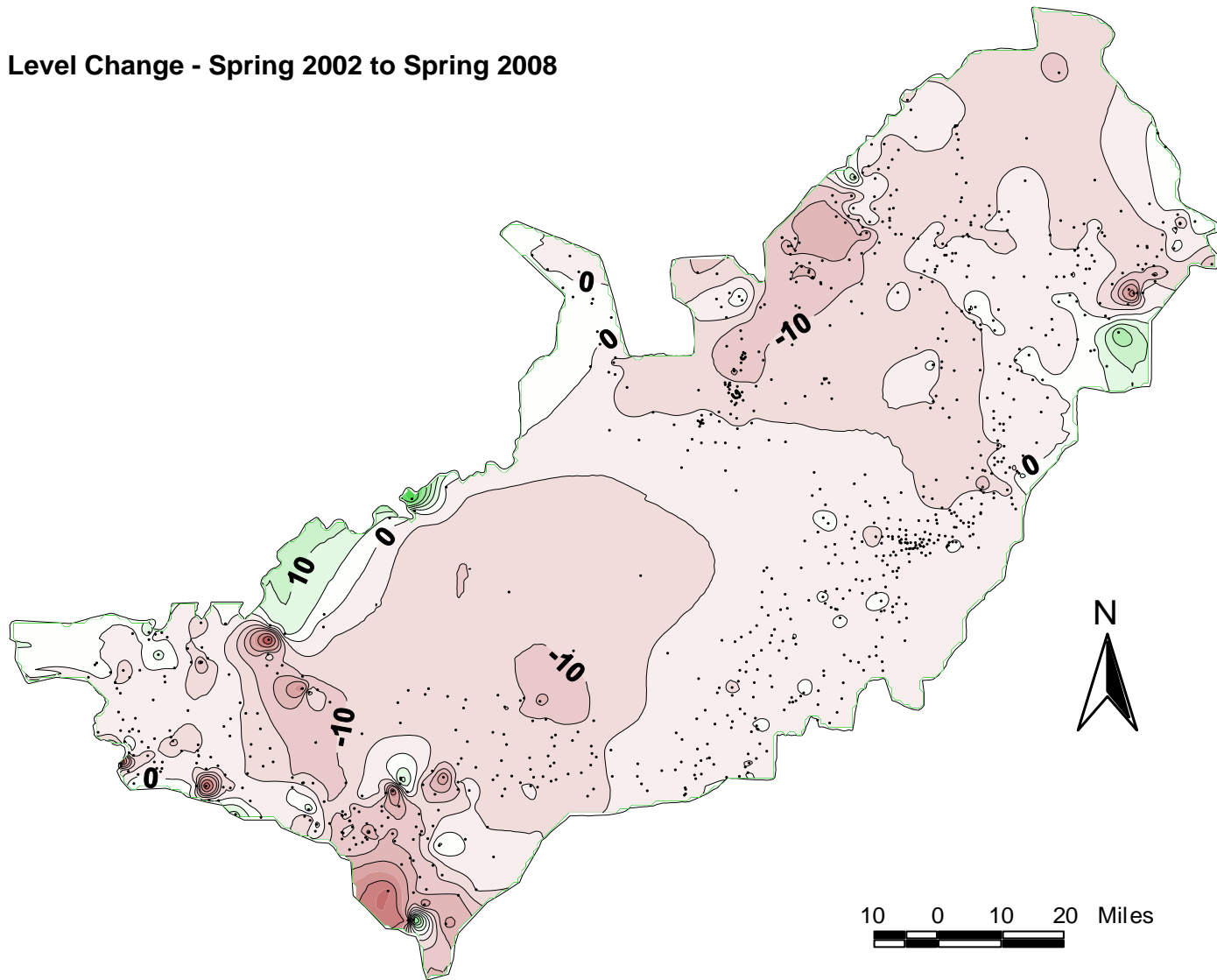
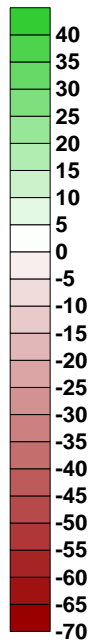


Figure 11. Water level change map, Spring 2002 – Spring 2008.

DRAFT

Water Level Change - Spring 1980 to Spring 2008

Water Level
Change (ft)

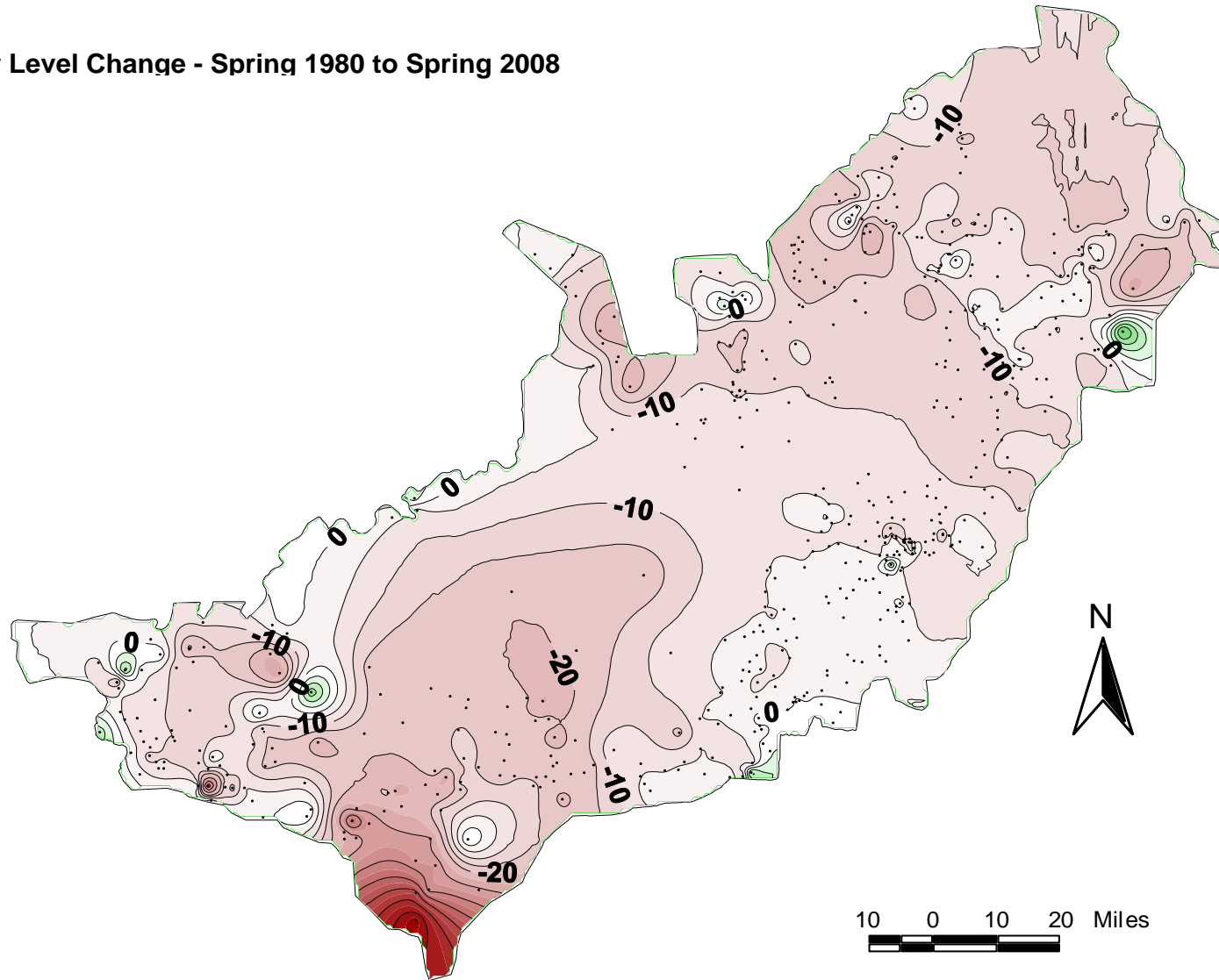
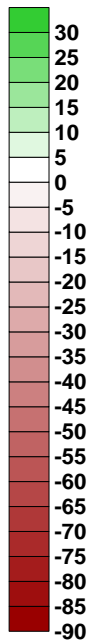
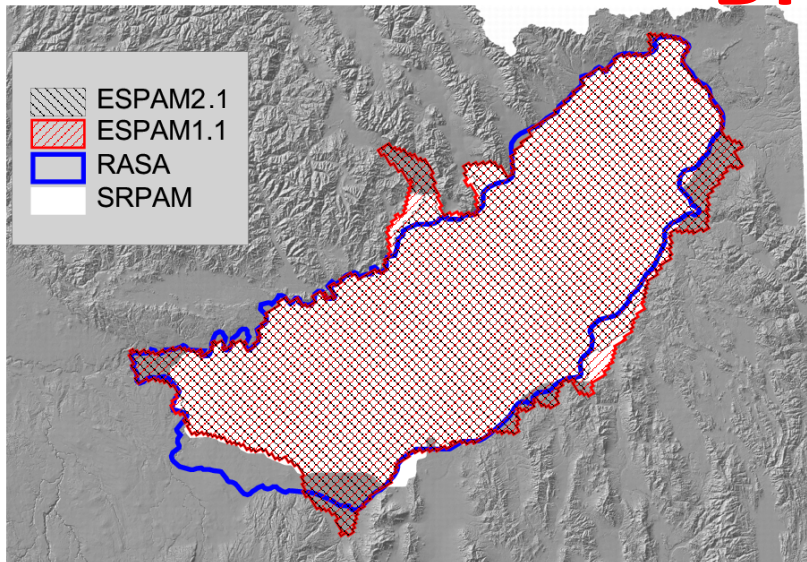


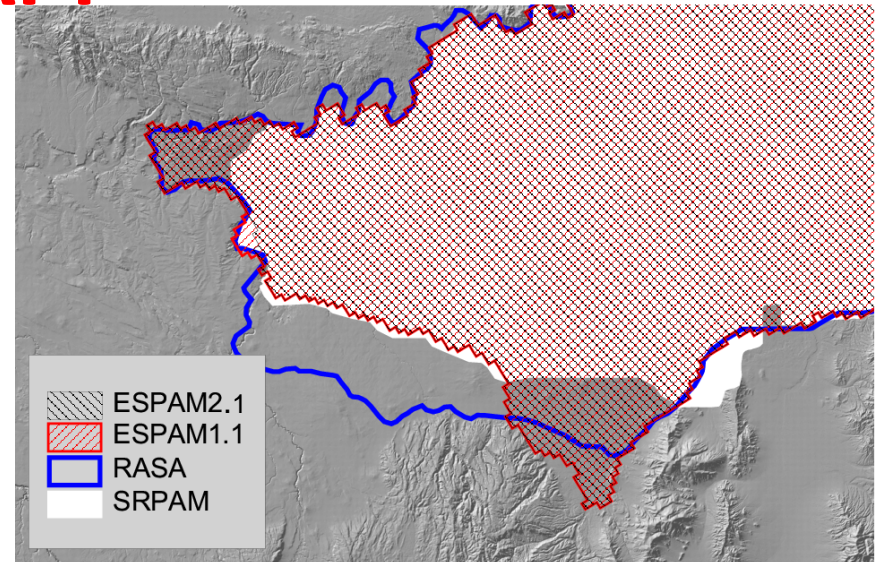
Figure 12. Water level change map, Spring 1980 - Spring 2008.

DRAFT



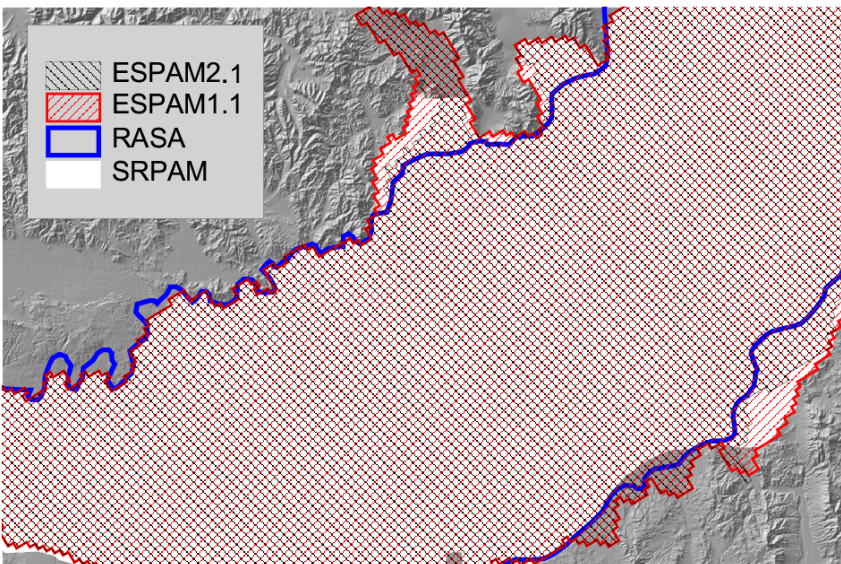
50 0 50 100 Miles

Figure 13a. Comparison of model boundaries.



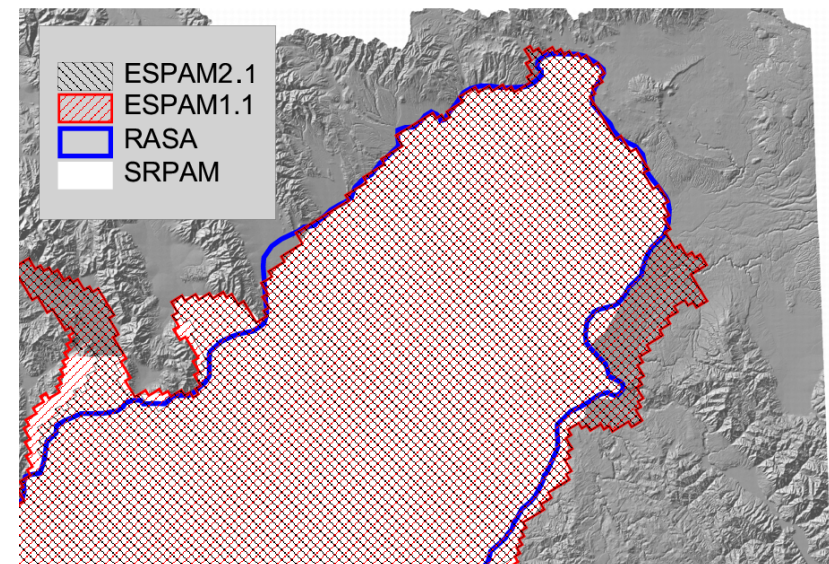
20 0 20 40 Miles

Figure 13b. Close-up of the southwestern area of Figure 15a.



20 0 20 40 Miles

Figure 13c. Close-up of the central area of Figure 15a.



20 0 20 40 Miles

Figure 13d. Close-up of the northeastern area of Figure 15a.

DRAFT

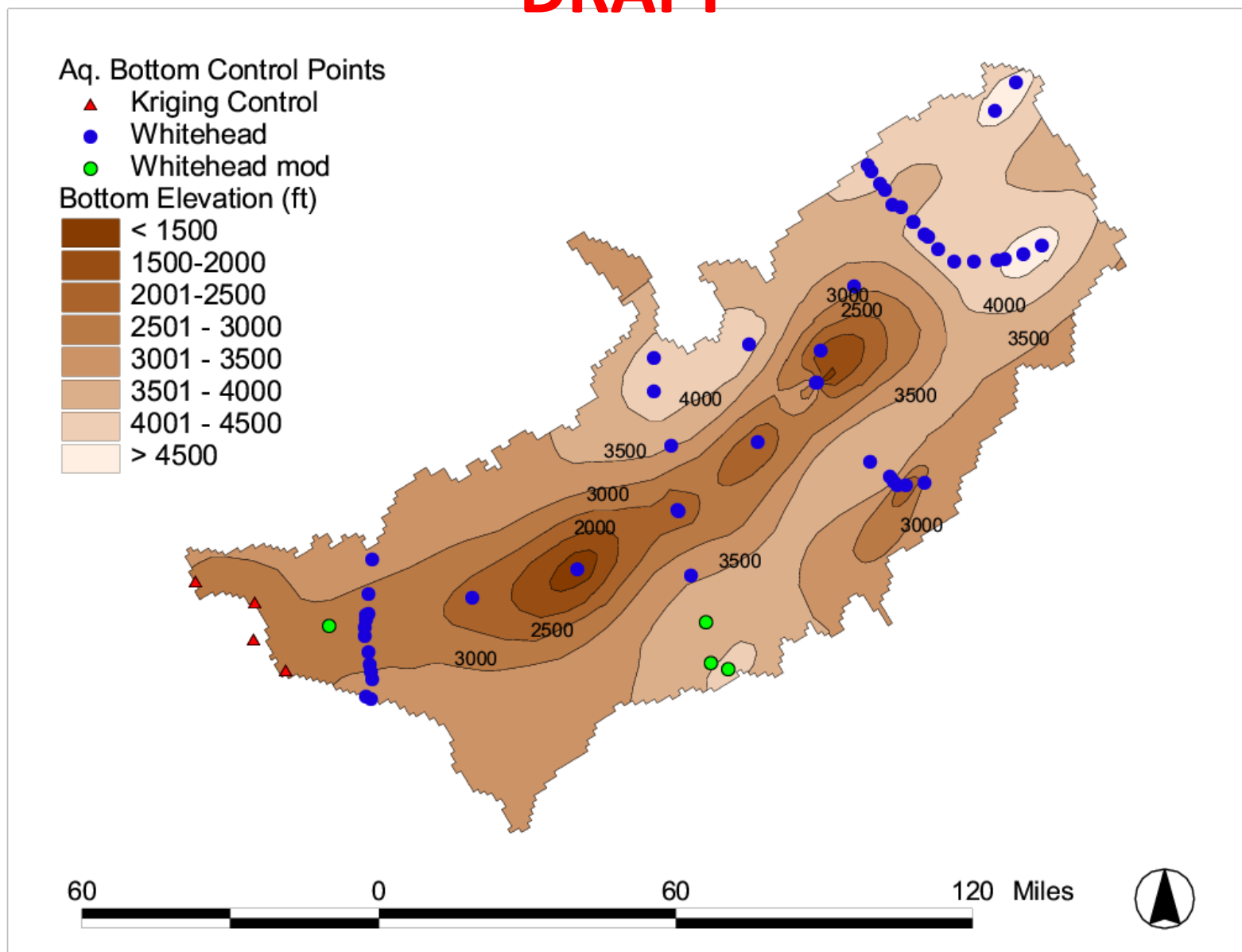


Figure 14. Aquifer bottom elevations with estimated elevation points. Based on modified Whitehead (1986) data. Blue dots represent locations used by Whitehead, green dots represent modified Whitehead data points, and red triangles represent points added to anchor the Kriged surface.

DRAFT

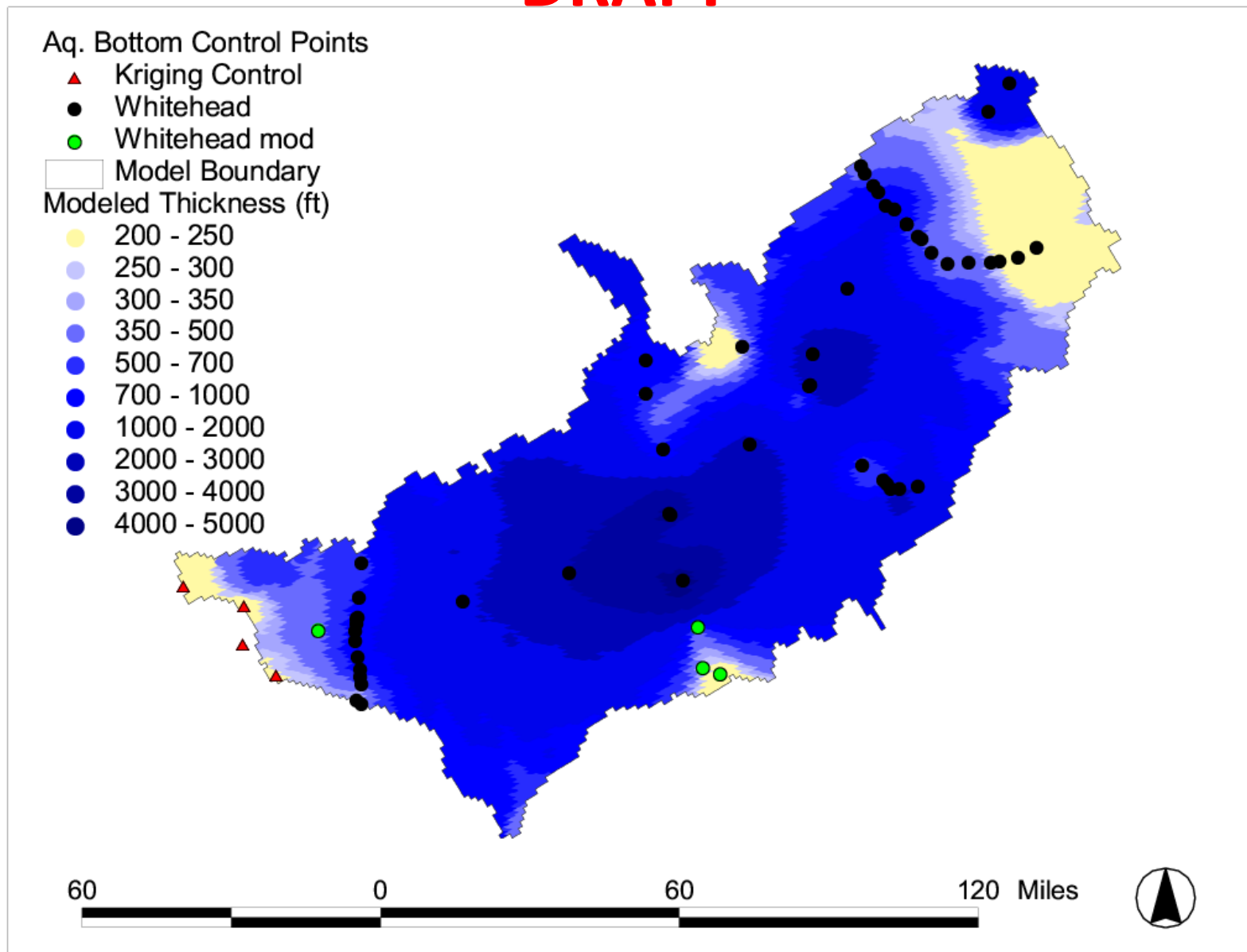


Figure 15. Delineation of aquifer thickness.

DRAFT

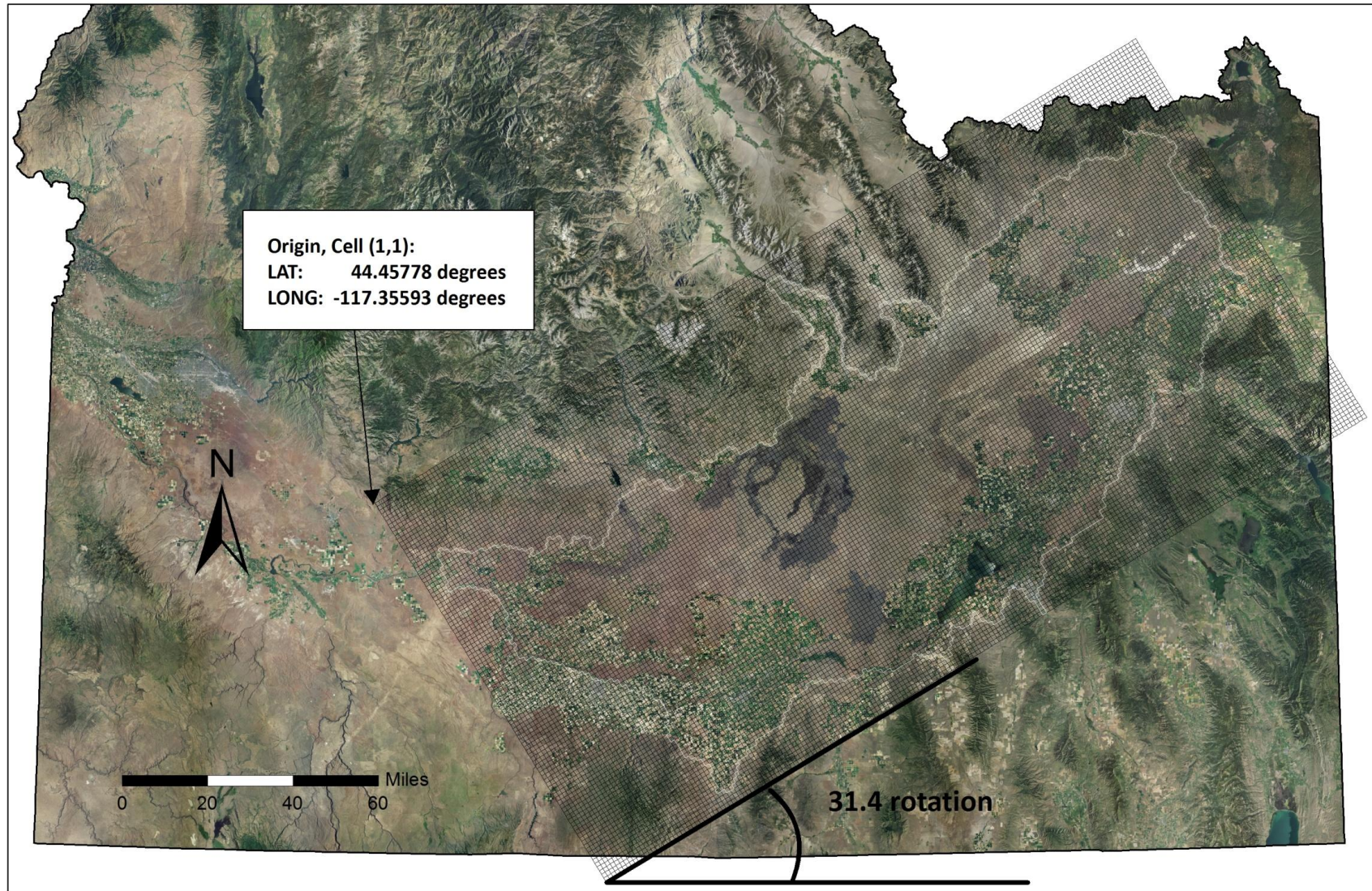


Figure16. Model grid and origin.

DRAFT

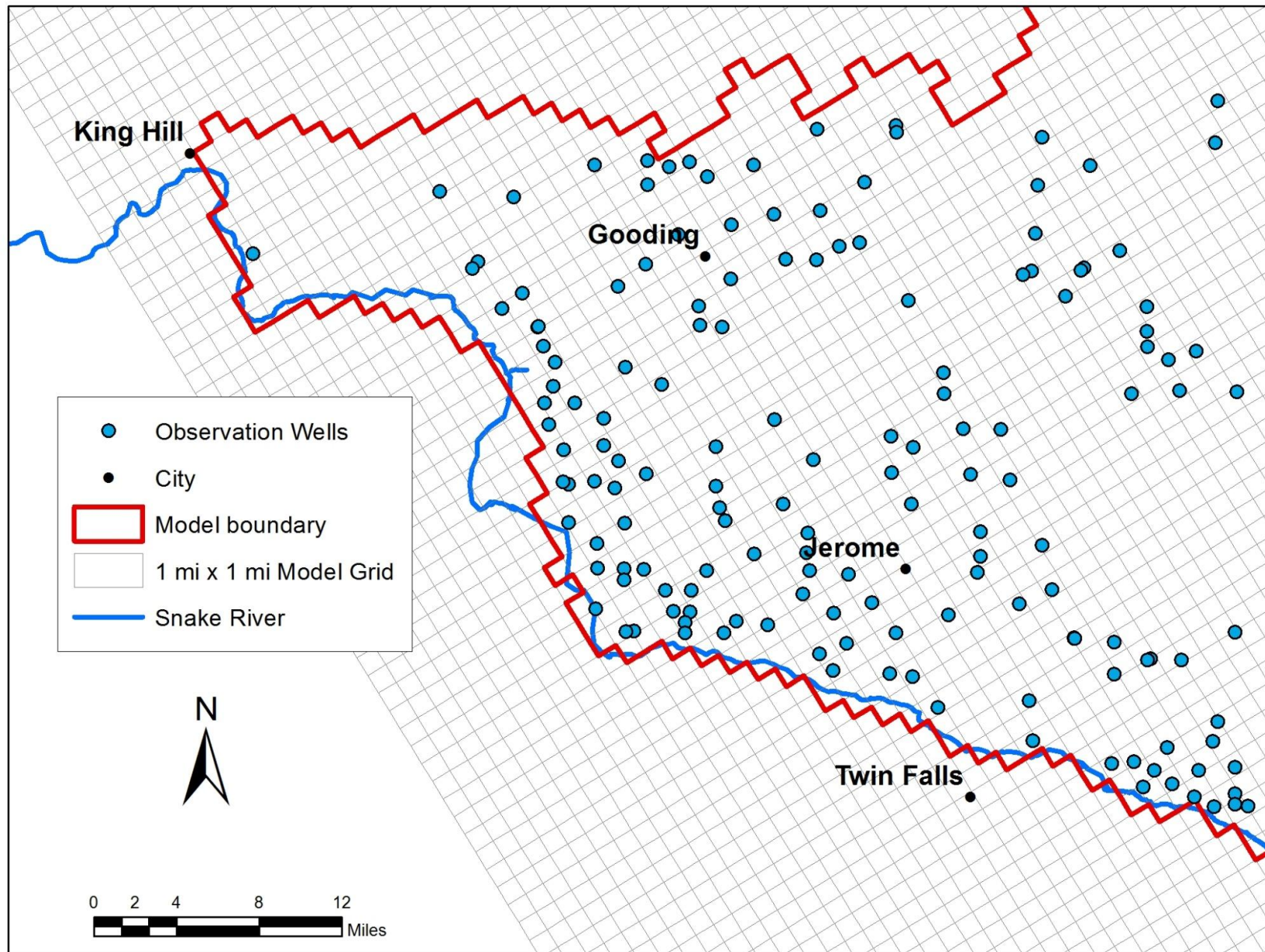


Figure 17. Close-up of model grid in the Thousand Springs area.

DRAFT

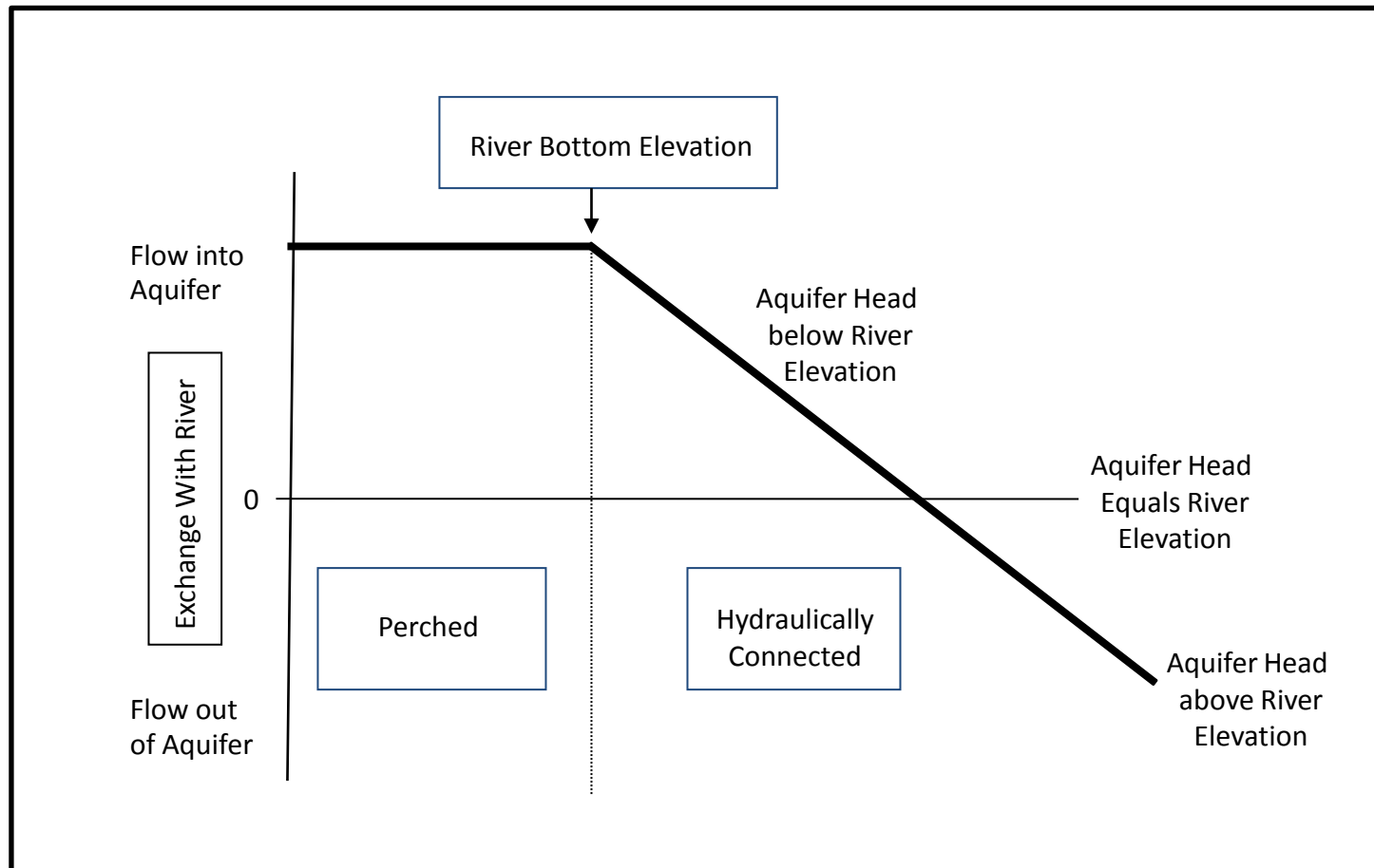


Figure 18. Conceptual illustration of river leakage computation in MODFLOW (after McDonald and Harbaugh, 1988).

DRAFT

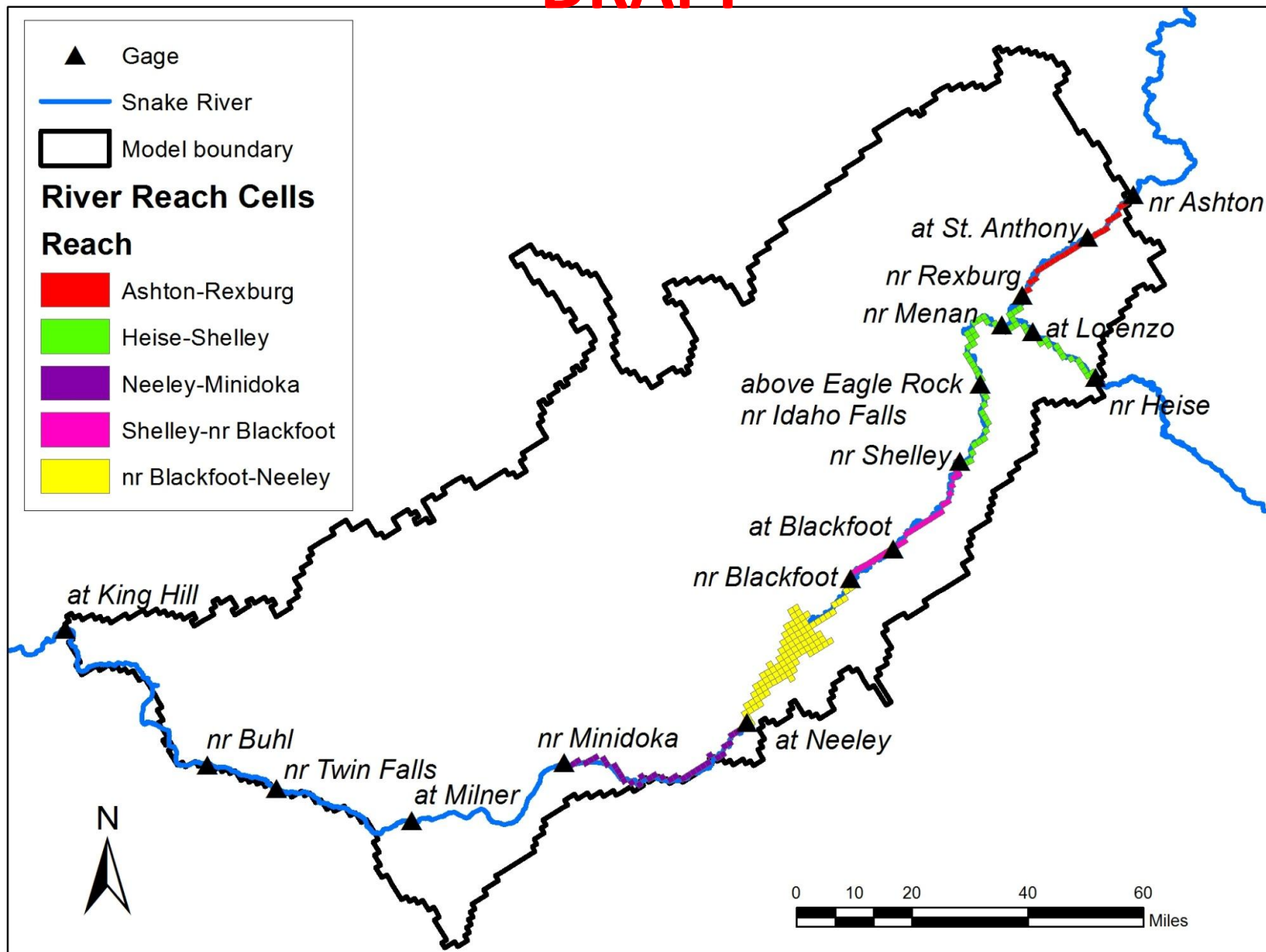


Figure 19. Head-dependent river reaches.

DRAFT

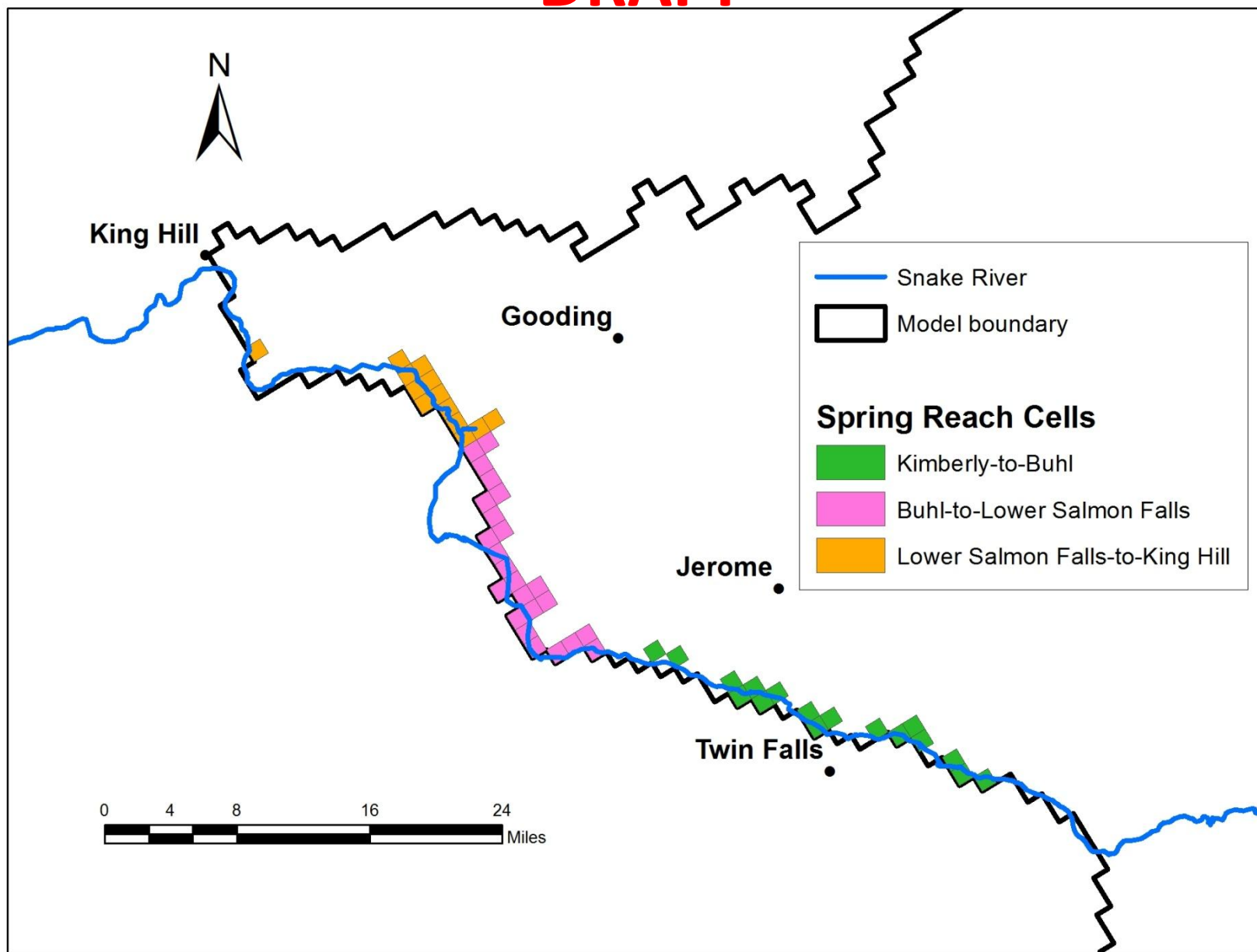


Figure 20. Head-dependent spring reaches.

DRAFT

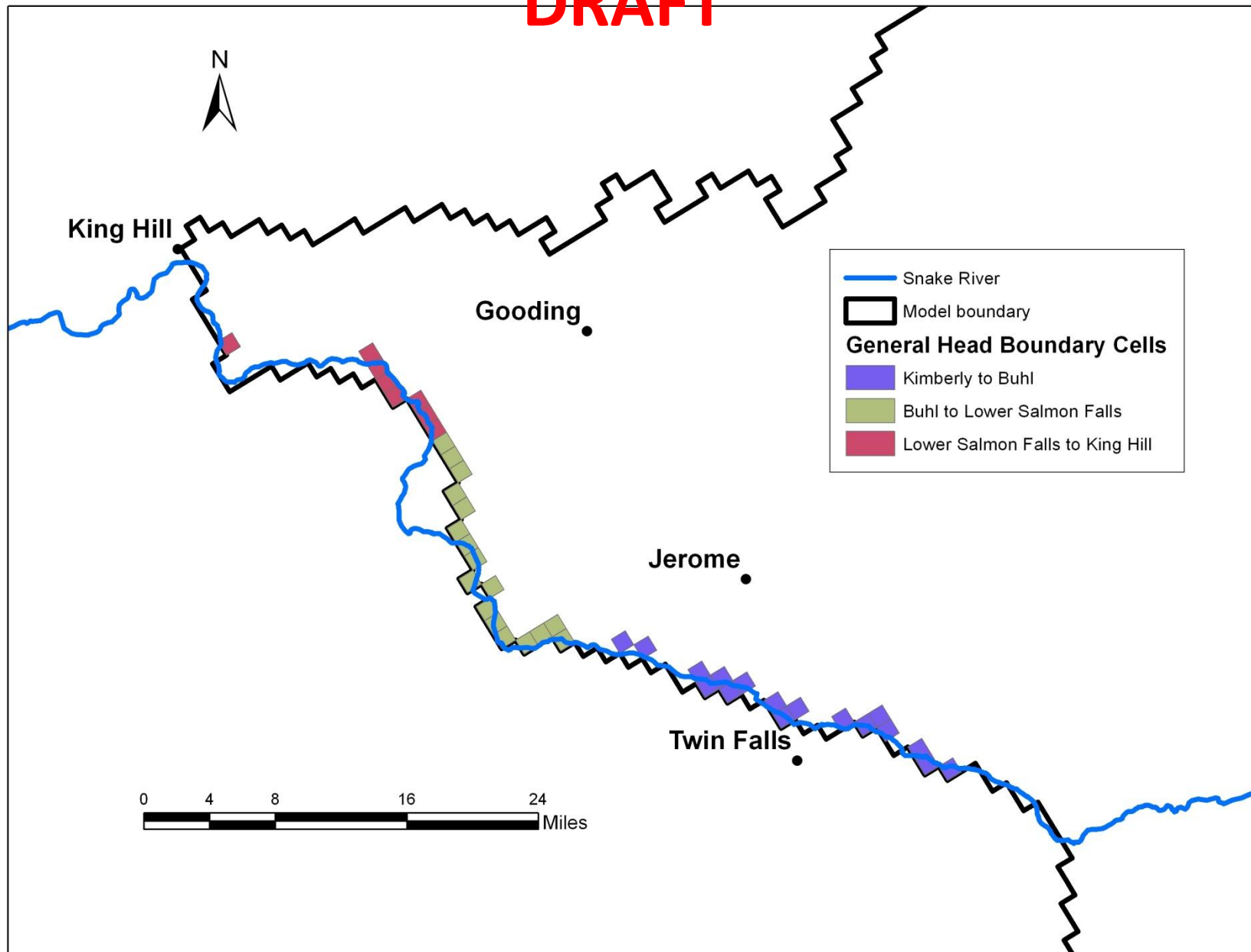


Figure 21. General head boundary cells.

DRAFT

Figure 22a – 22f. Irrigated lands for the years 1980, 1986, 1992, 2000, 2002, and 2006.
See 11x17 Figures.

DRAFT

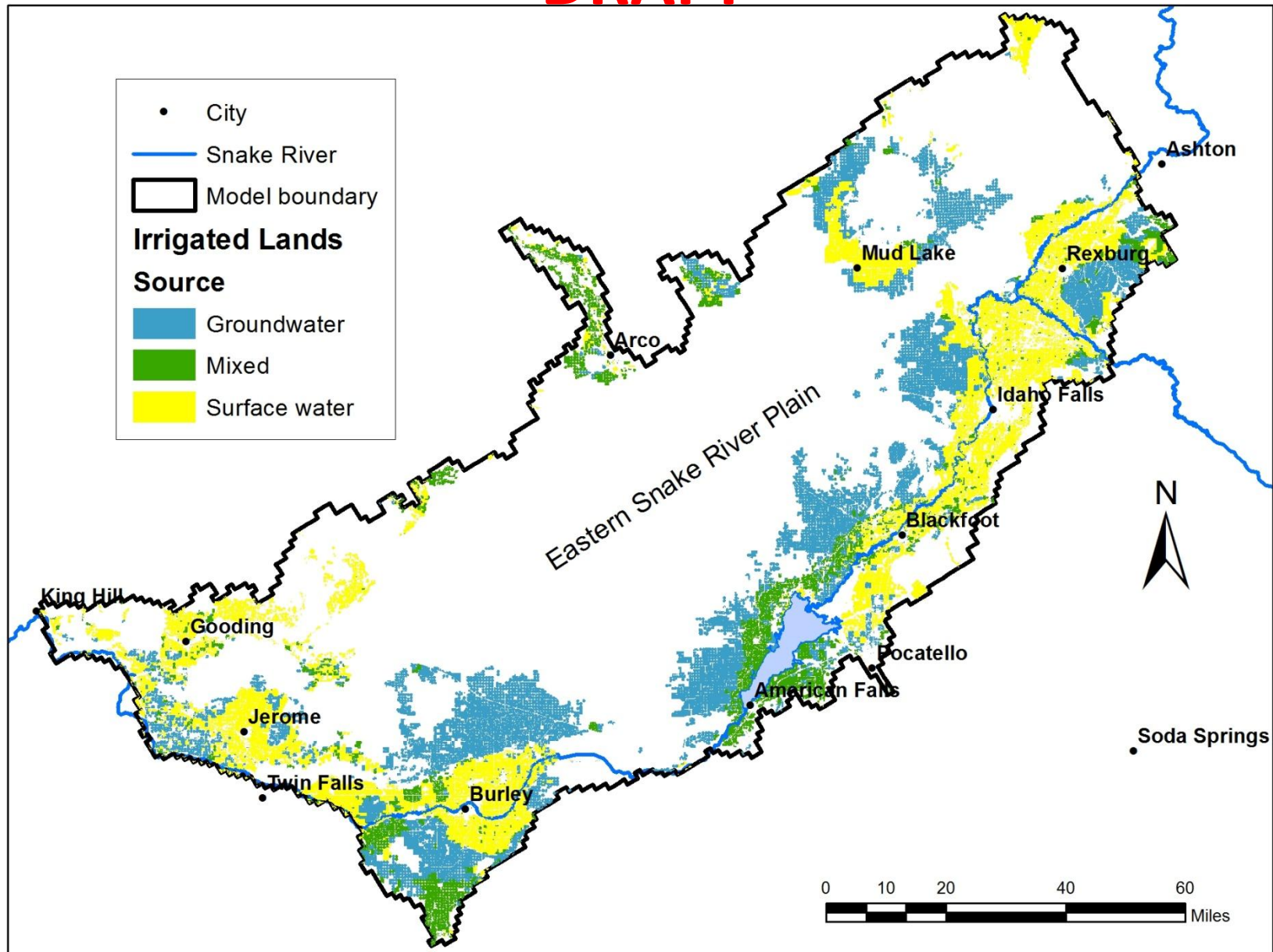


Figure 23. Irrigation water source determined from adjudication data. Water source was adjusted in Mud Lake and Montevideo area to account for water delivery from offsite irrigation wells.

DRAFT

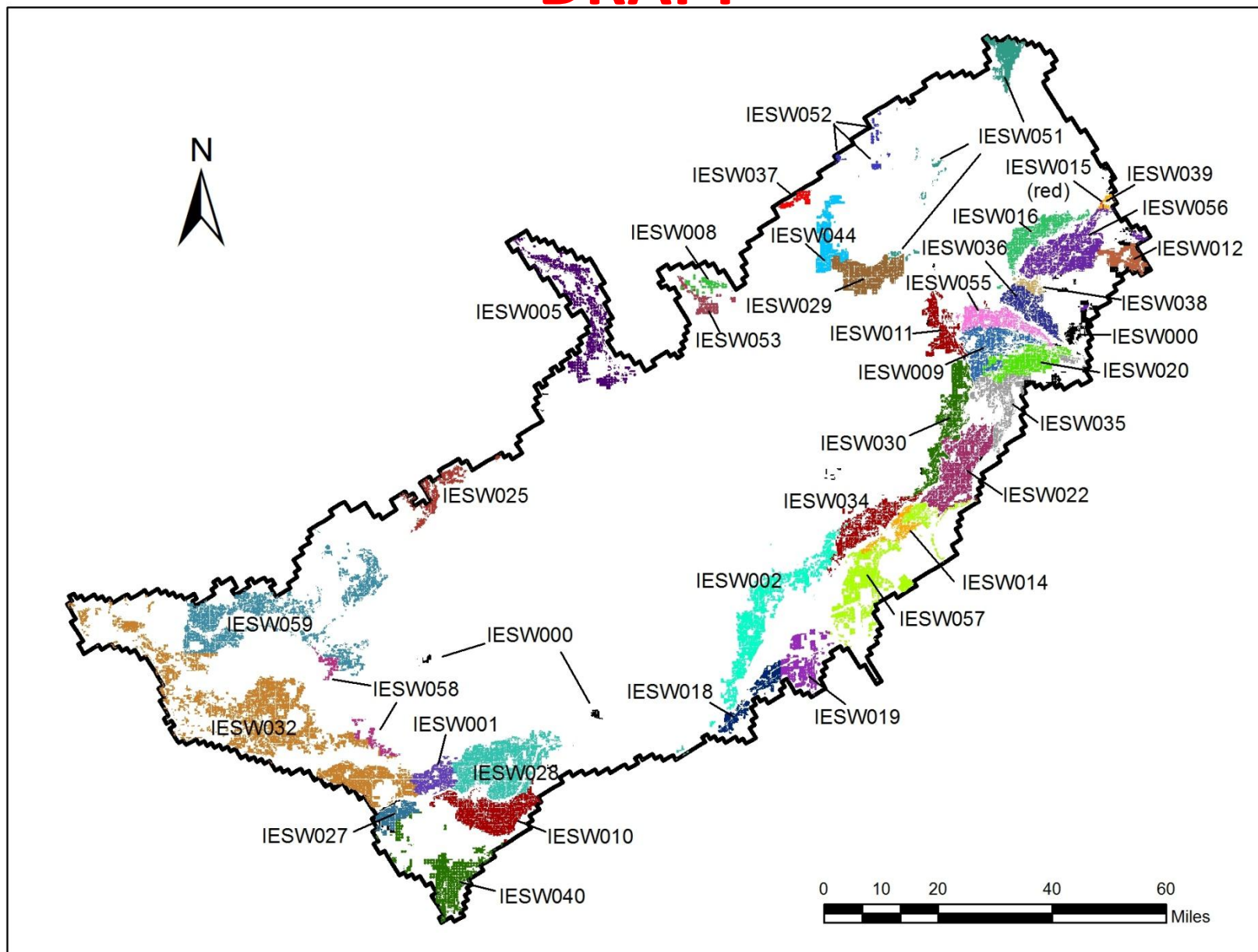


Figure 24. Surface-water irrigation entities.

DRAFT

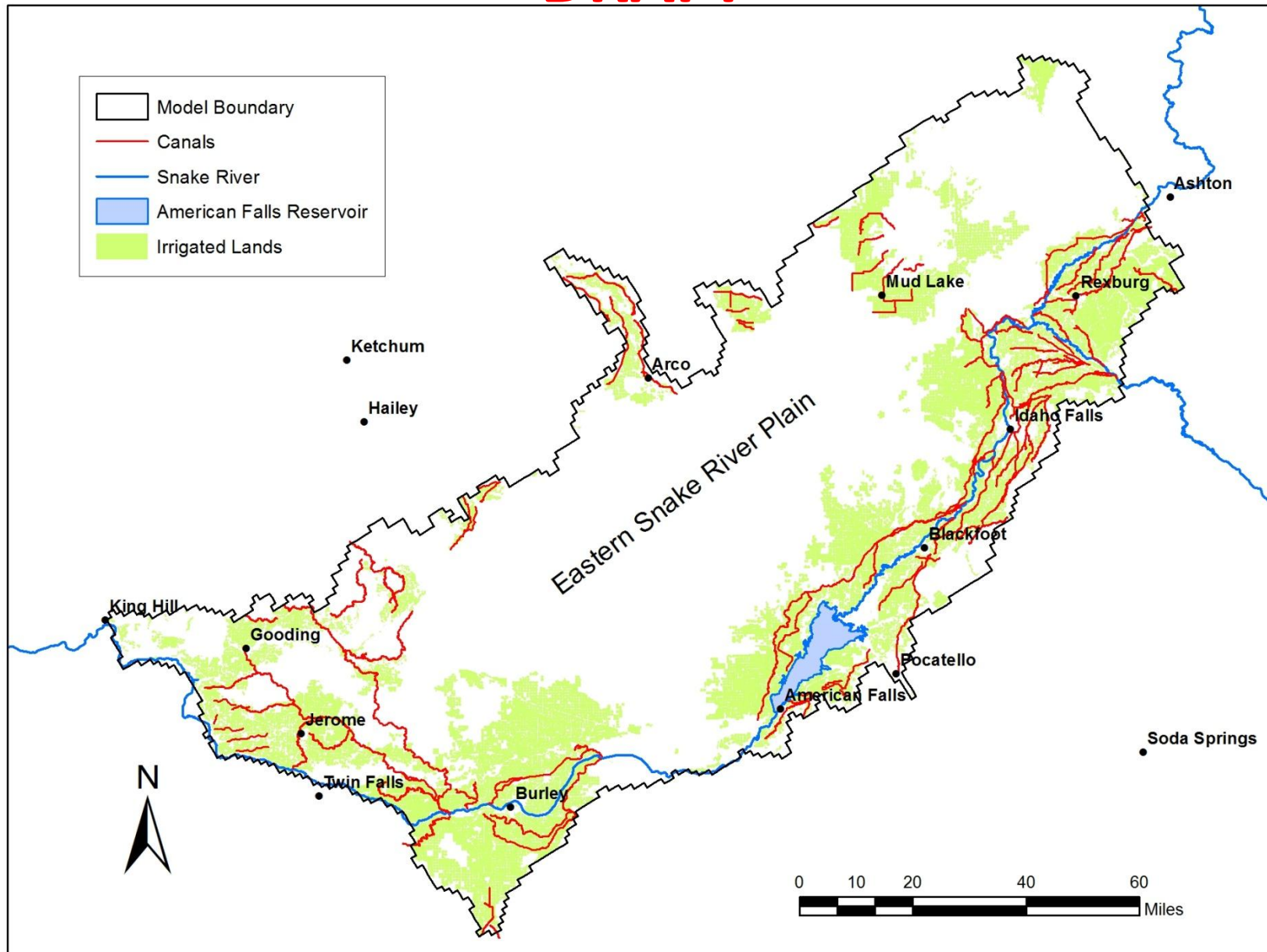


Figure 25. Locations of canals where leakage is simulated in the model.

DRAFT

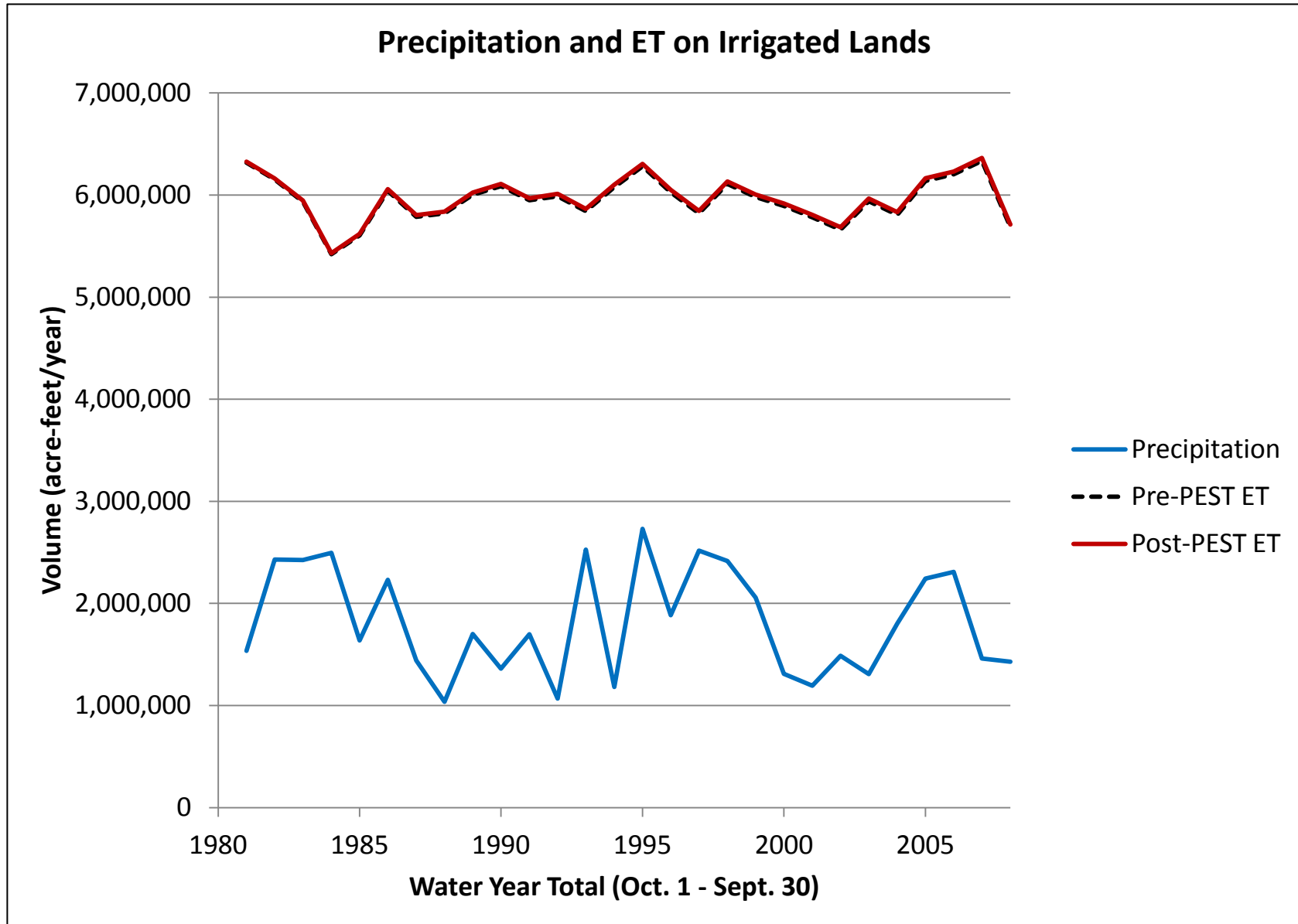


Figure 26. Precipitation and evapotranspiration (ET) for irrigated lands for water years 1981-2008.

DRAFT

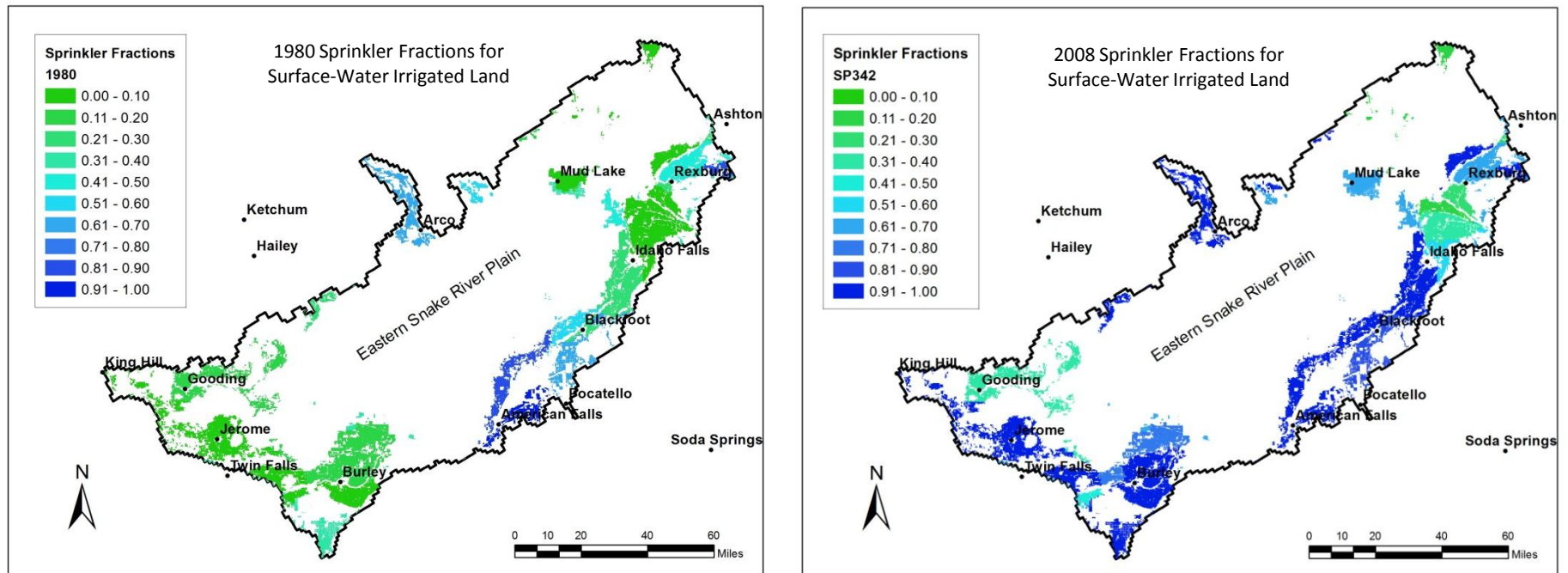


Figure 28. Sprinkler fraction by surface-water entity, 1980 and 2008.

DRAFT

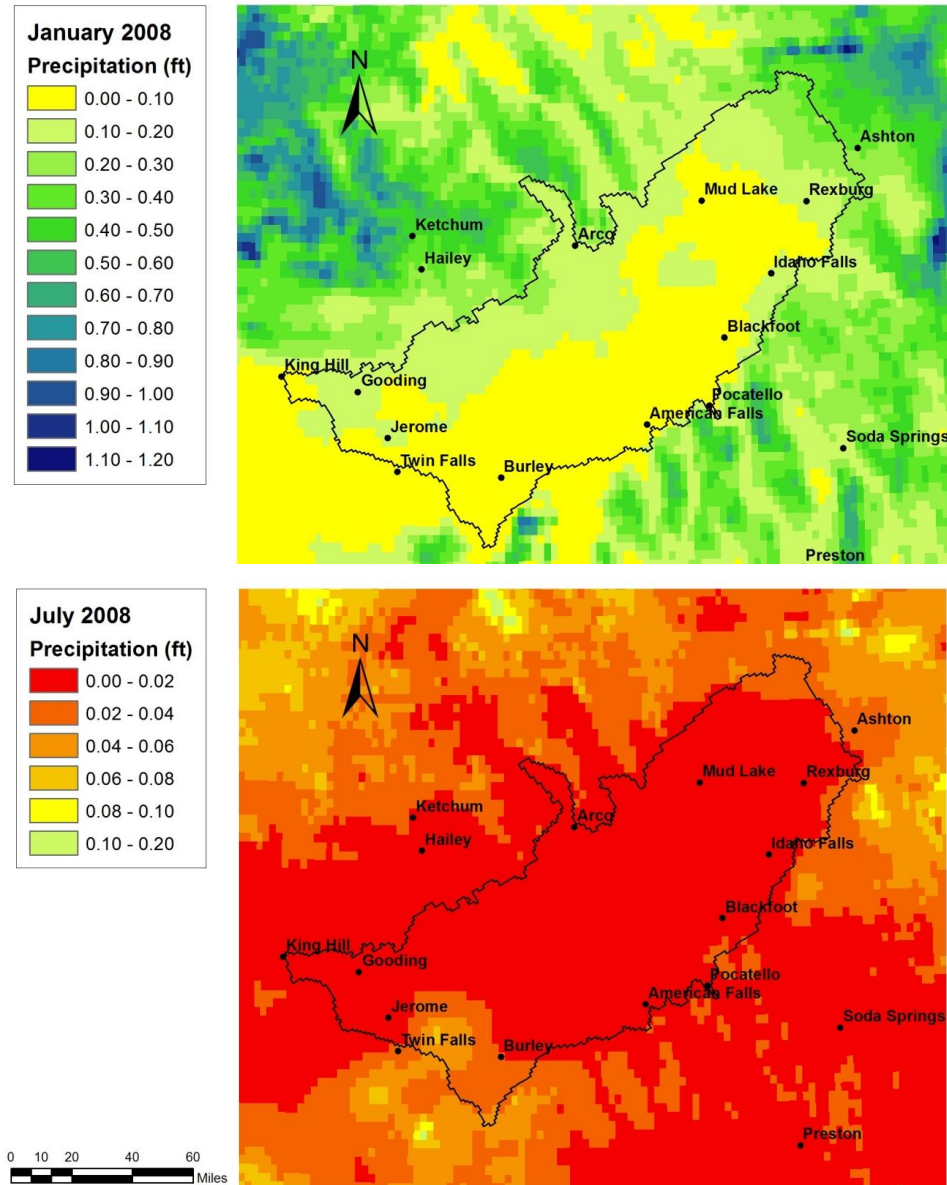


Figure 29. PRISM precipitation maps for one month in the non-irrigation season (January 2008 - top) and the irrigation season (July 2008 - bottom).

DRAFT

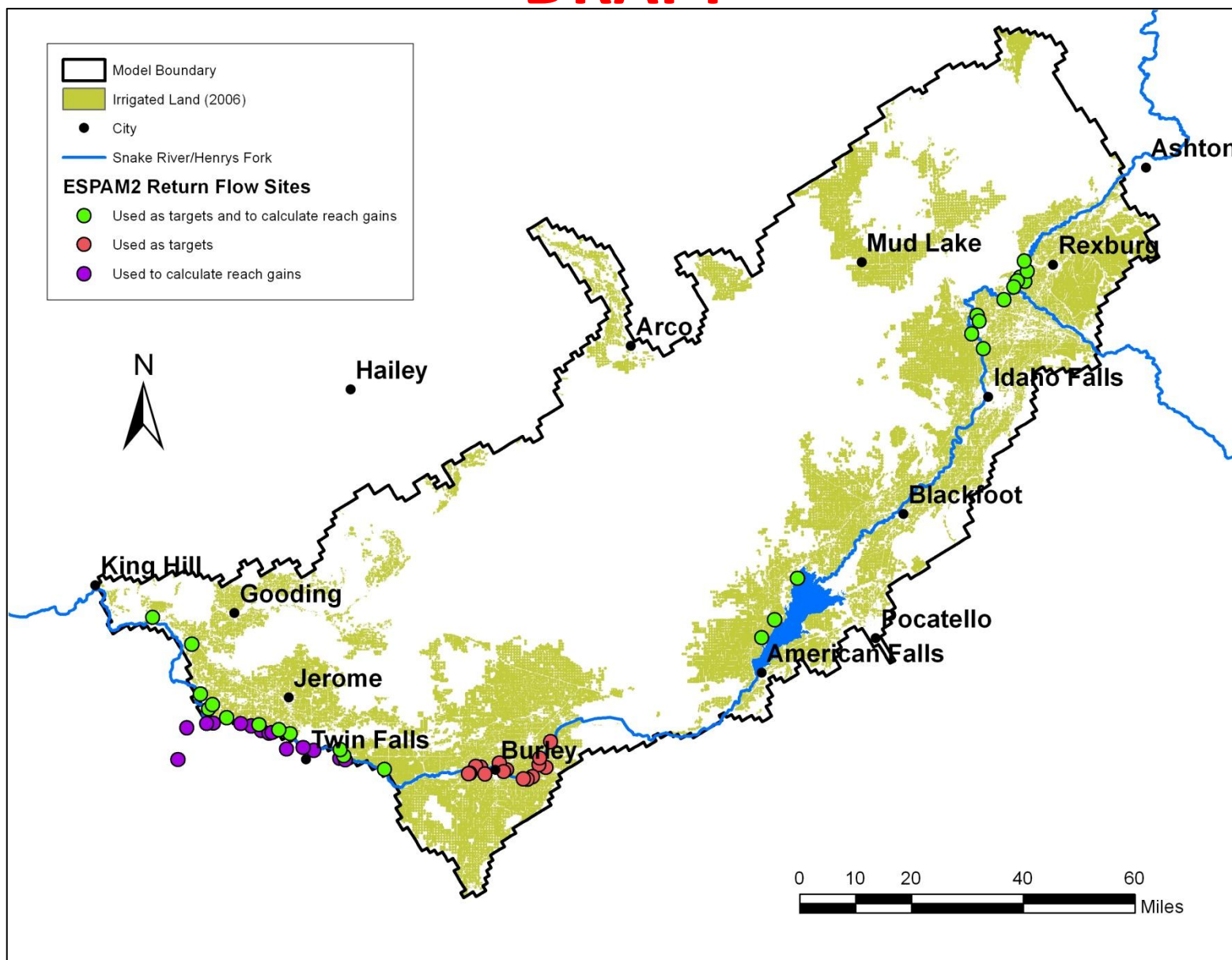


Figure 30. Return-flow measurement locations.

DRAFT

Canal Seepage and Recharge in ESPAM2.1 Surface Water Entities

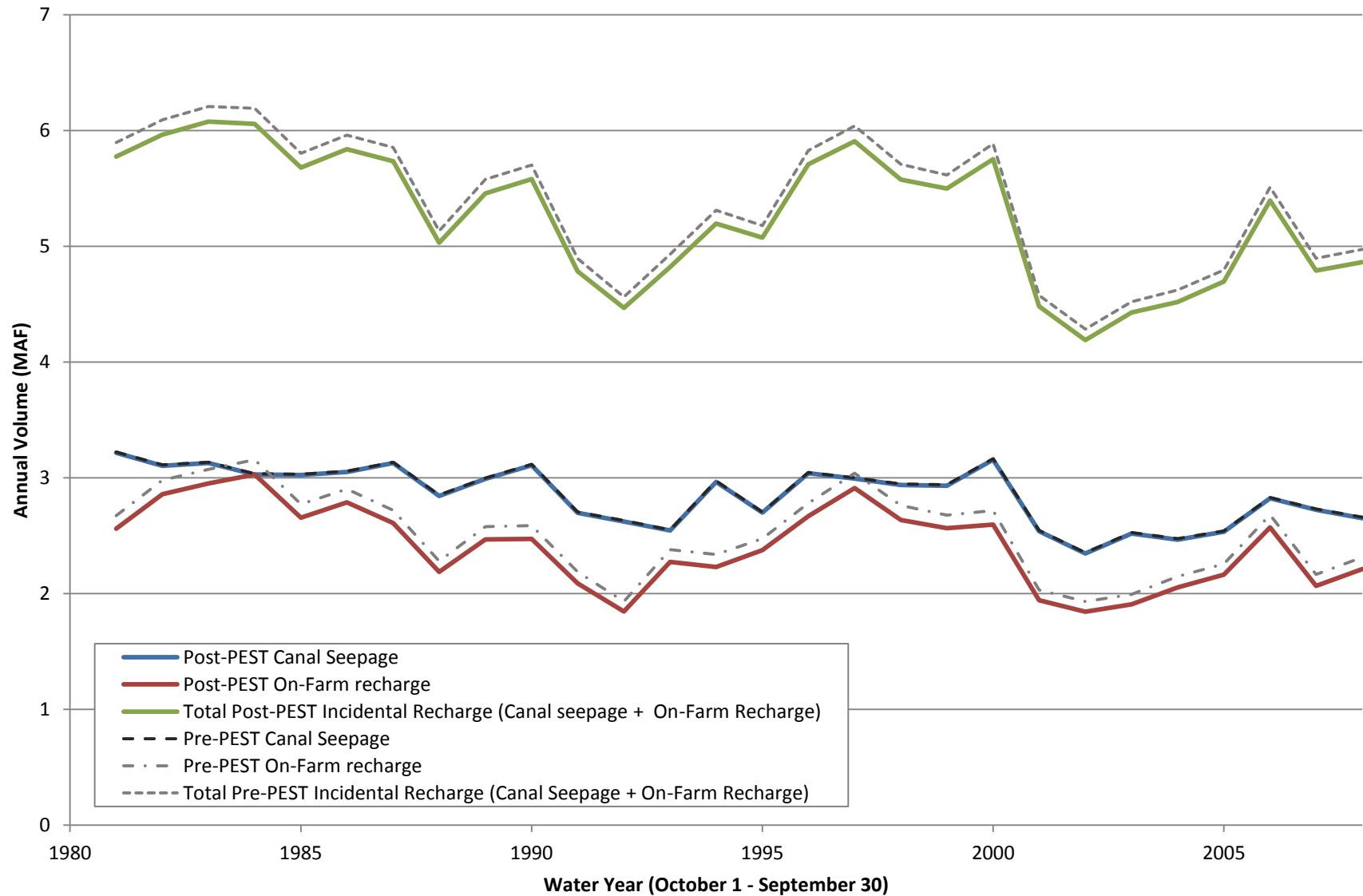


Figure 31. Annual volume of canal seepage and recharge incidental to irrigation in ESPAM2.1 surface water entities.

DRAFT

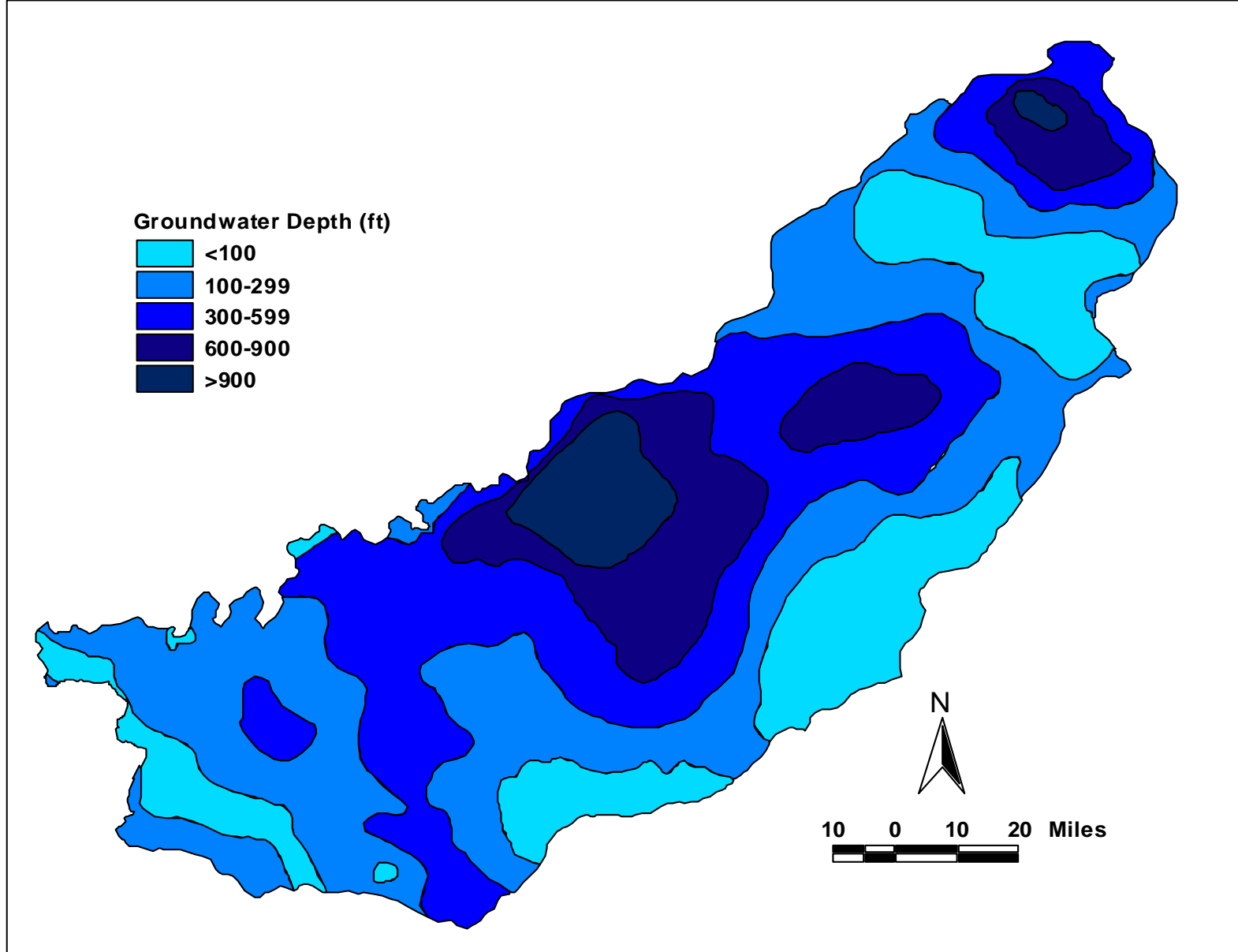


Figure 32. Depth to water in 1980 (digitized from Lindholm and others, 1988).

DRAFT

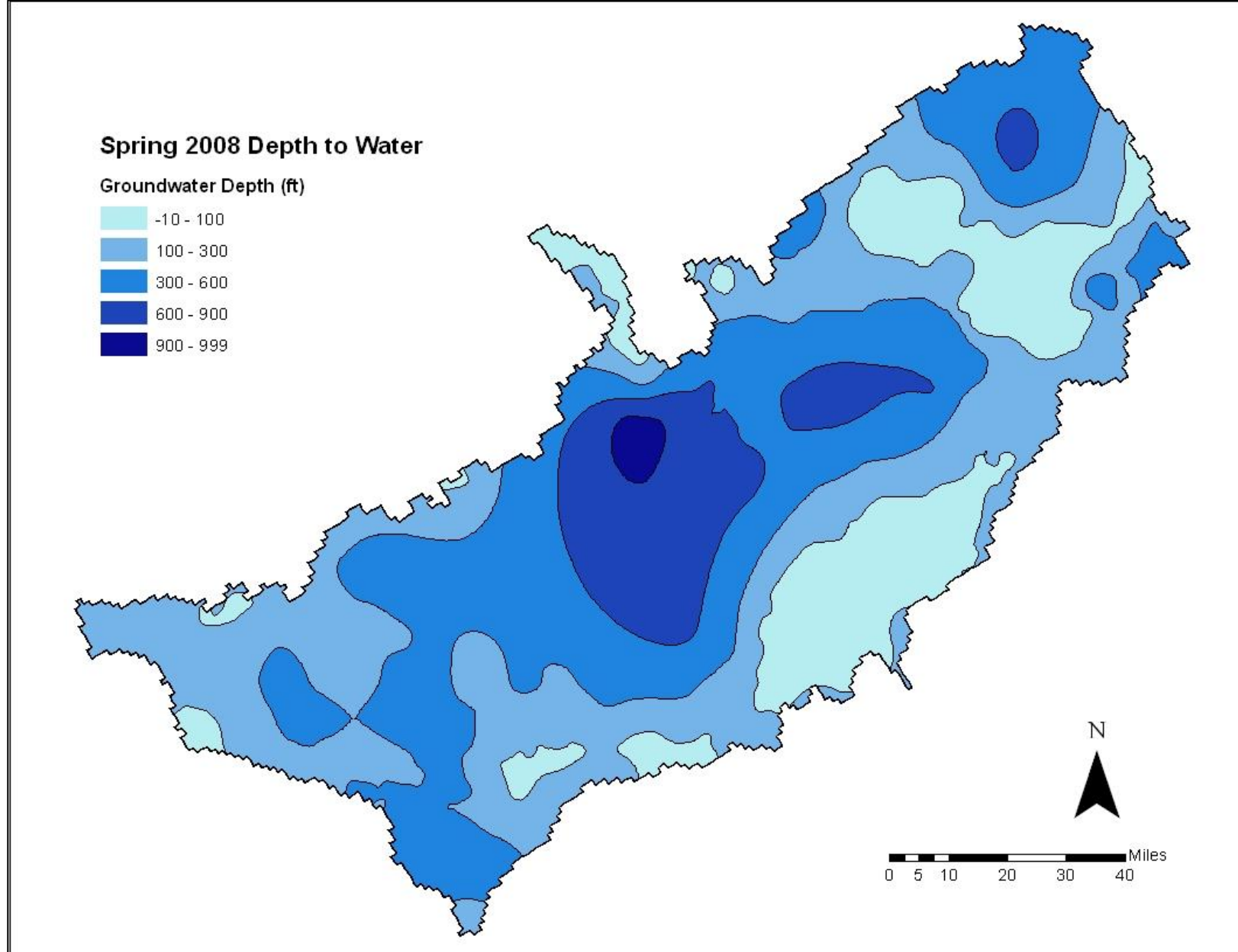


Figure 33. Depth to water based on Spring 2008 synoptic water levels.

DRAFT

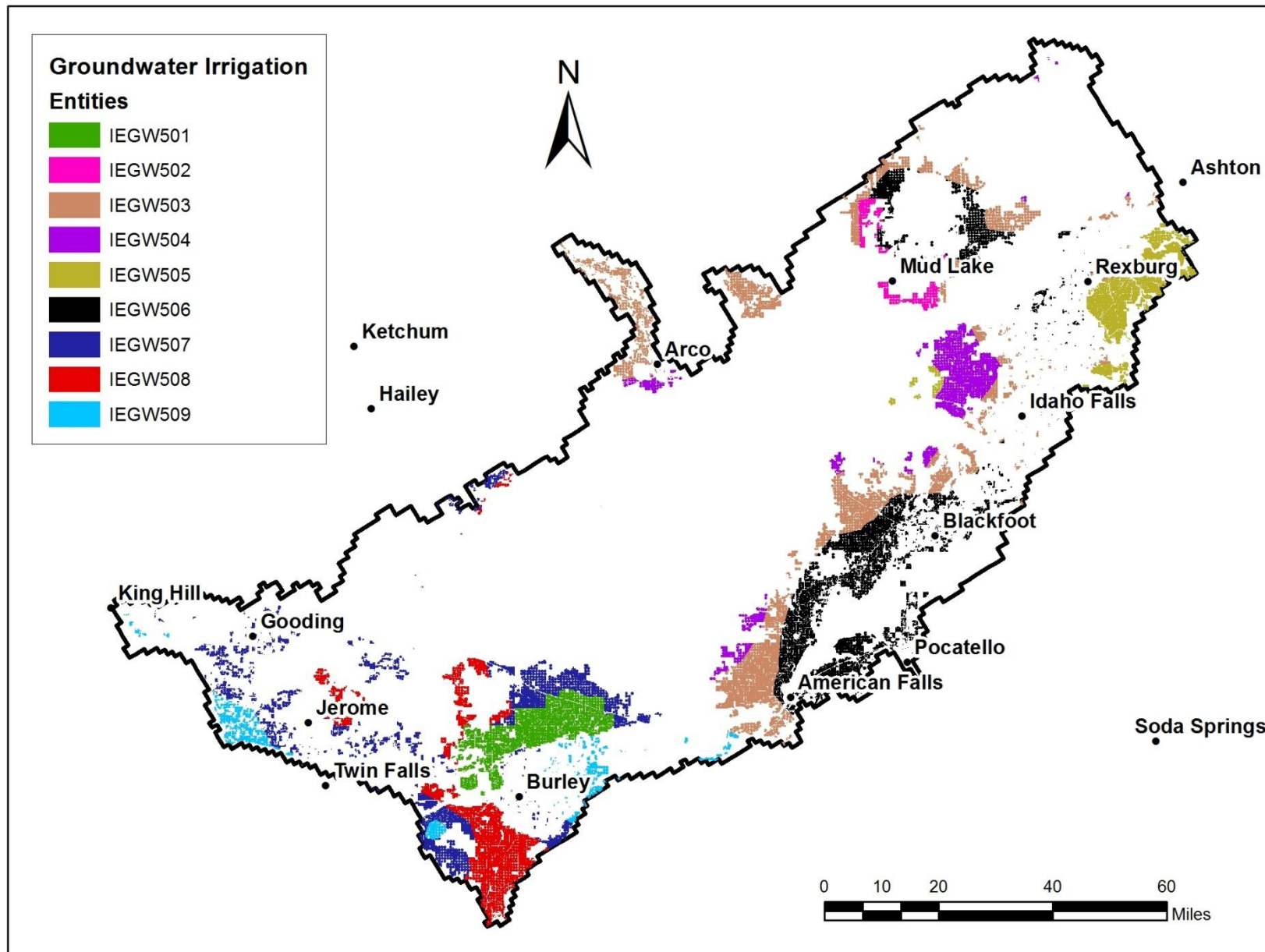


Figure 34. Groundwater irrigation polygons. The central portion of the plain absent of irrigation is represented as IEGW600 (not labeled in the figure).

DRAFT

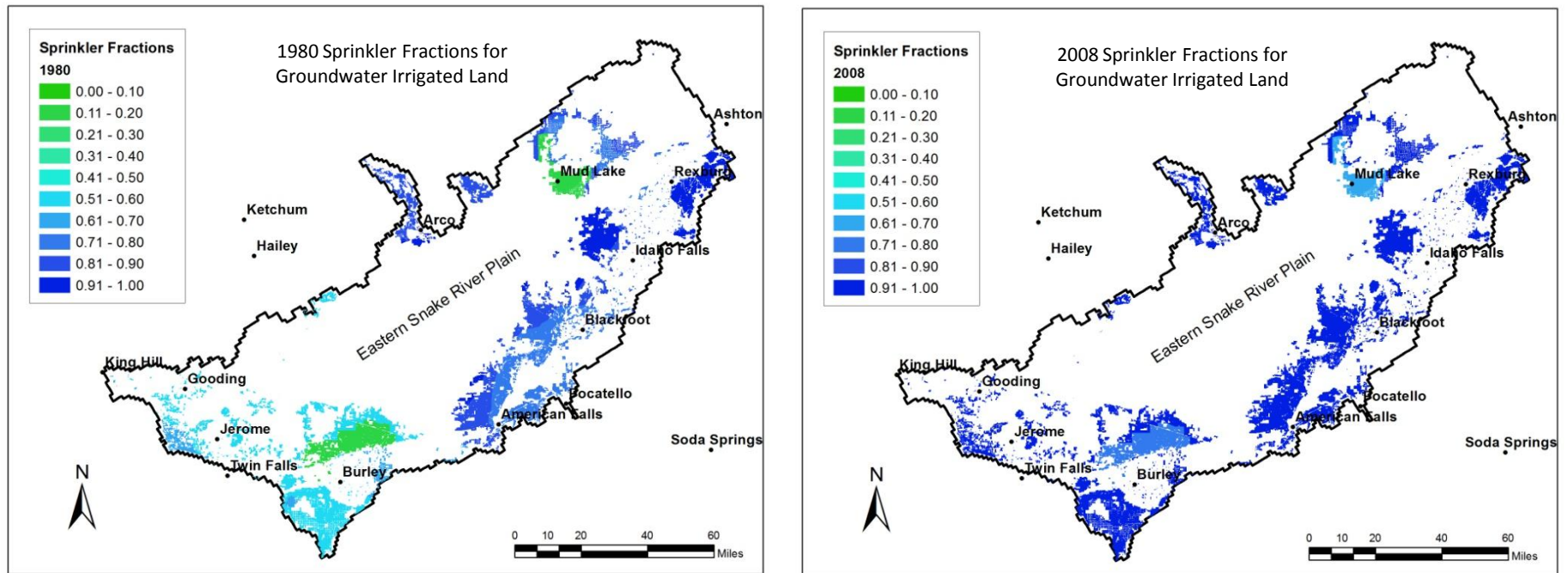


Figure 35. Sprinkler fraction by groundwater polygon, 1980 and 2008.

DRAFT

Net Extraction Attributed to Groundwater Polygons and Total Extraction from Offsite and Exchange Wells

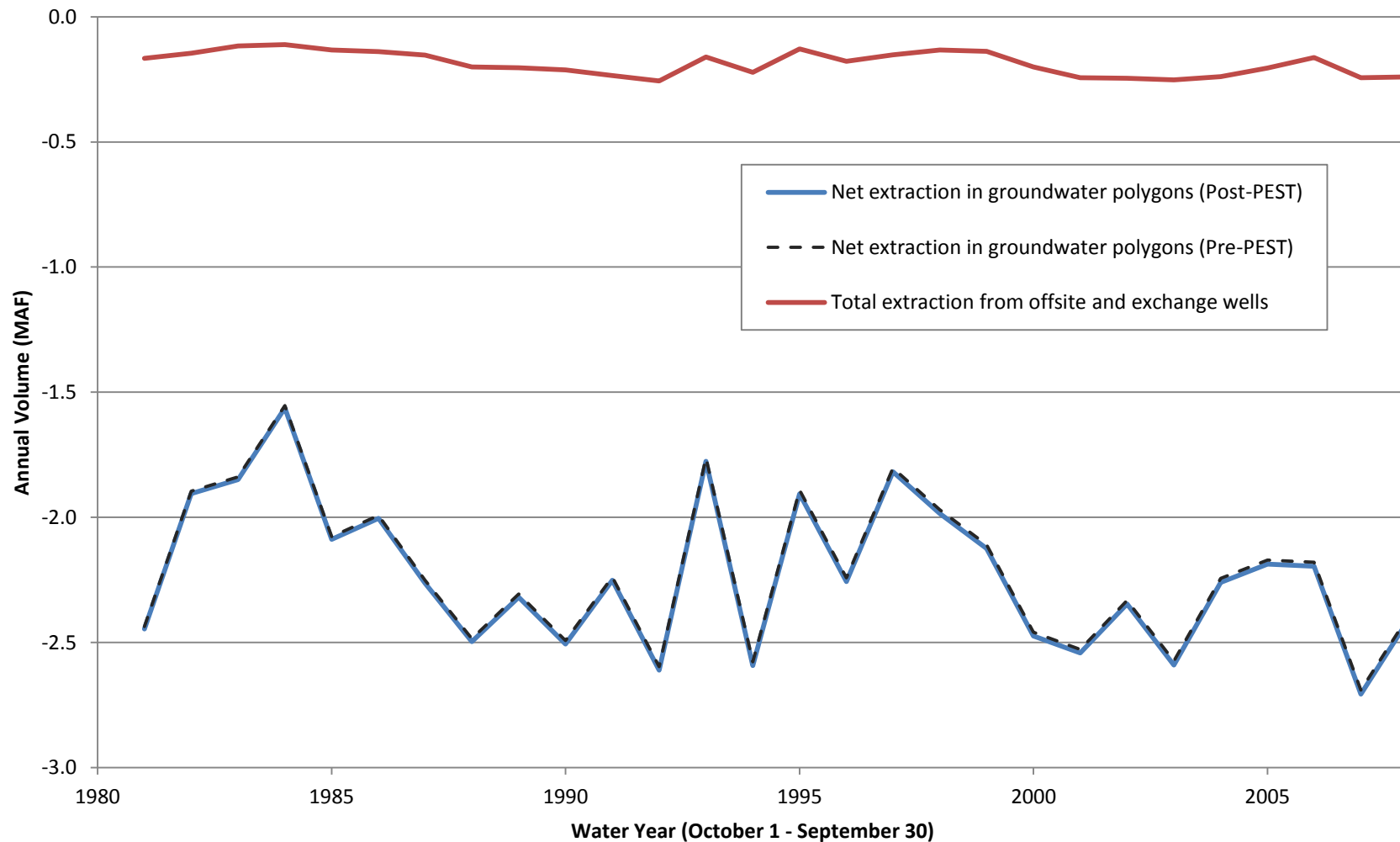


Figure 36. Net extraction in groundwater polygons and total extraction from offsite and exchange wells. Net extraction in groundwater polygons is equivalent to the crop irrigation requirement attributed to groundwater polygons. Total extraction from offsite and exchange wells includes water recharged via canal seepage and On-Farm recharge. Extraction from offsite and exchange wells is not adjusted during model calibration.

DRAFT

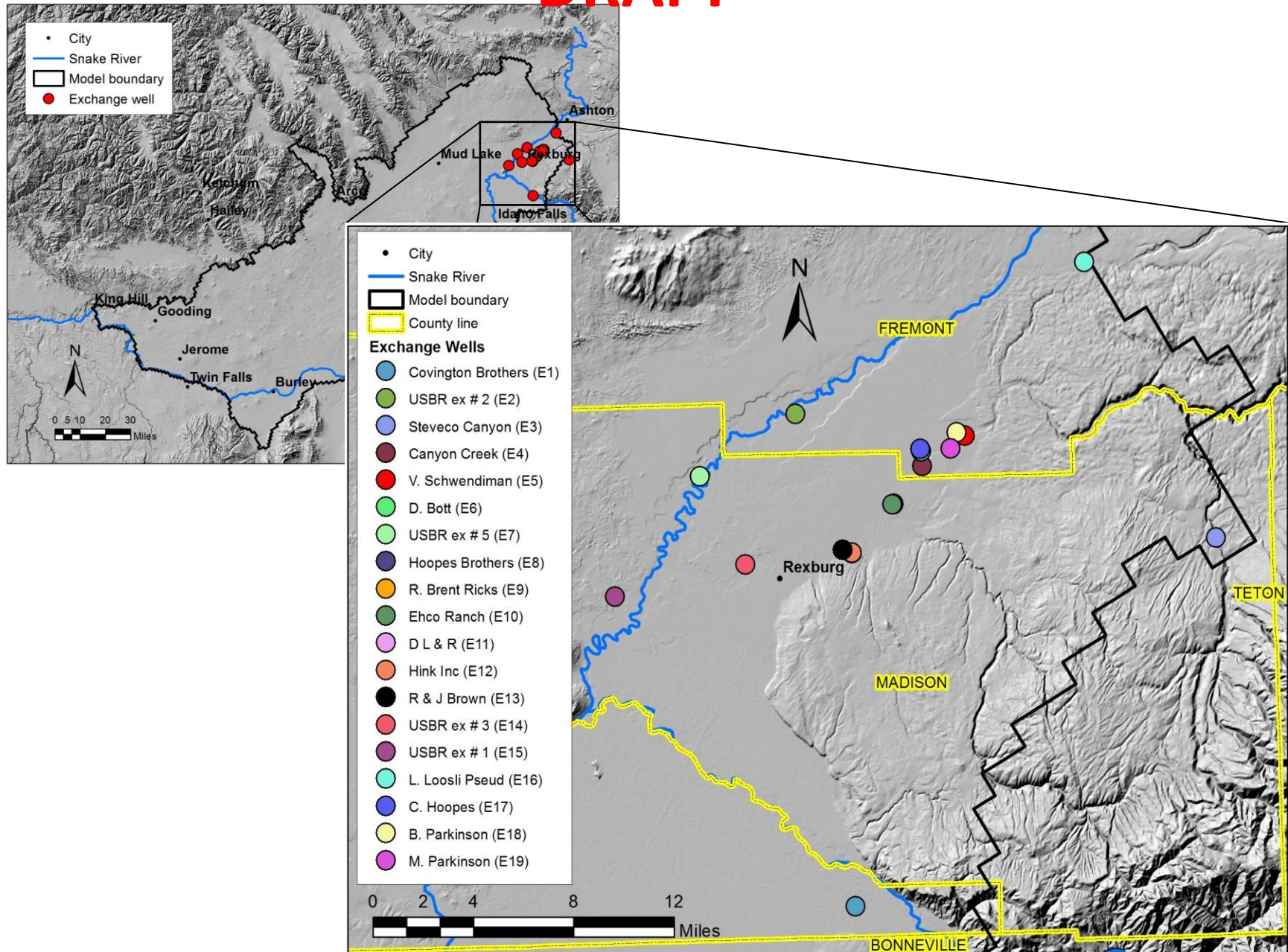


Figure 37. Teton and Snake River exchange wells.

DRAFT

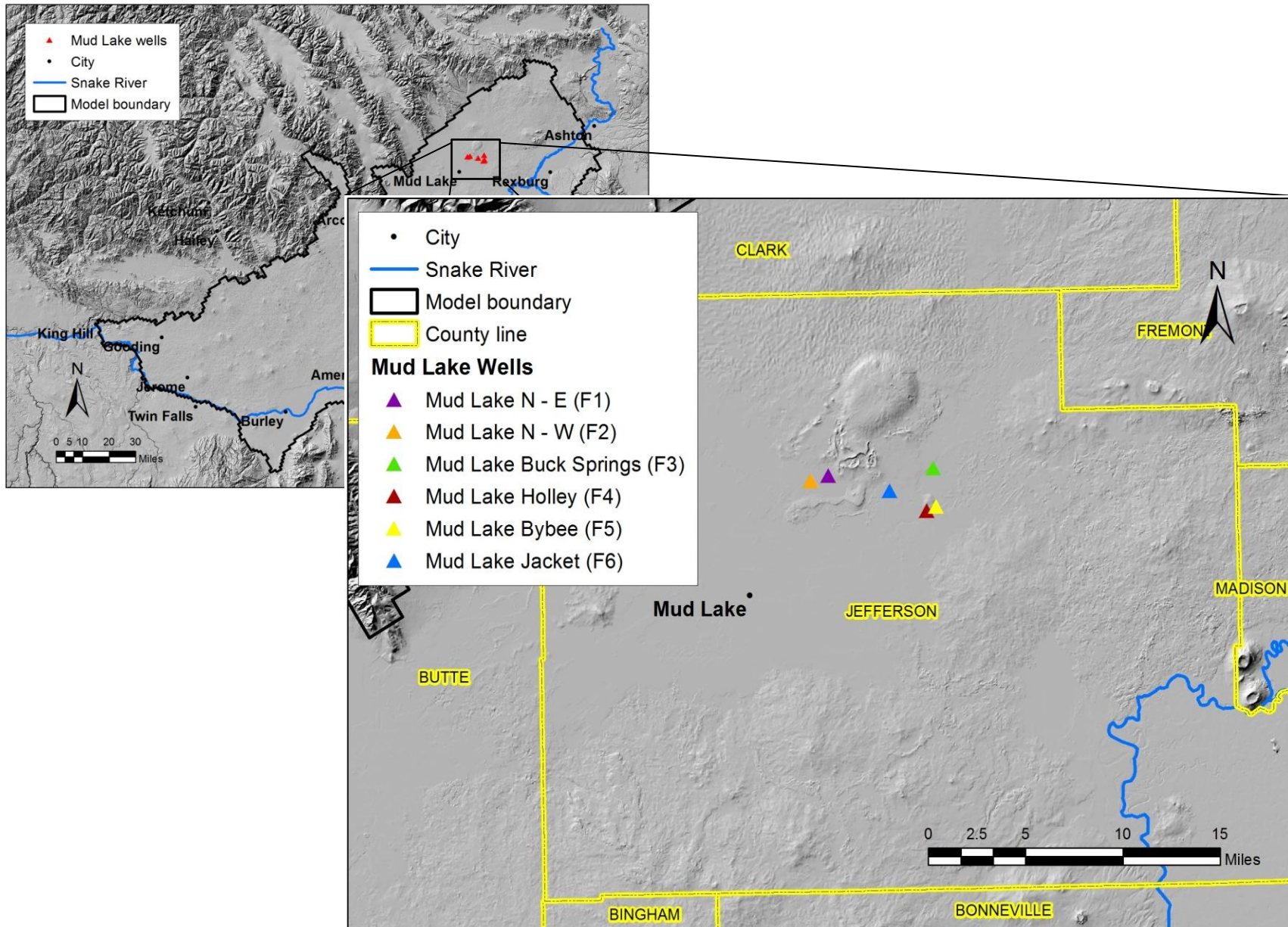


Figure 38. Mud Lake area exchange well groups.

DRAFT

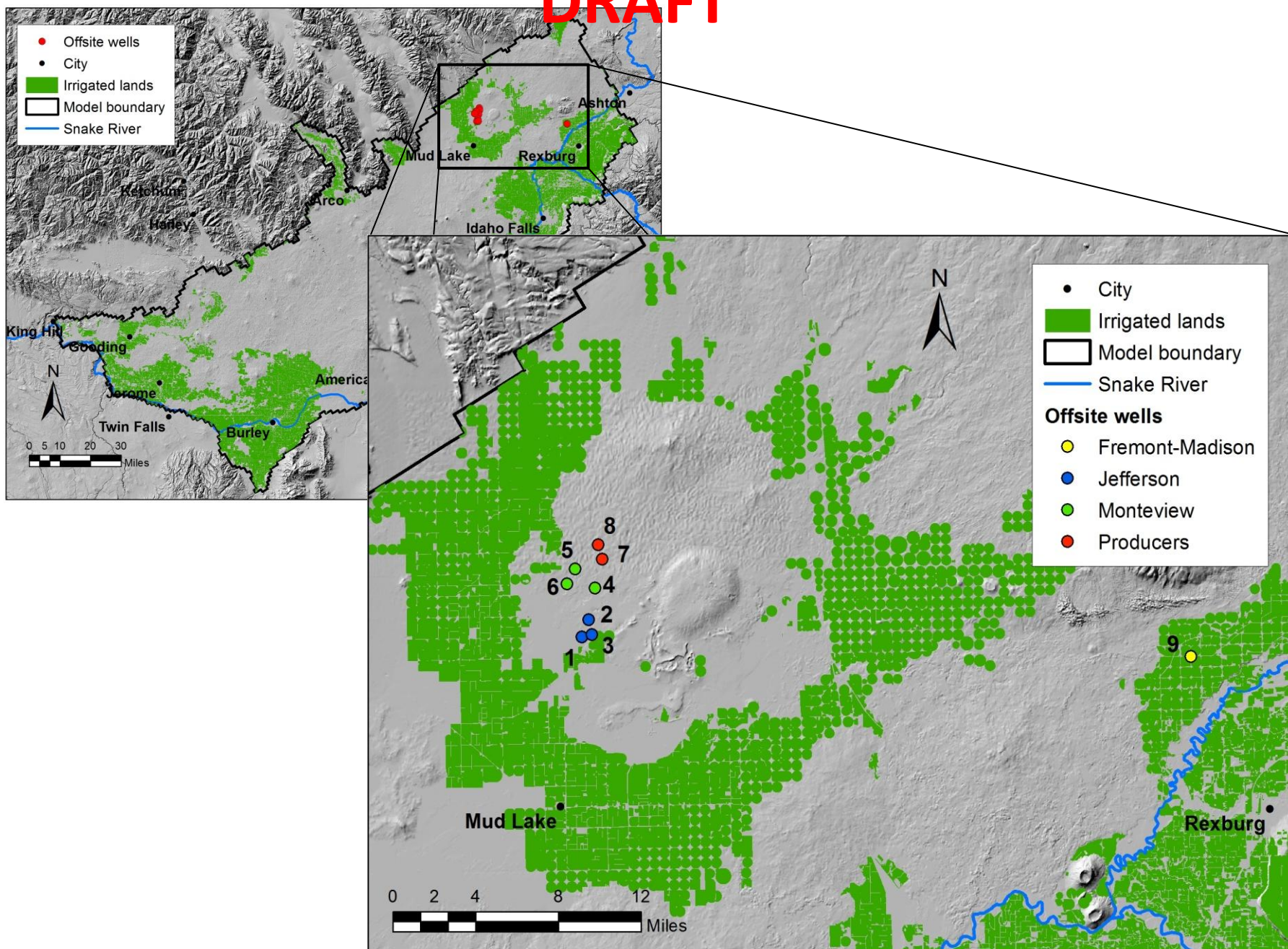


Figure 39. Offsite pumping locations.

DRAFT

Figure 40a – 40d. Time series of fixed point pumping volumes for exchange wells. See 11x17 Figures.

DRAFT

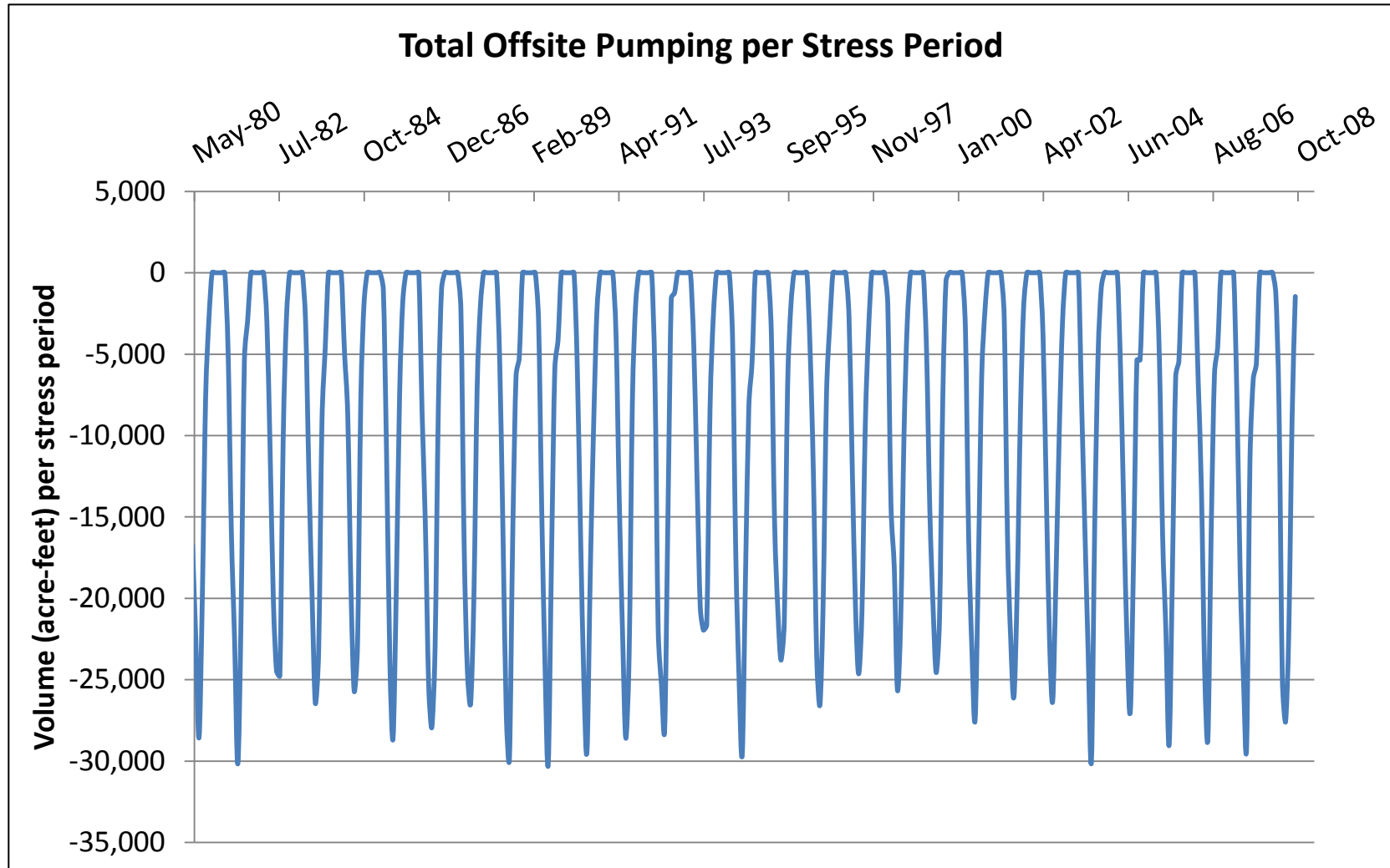


Figure 41. Time series of total offsite pumping in the eastern Snake River Plain aquifer.

DRAFT

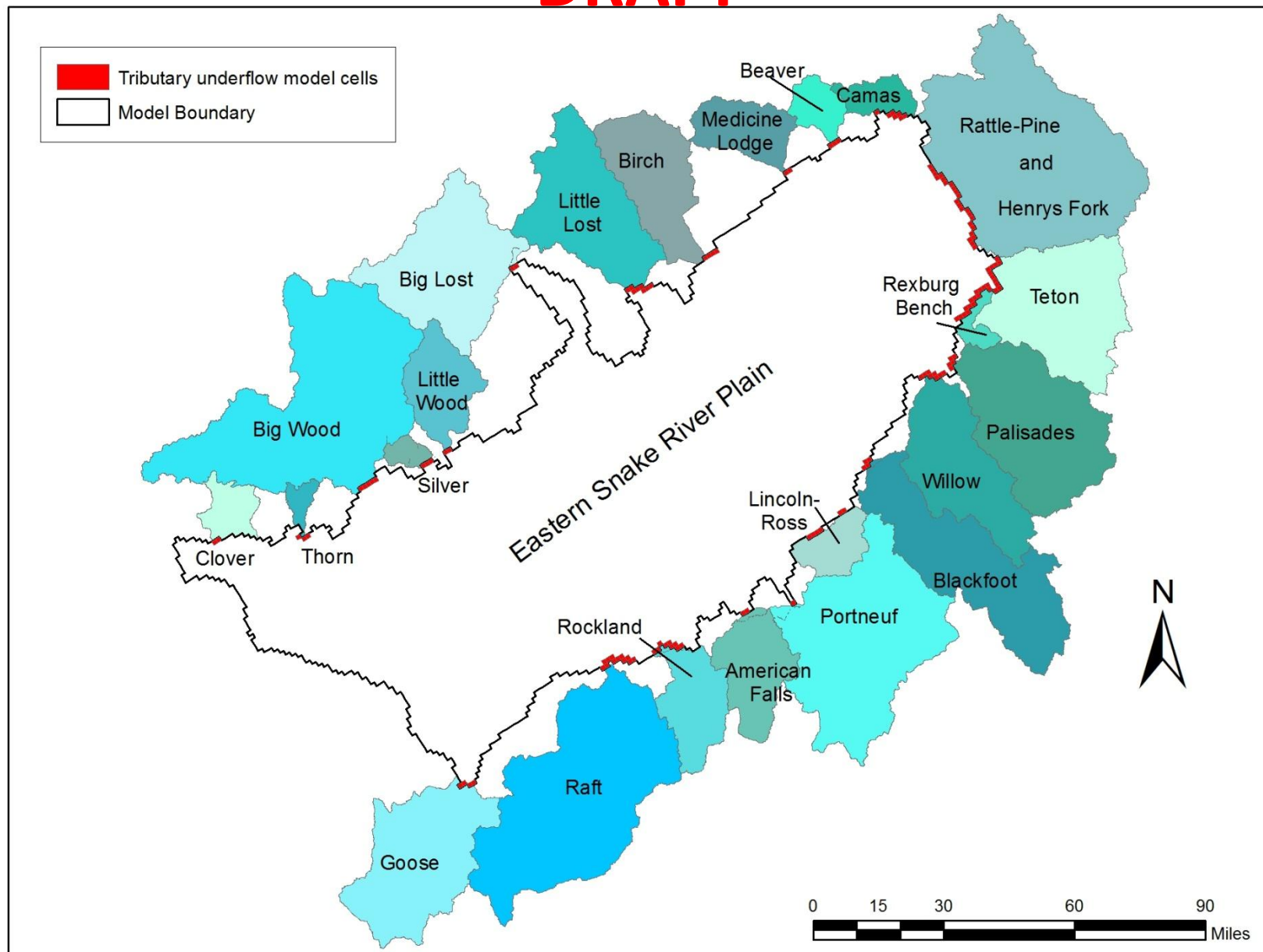


Figure 42. Tributary underflow basins and model cells.

DRAFT

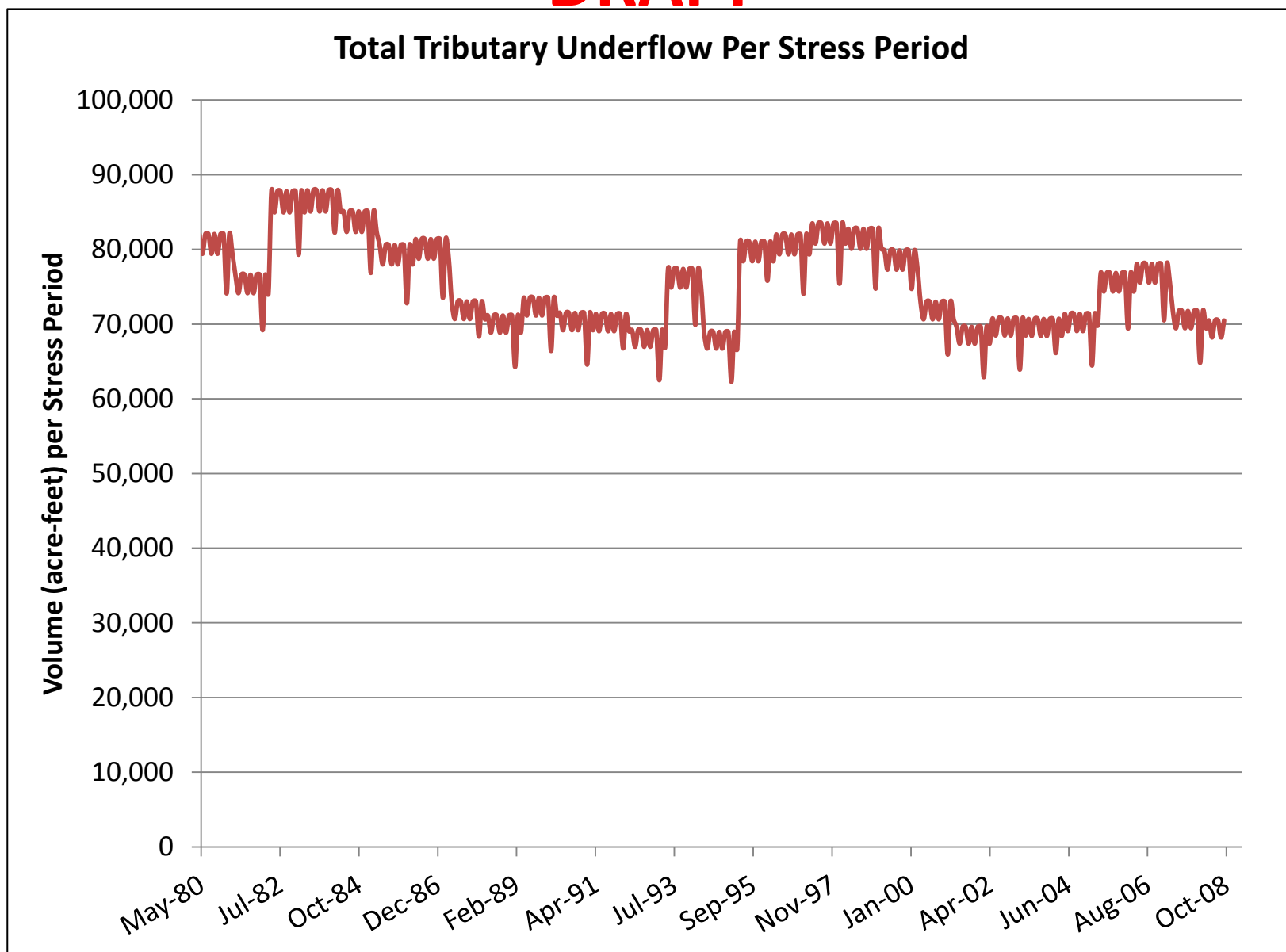


Figure 43. Pre-PEST tributary underflow volume over the calibration period 1980-2008.

DRAFT

Figure 44a – 44f. Pre-PEST tributary underflow in volume (acre-feet) in individual tributary basins.
See 11x17 Figures.

DRAFT

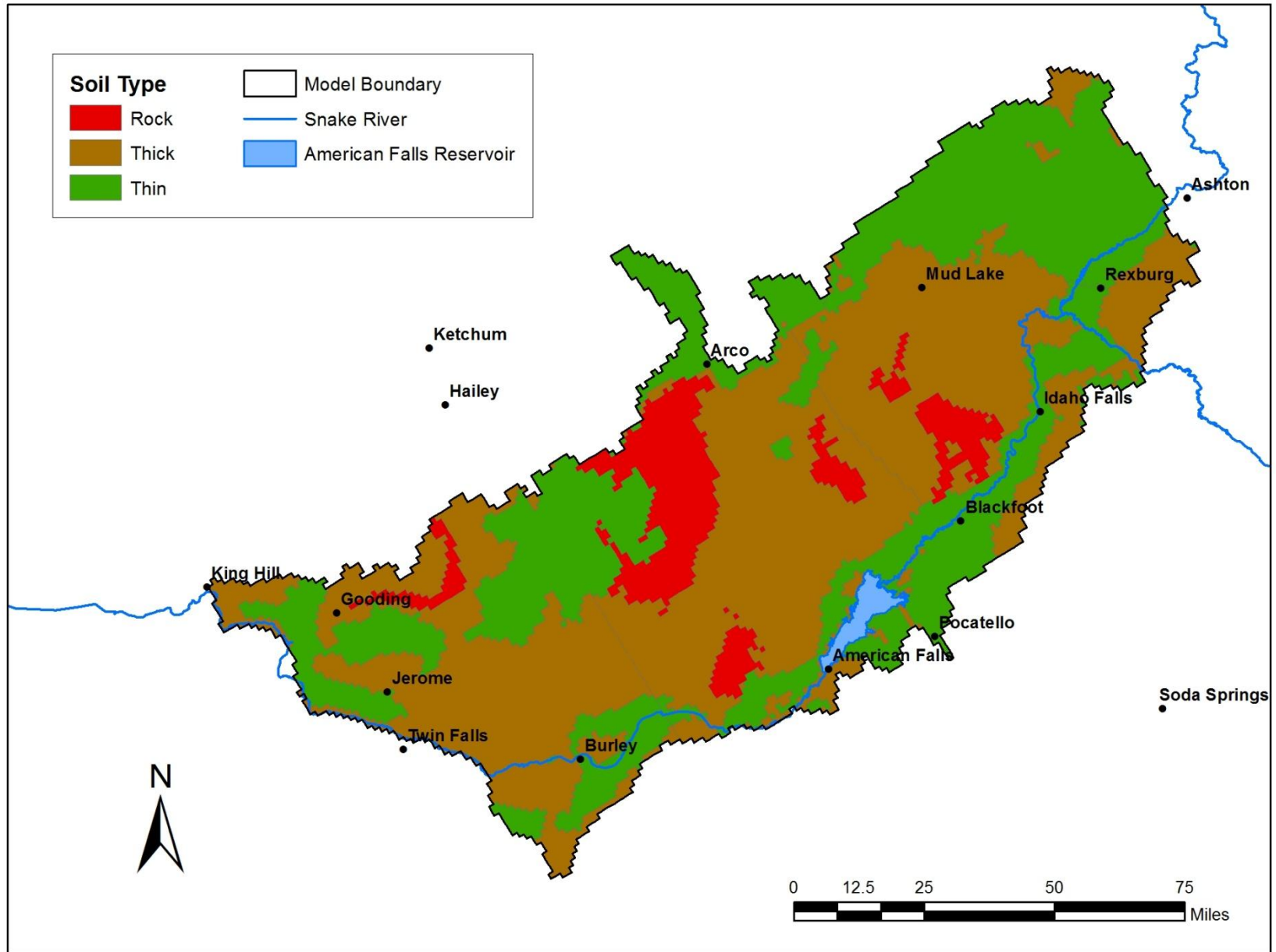


Figure 45. Generalized soil type.

DRAFT

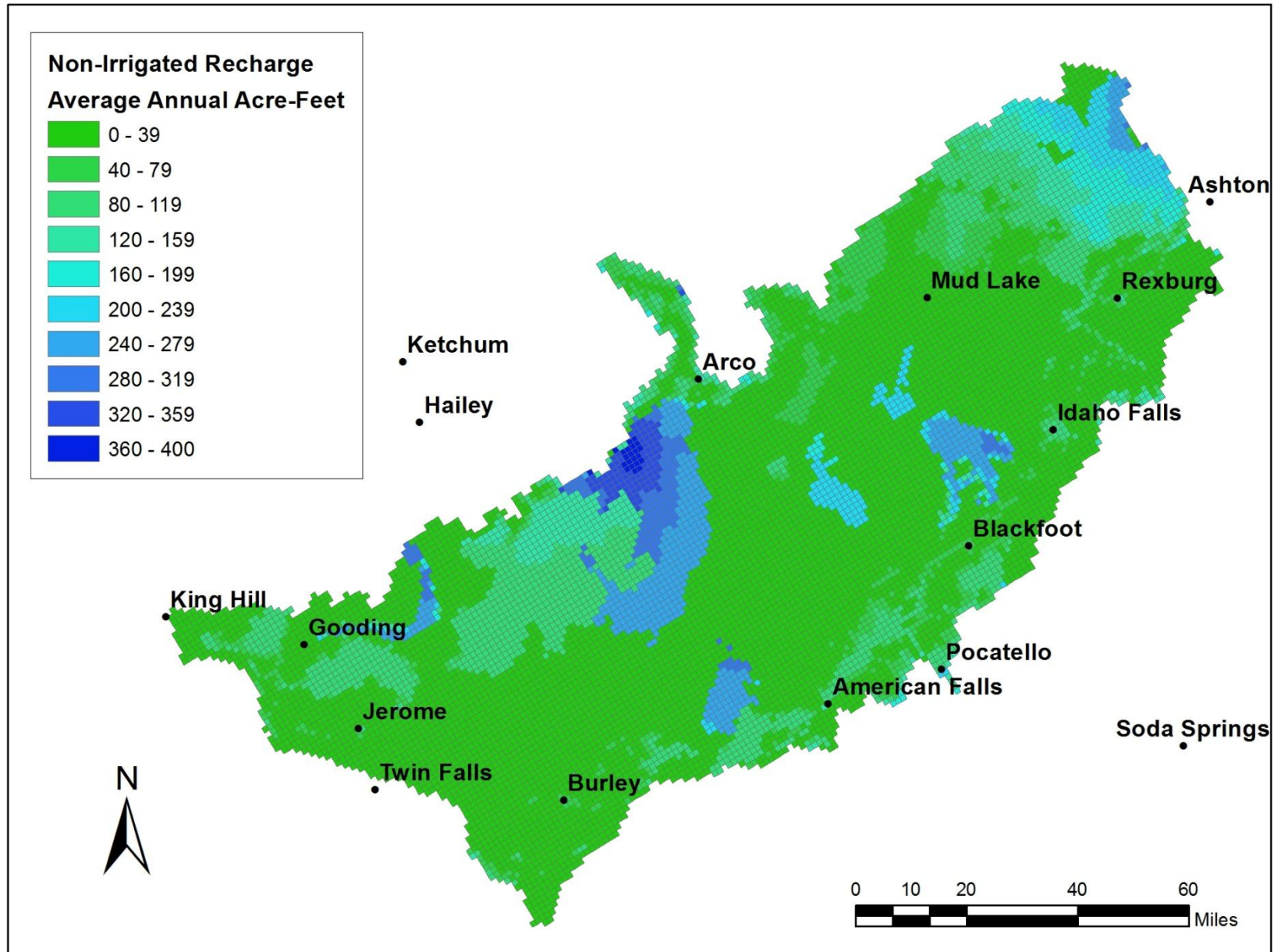


Figure 46. Spatial distribution of pre-PEST non-irrigated recharge averaged for water years 1981-2008.

DRAFT

Figure 47a-47d. Time series of Pre-PEST non-irrigated recharge. See 11x17 figures.

DRAFT

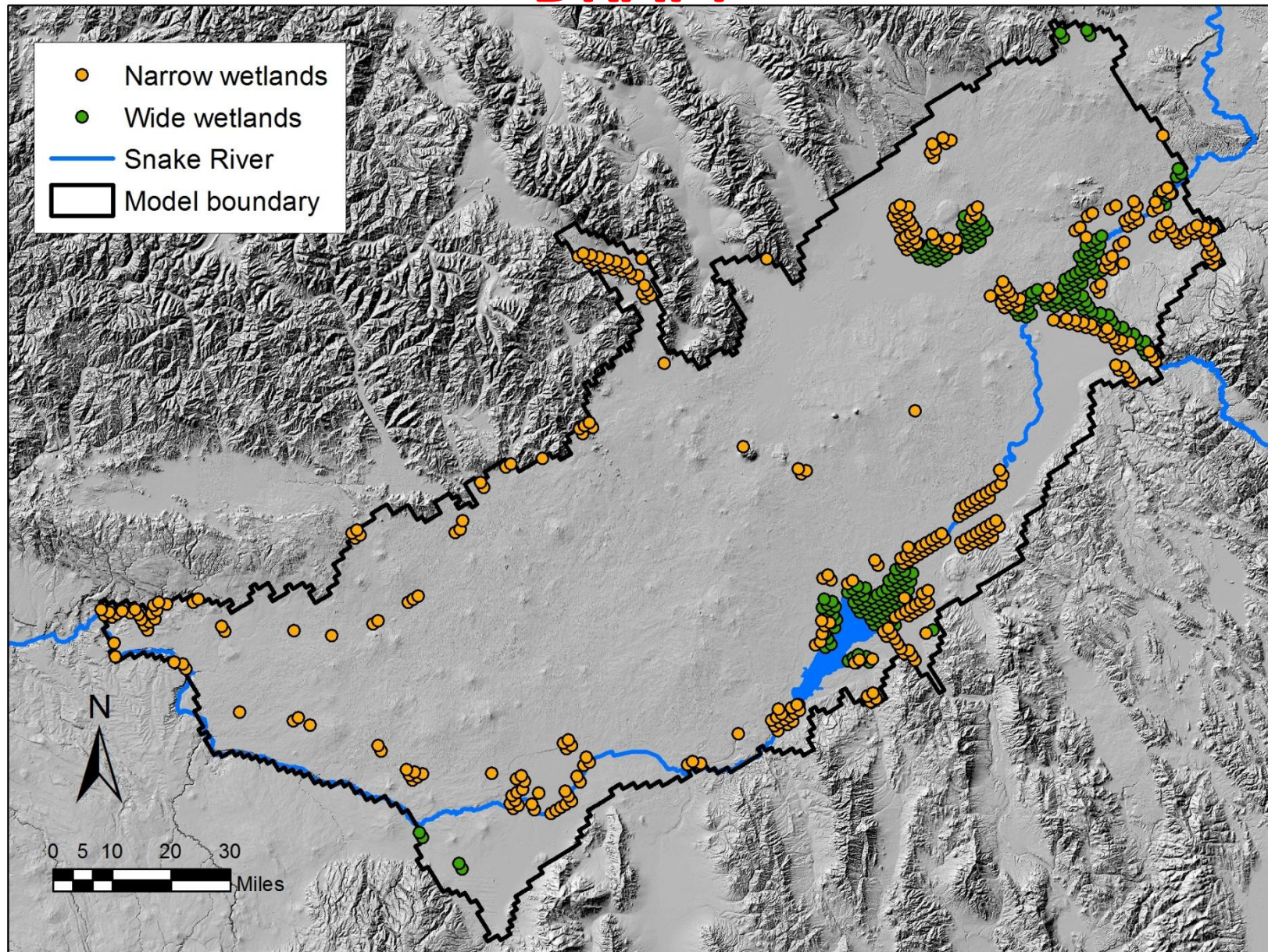


Figure 48. Locations of wetlands represented in the fixed point extraction dataset.

DRAFT

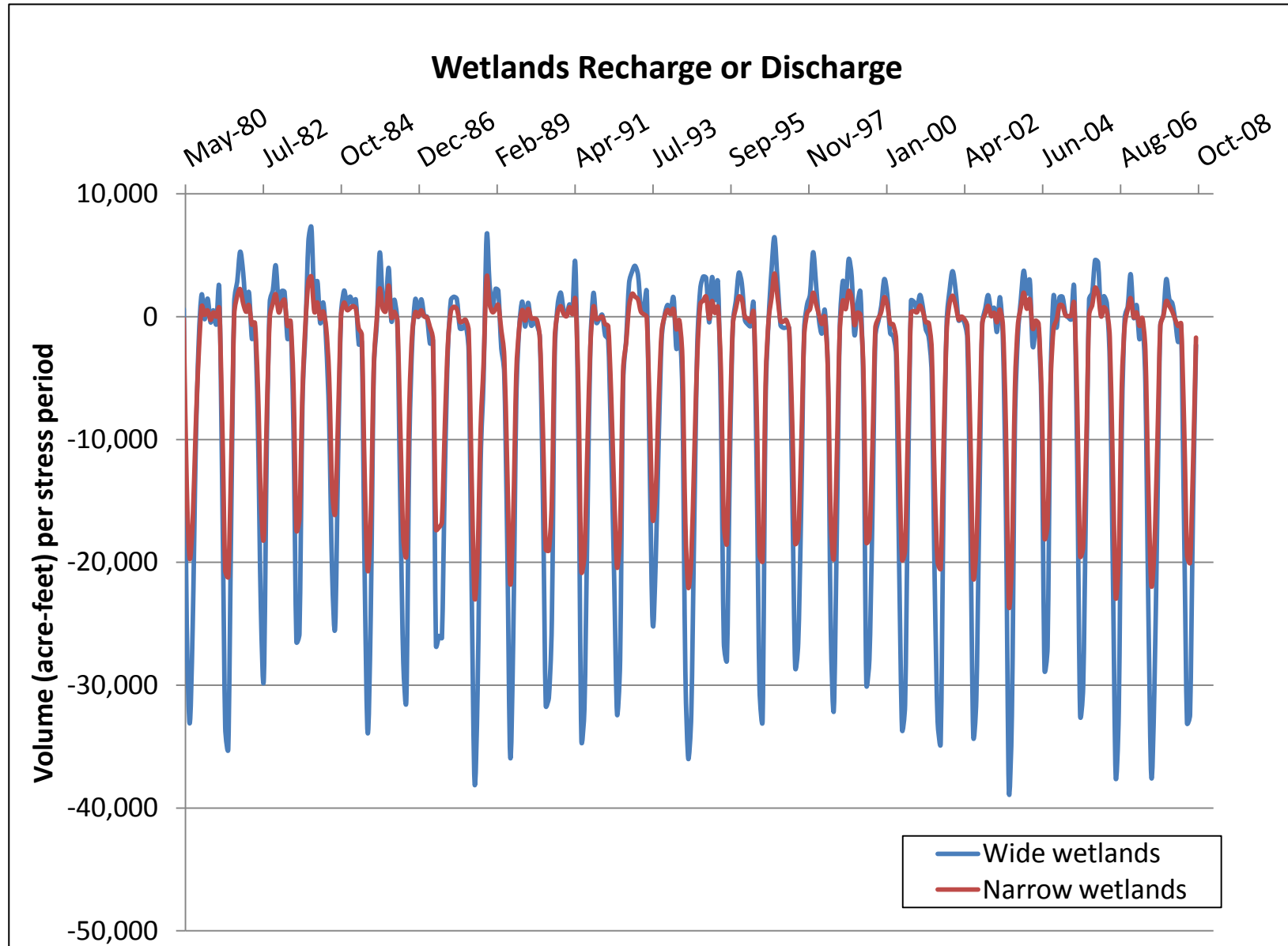


Figure 49. Time series of pre-PEST recharge or discharge from wetlands (wide and narrow). Recharge is indicated by negative values and discharge is indicated by positive values.

DRAFT

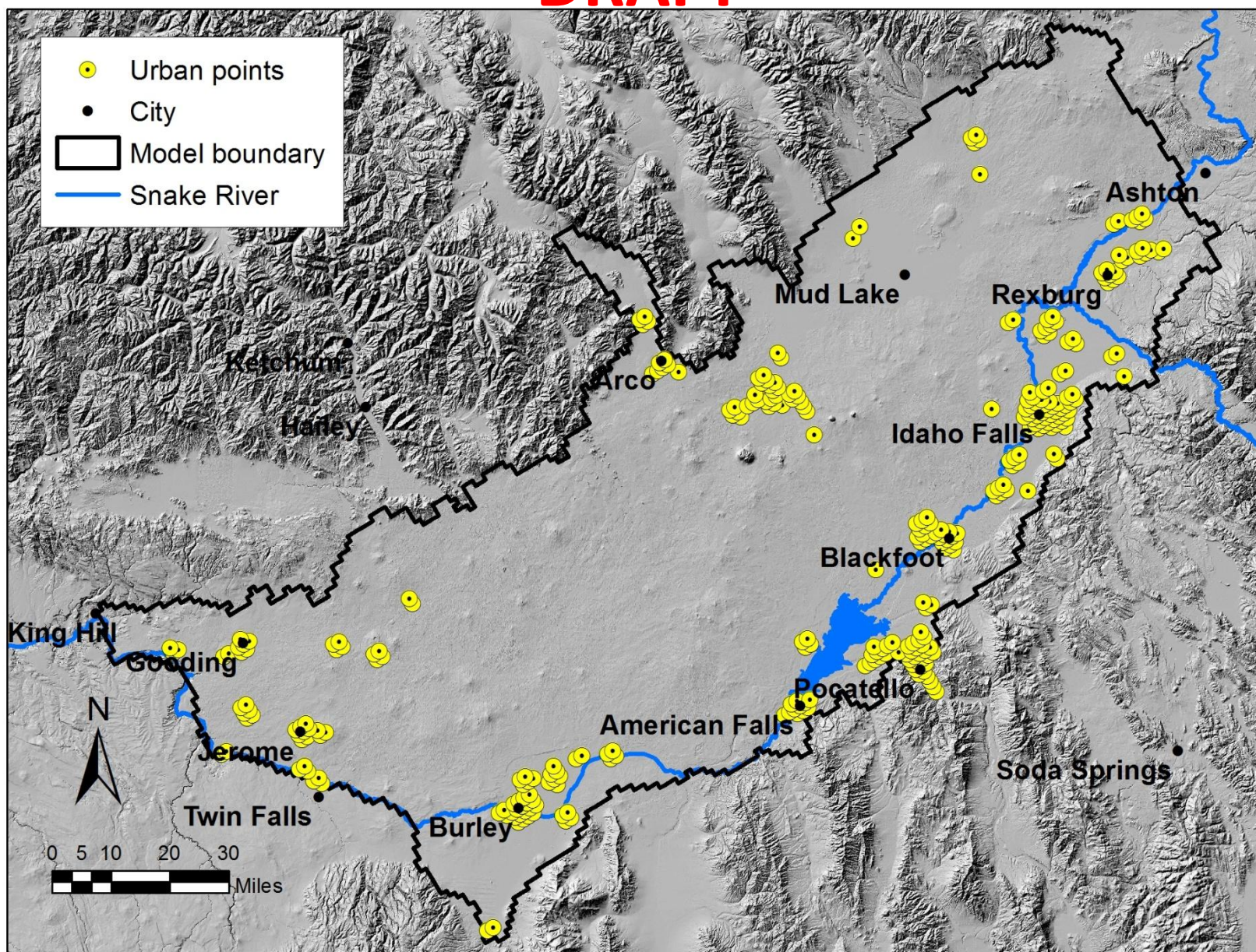


Figure 50. Locations of urban extraction points represented in fixed point extraction dataset.

DRAFT

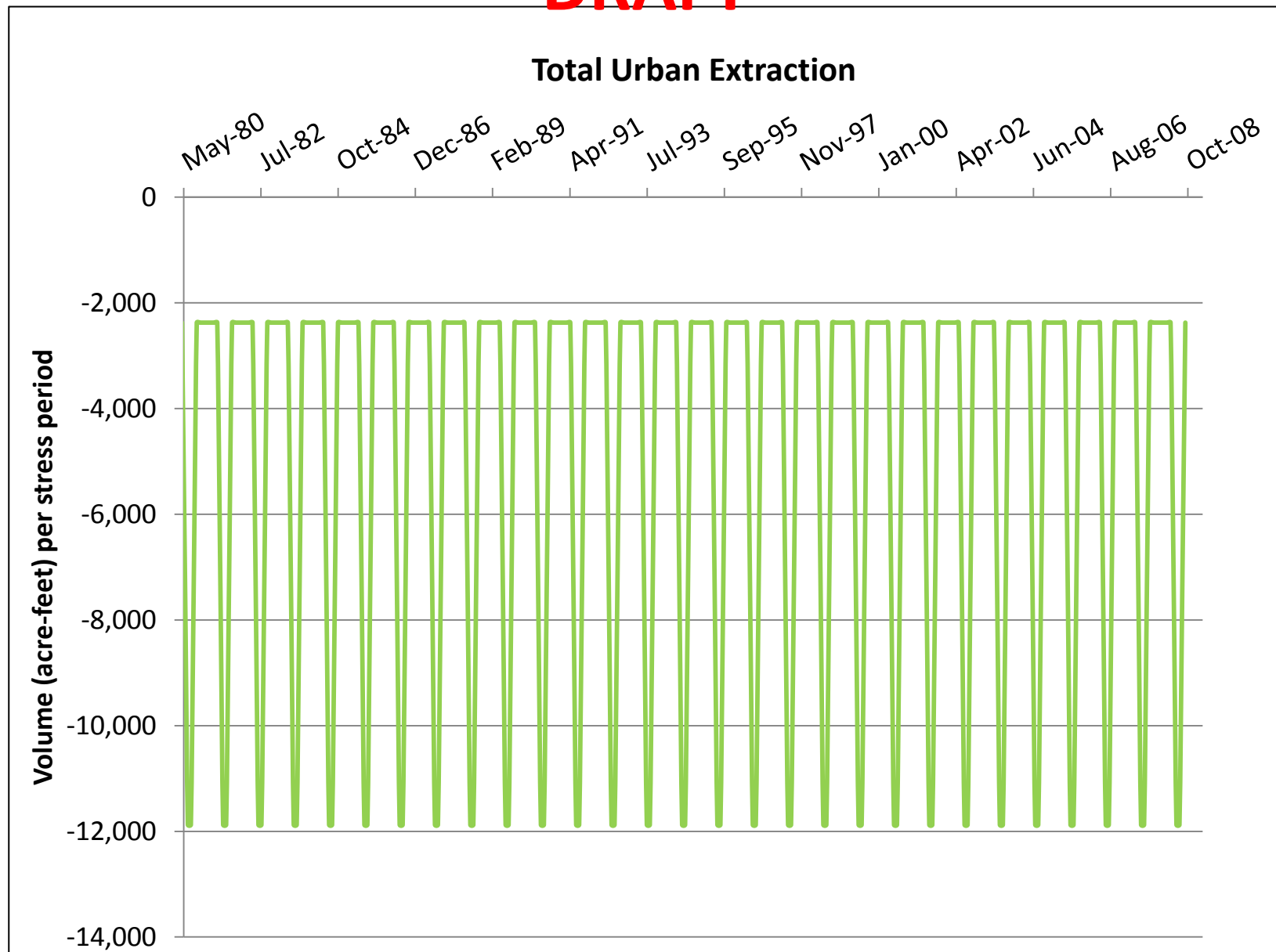


Figure 51. Time series of urban extraction.

DRAFT

Figure 52a – 52c. Non-Snake River sources of surface water seepage. See 11x17 figures.

DRAFT

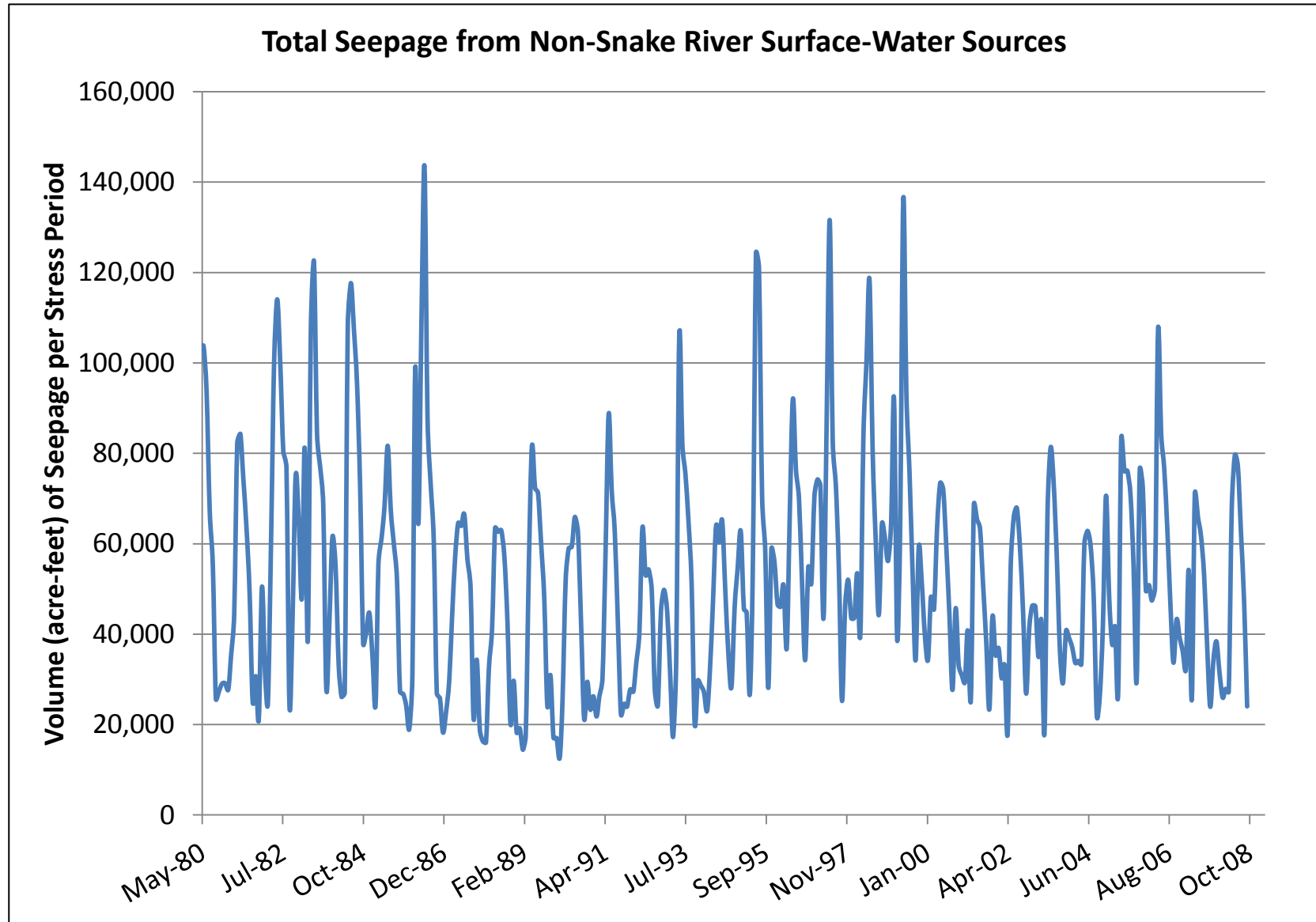


Figure 53. Total volume of seepage from non-Snake River surface-water sources.

DRAFT

Figure 54a – 54d. Pre-PEST volume of seepage per stress period from
non-Snake River surface-water sources.
See 11x17 figures.

DRAFT

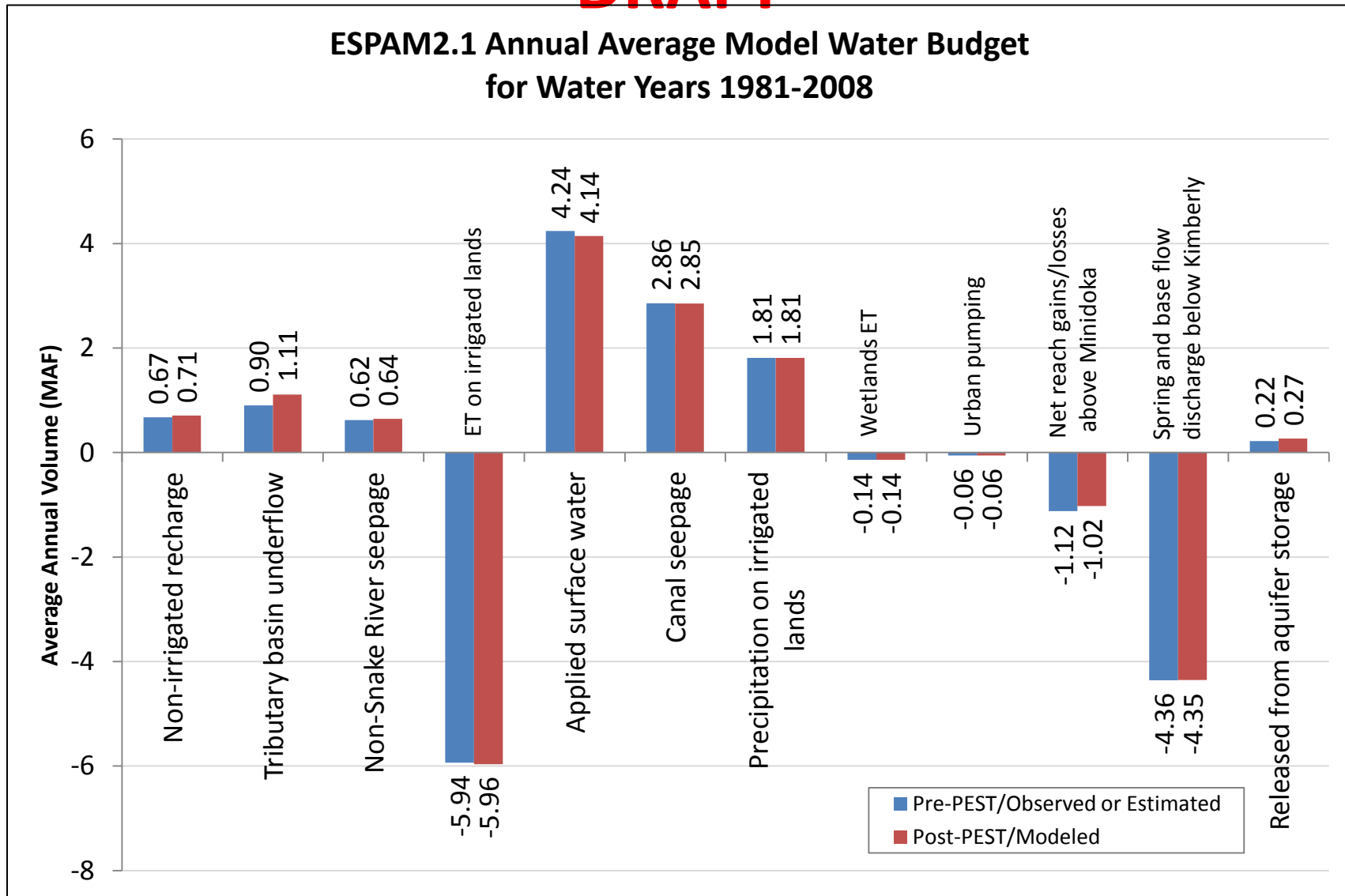


Figure 55. Enhanced Snake Plain Aquifer Model 2.1 average annual model water budget. Positive values of aquifer storage represent water released from storage into the aquifer flow system. Negative values of aquifer storage represent water placed into storage. Applied surface water is defined as (*Agricultural diversions – canal seepage – returns – offsite, exchange, and Mud Lake pumping*). Precipitation on agricultural lands and urban pumping were not adjustable during model calibration.

DRAFT

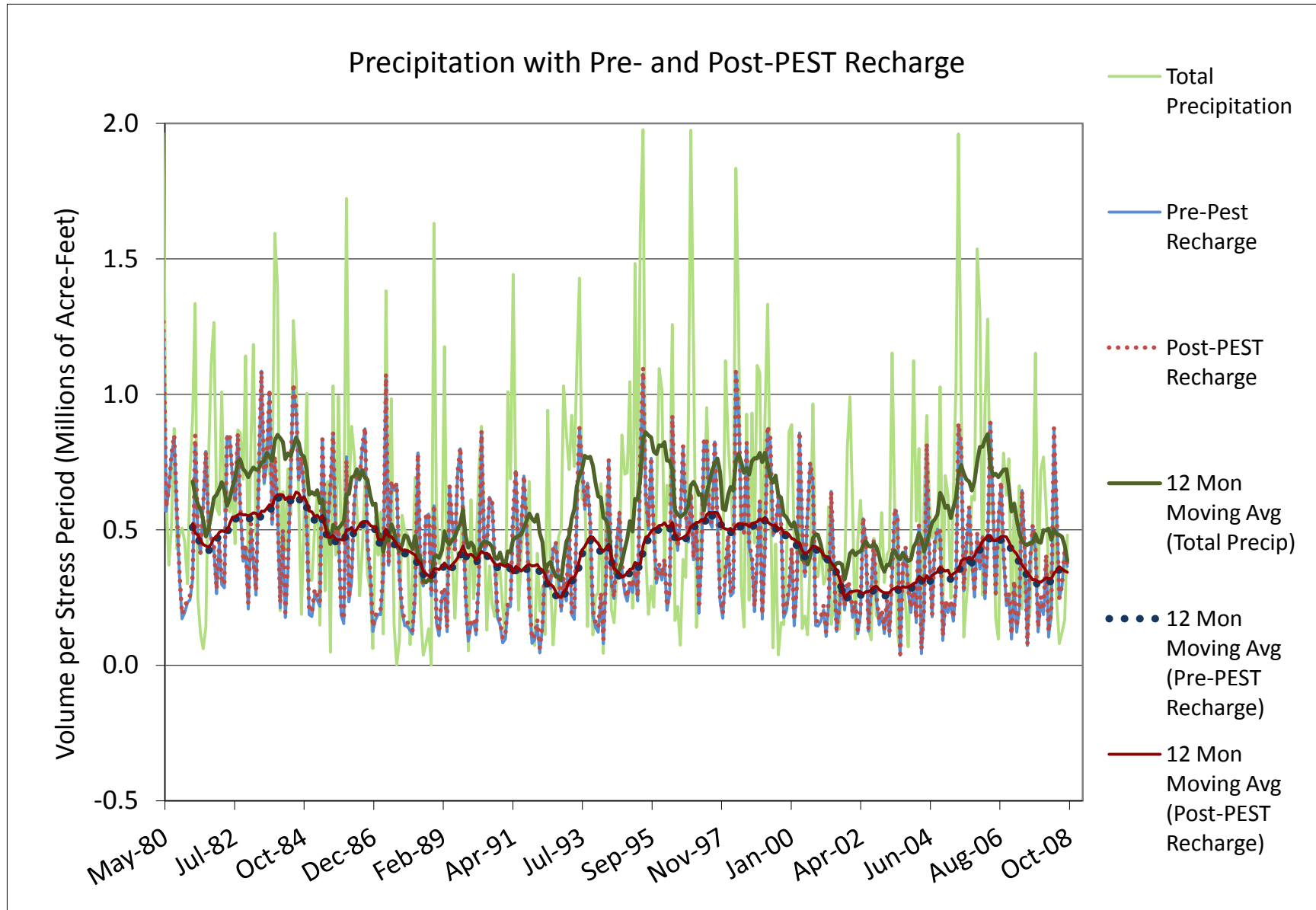


Figure 56. Pre-PEST and Post-PEST net recharge plotted over time in comparison with total precipitation for the transient ESPAM model.

DRAFT

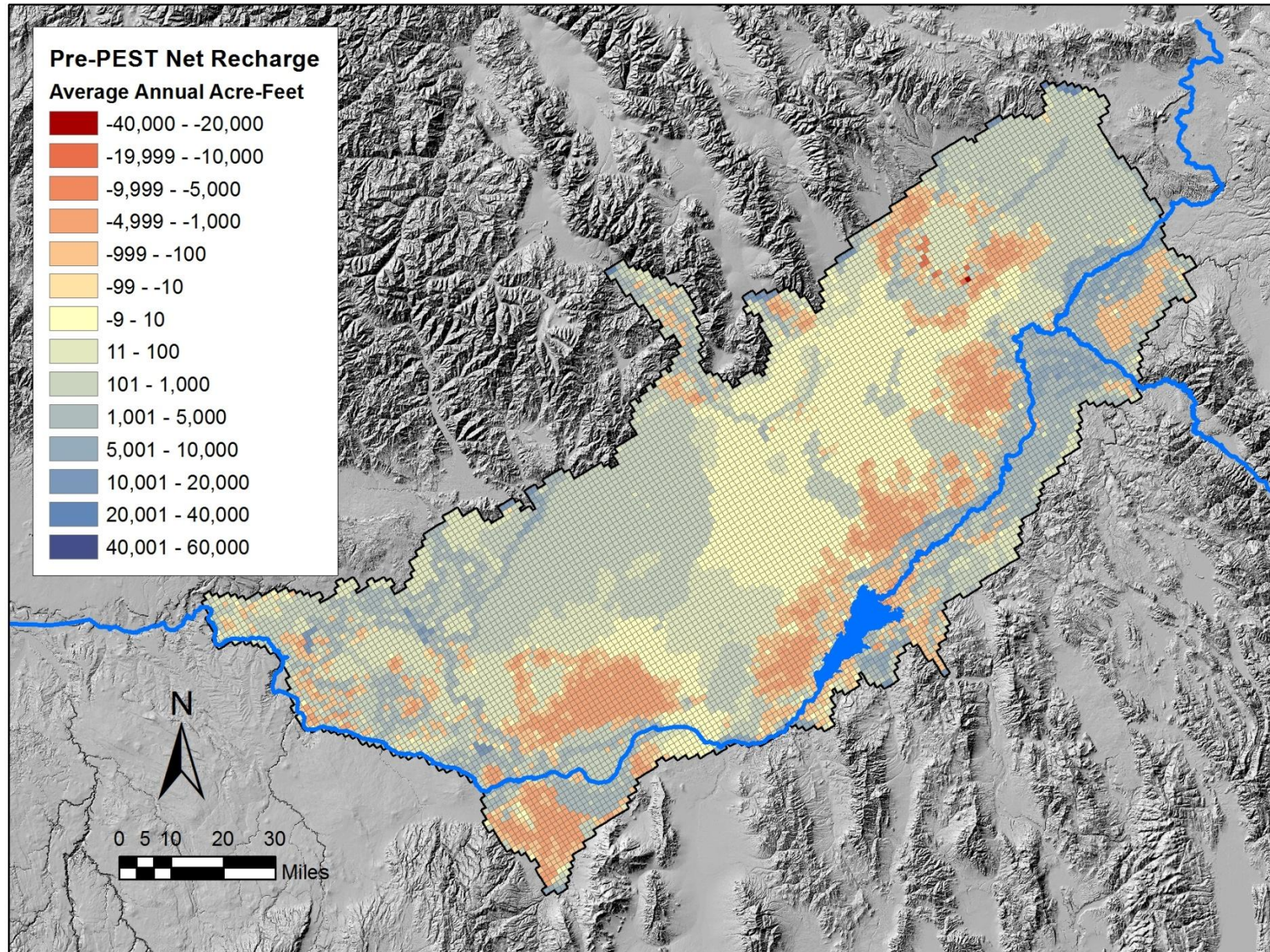


Figure 57. Pre-PEST areal distribution of net recharge (average annual water year values).

DRAFT

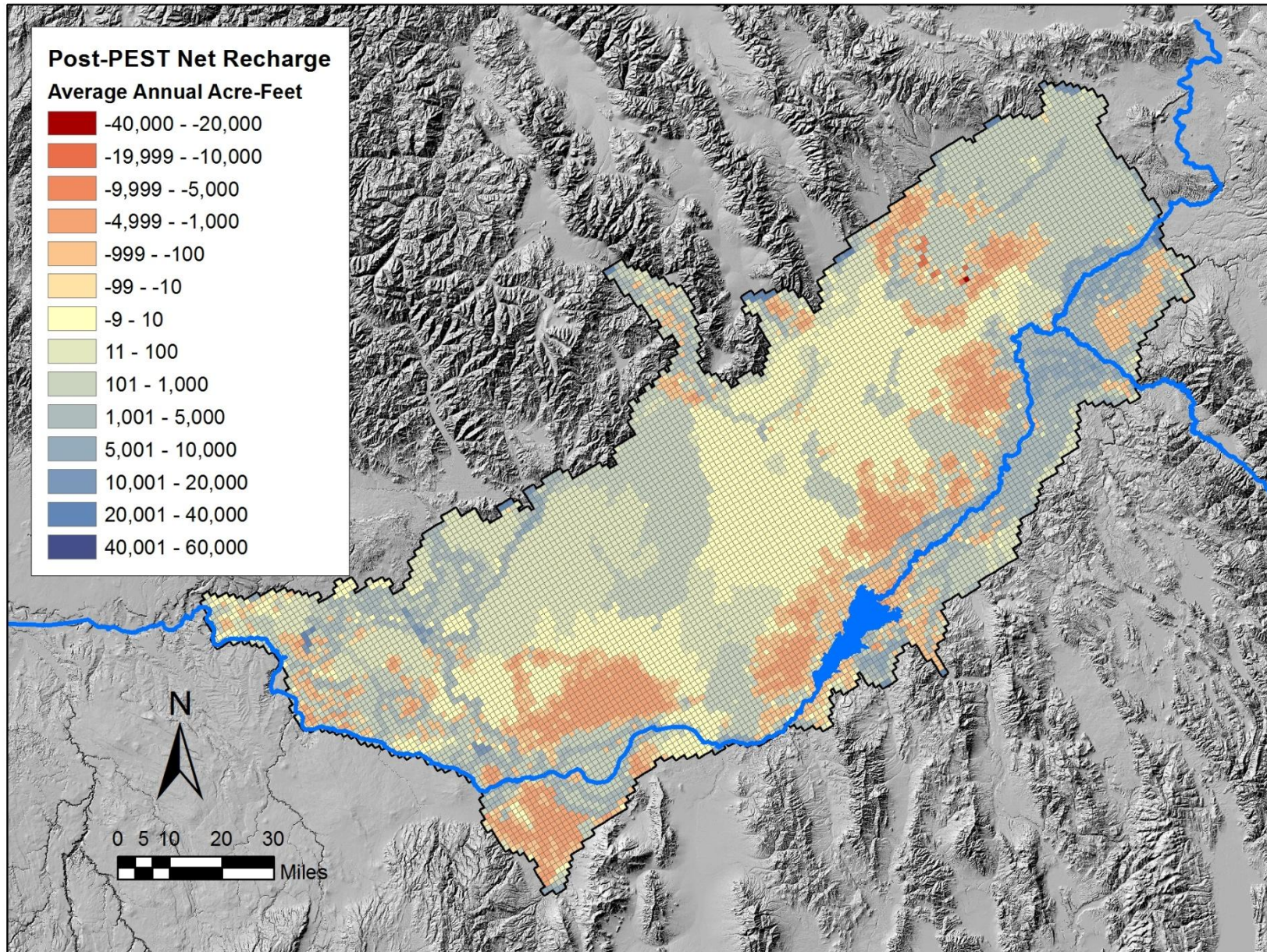


Figure 58. Post-PEST areal distribution of net recharge (average annual water year values).

DRAFT

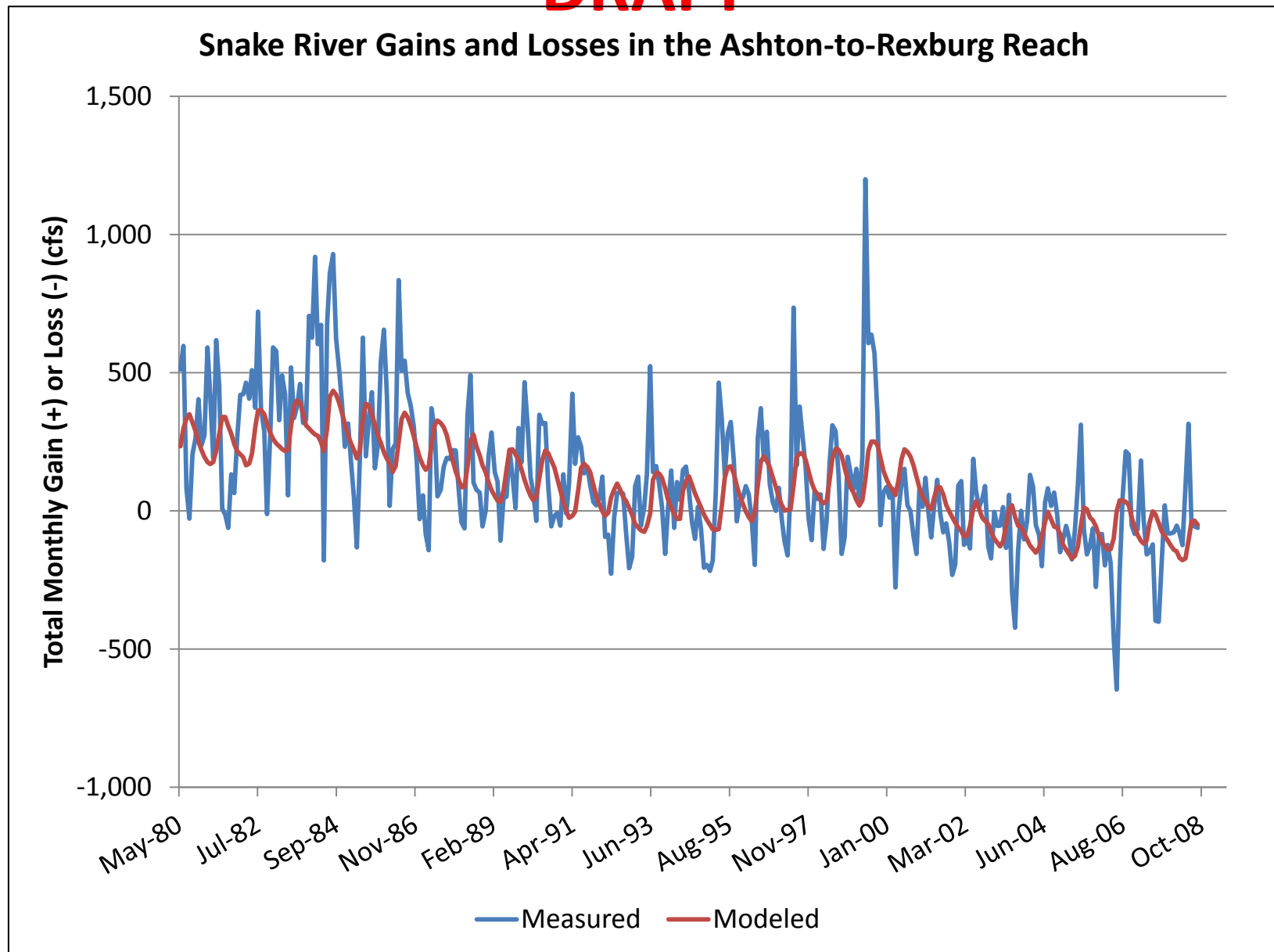


Figure 59. Monthly Snake River gains and losses in the Ashton-to-Rexburg reach.

DRAFT

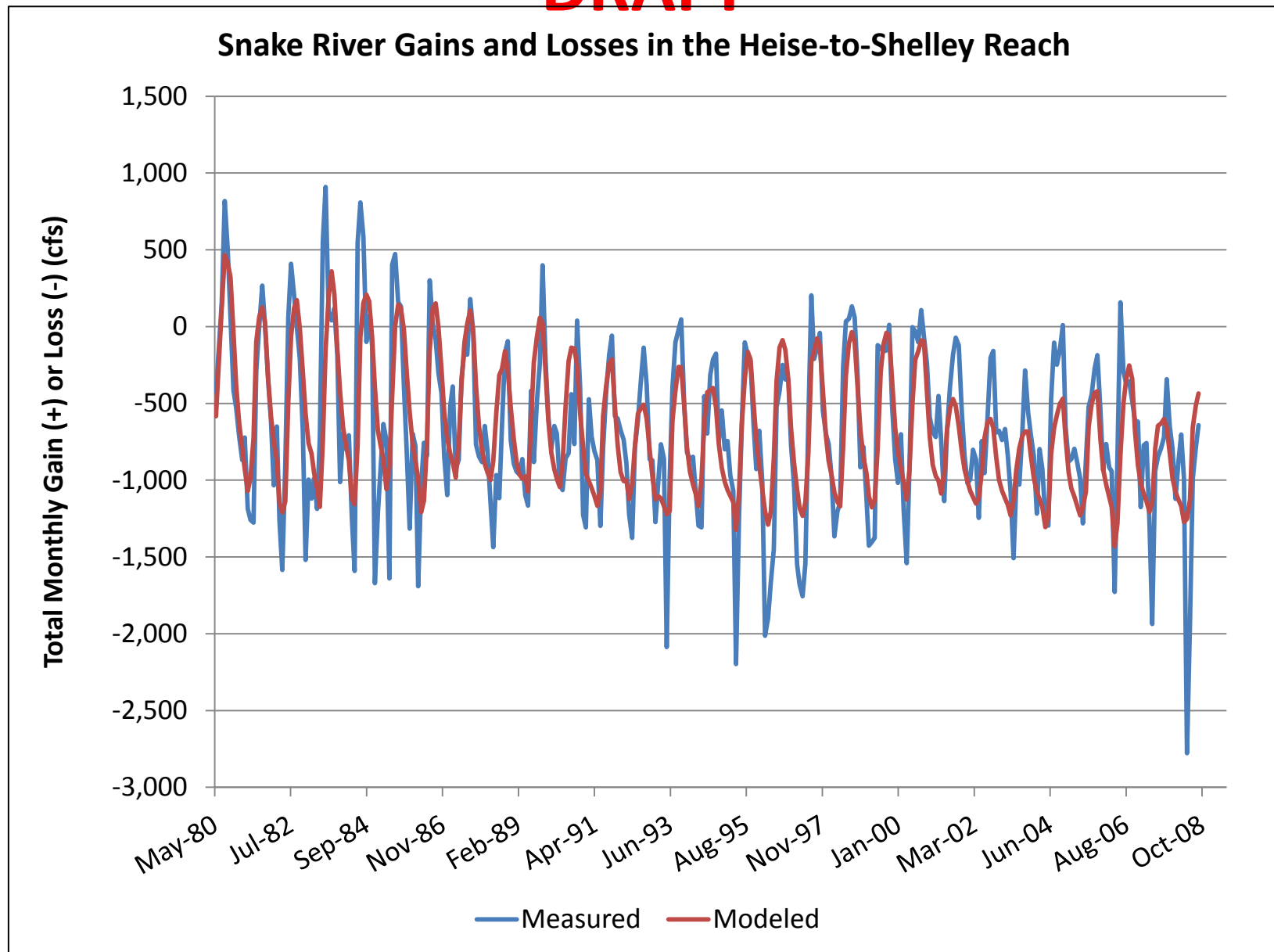


Figure 60. Monthly Snake River gains and losses in the Heise-to-Shelley reach.

DRAFT

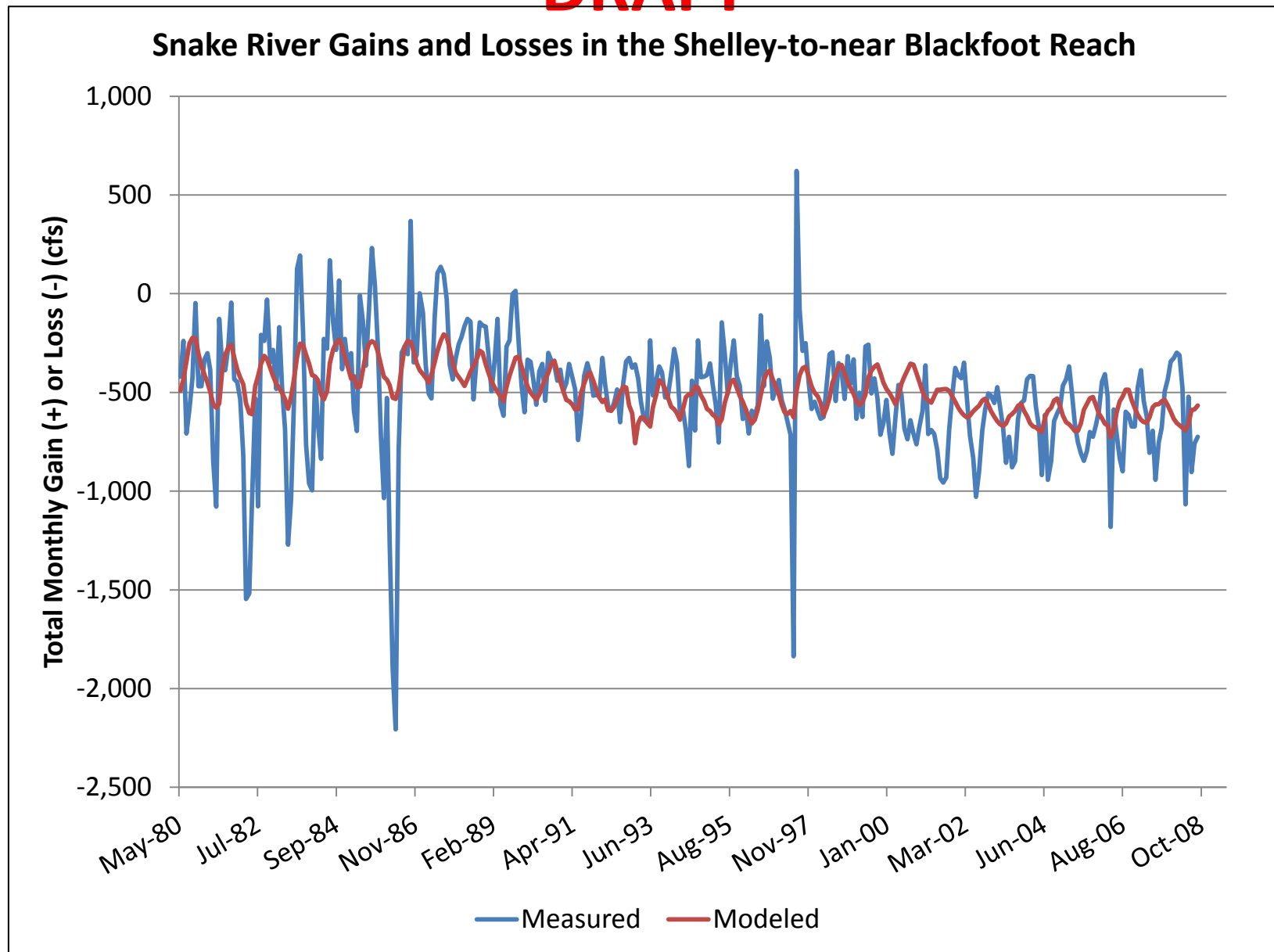


Figure 61. Monthly Snake River gains and losses in the Shelley-to-near Blackfoot reach.

DRAFT

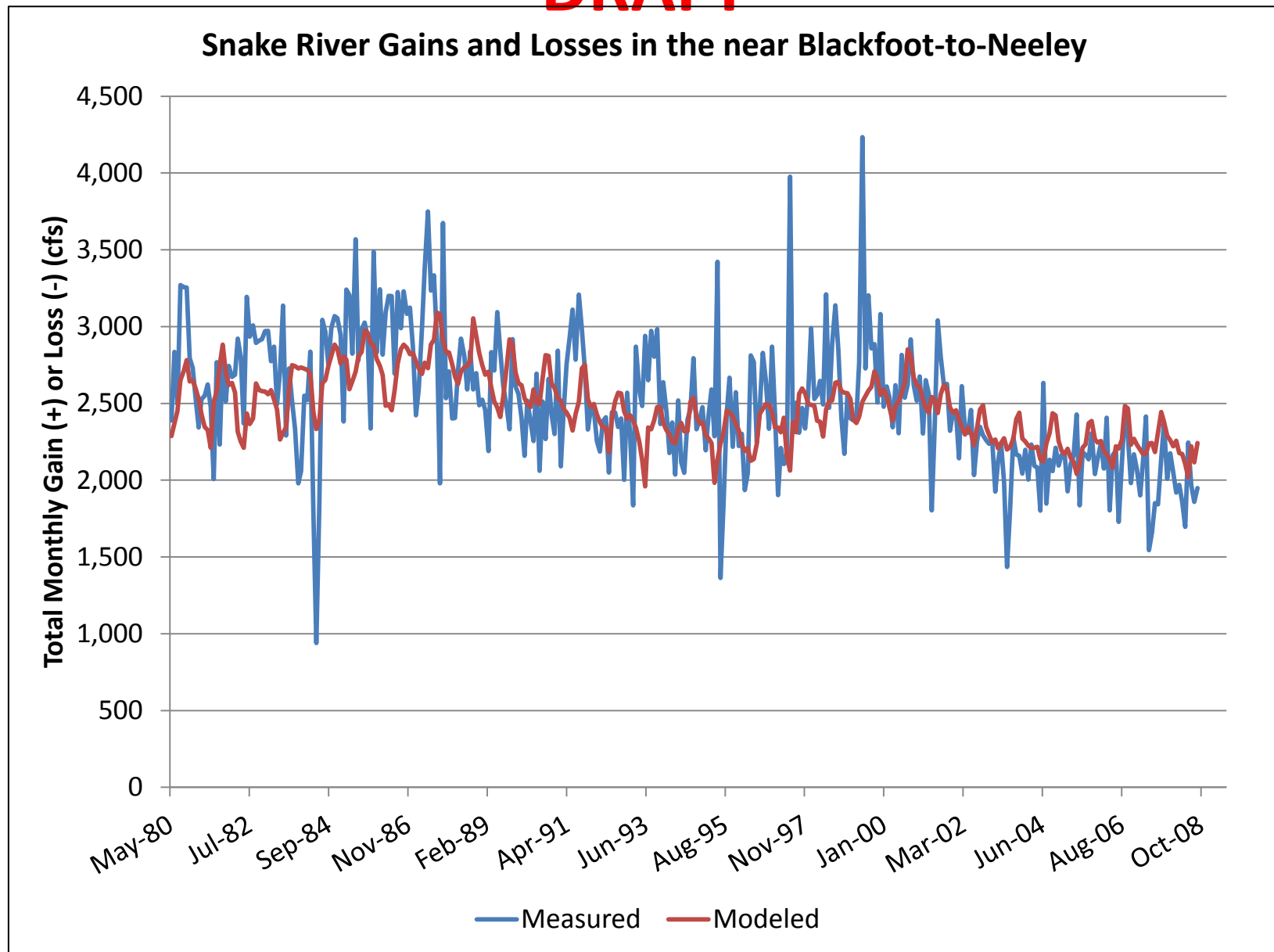


Figure 62. Monthly Snake River gains and losses in the near Blackfoot-to-Neeley reach.

DRAFT

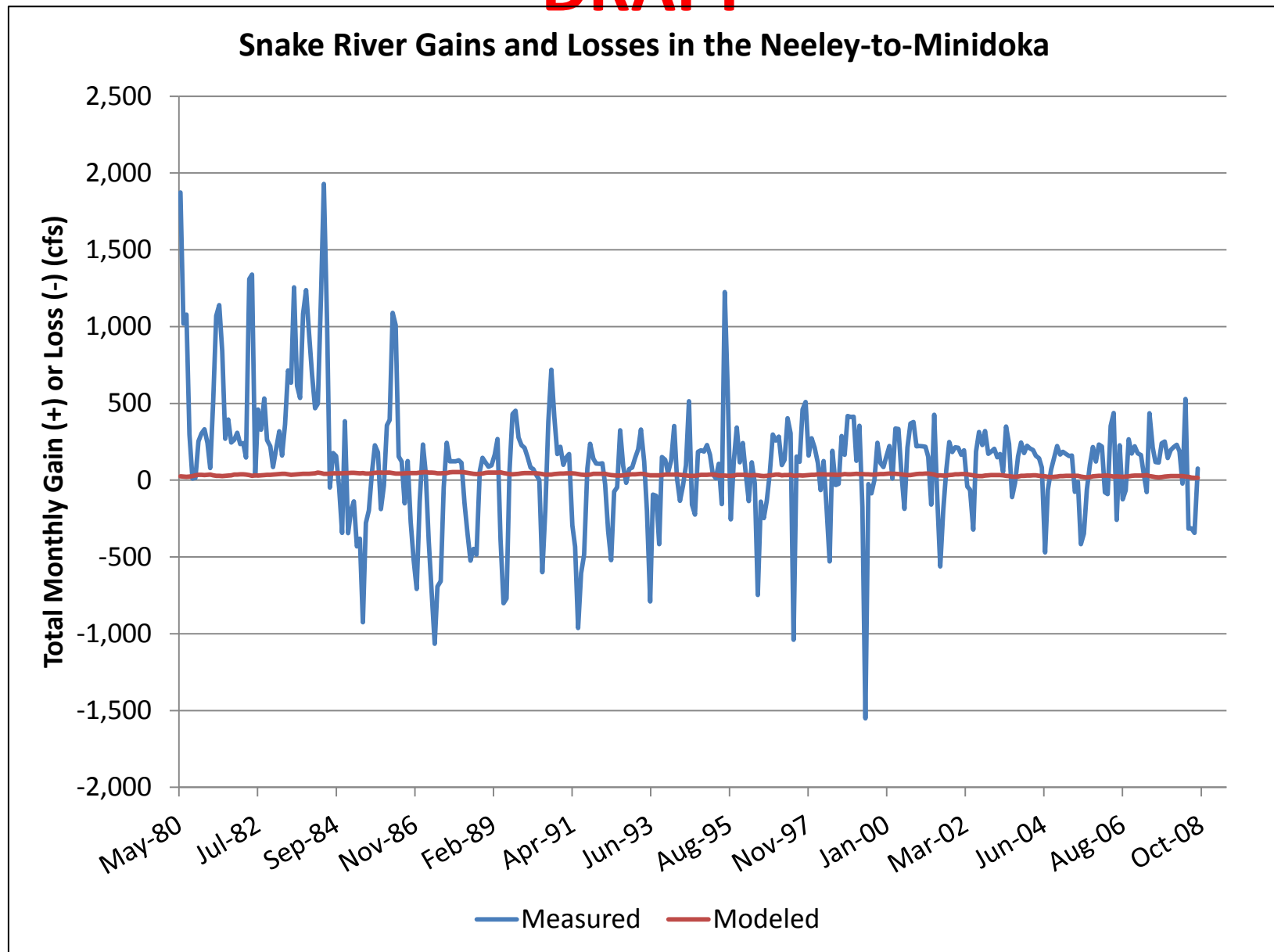


Figure 63. Monthly Snake River gains and losses in the Neeley-to-Minidoka reach.

DRAFT

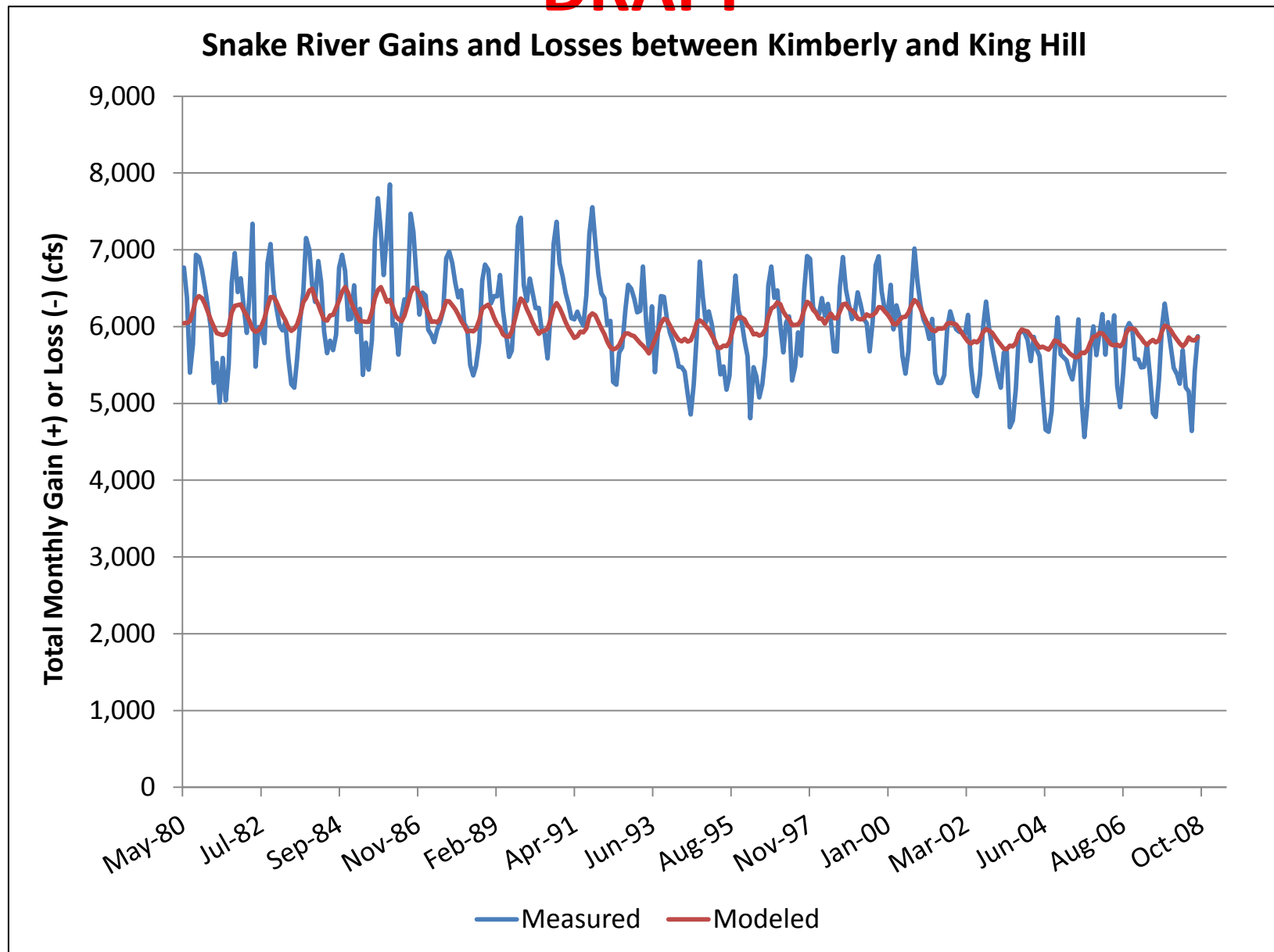


Figure 64. Monthly Snake River gains and losses between Kimberly and King Hill.

DRAFT

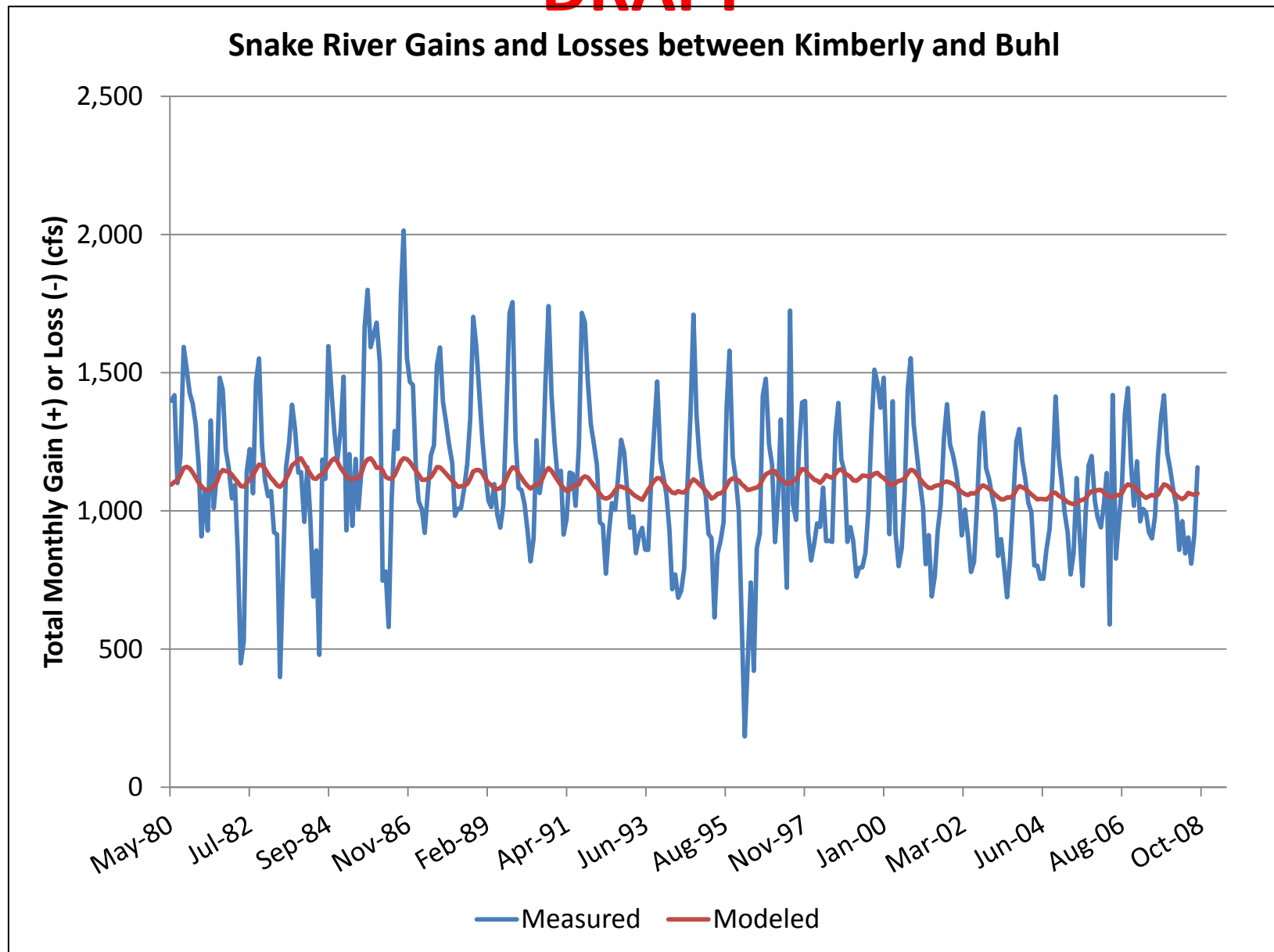


Figure 65. Monthly Snake River gains and losses between Kimberly and Buhl.

DRAFT

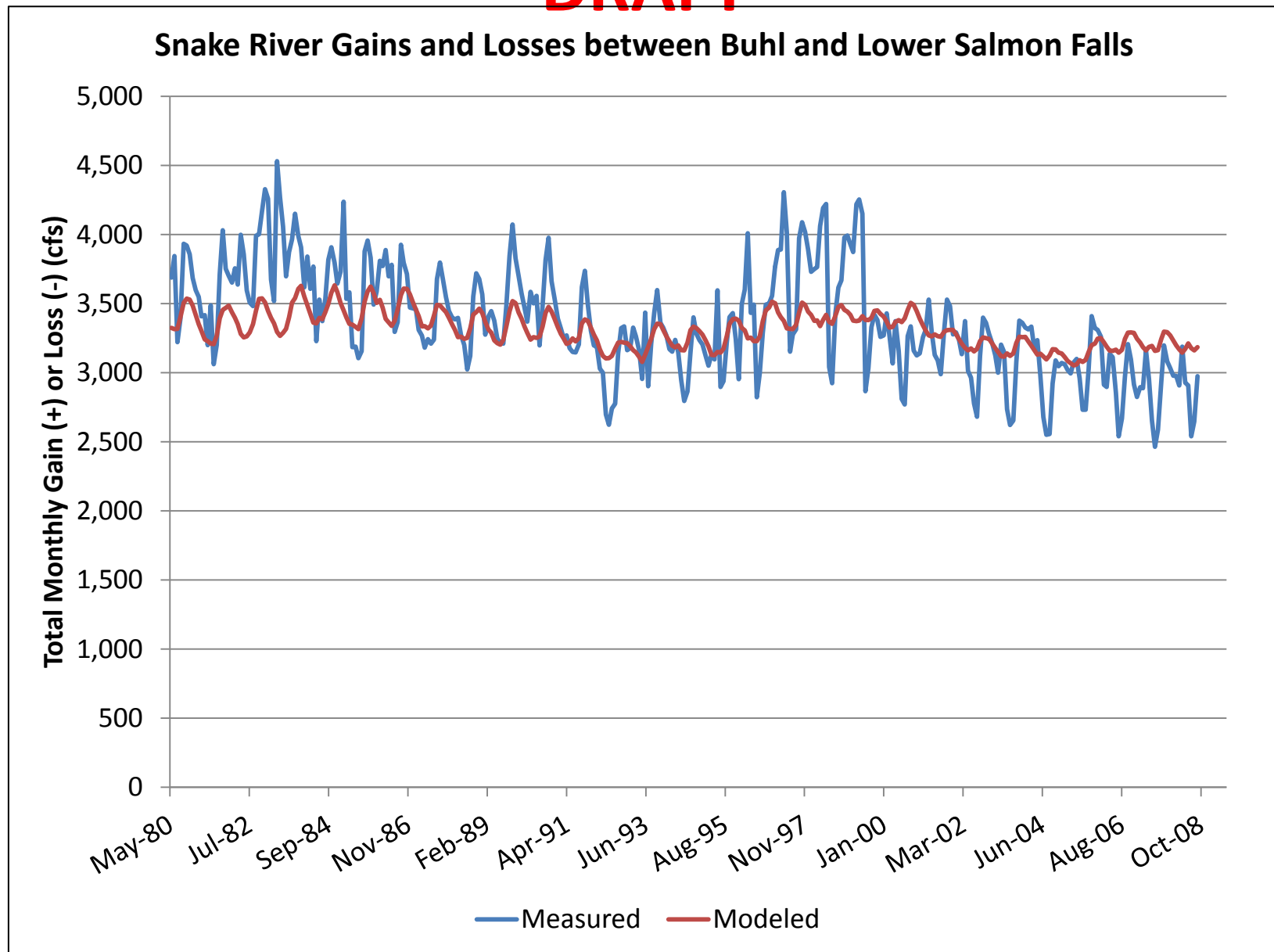


Figure 66. Monthly Snake River gains and losses between Buhl and Lower Salmon Falls.

DRAFT

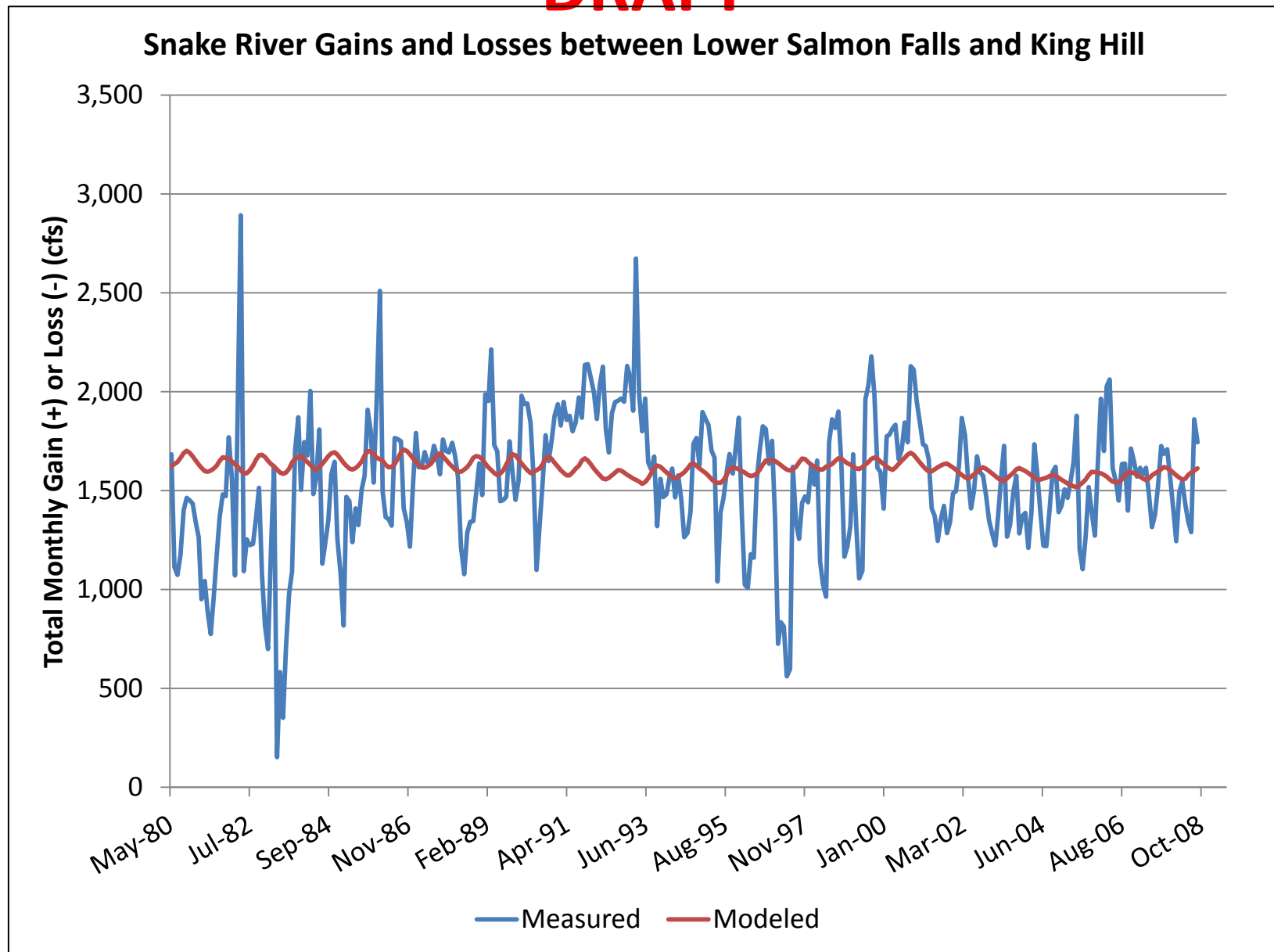


Figure 67. Monthly Snake River gains and losses between Lower Salmon Falls and King Hill.

DRAFT

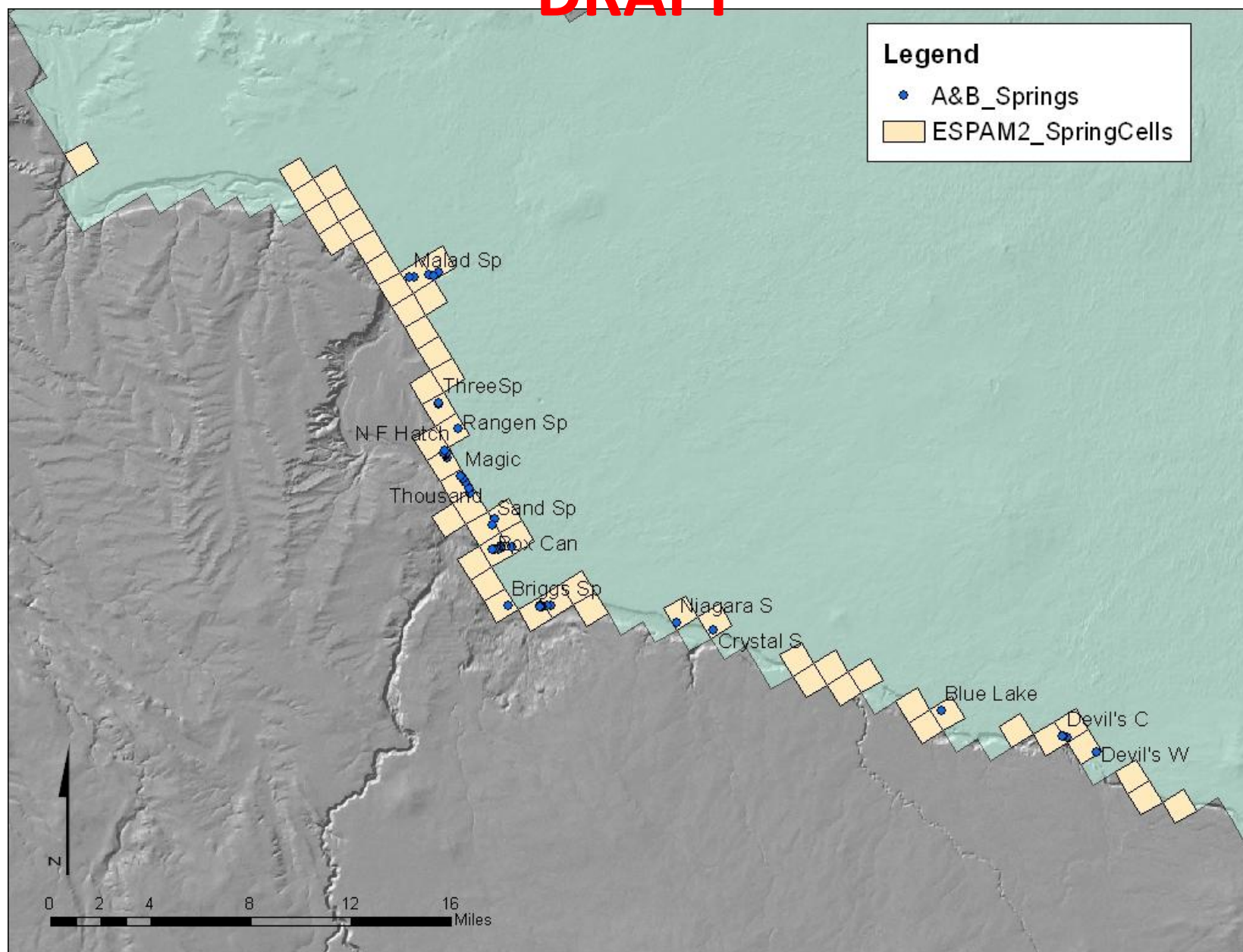


Figure 68. Location of Group A and B springs used as calibration targets.

DRAFT

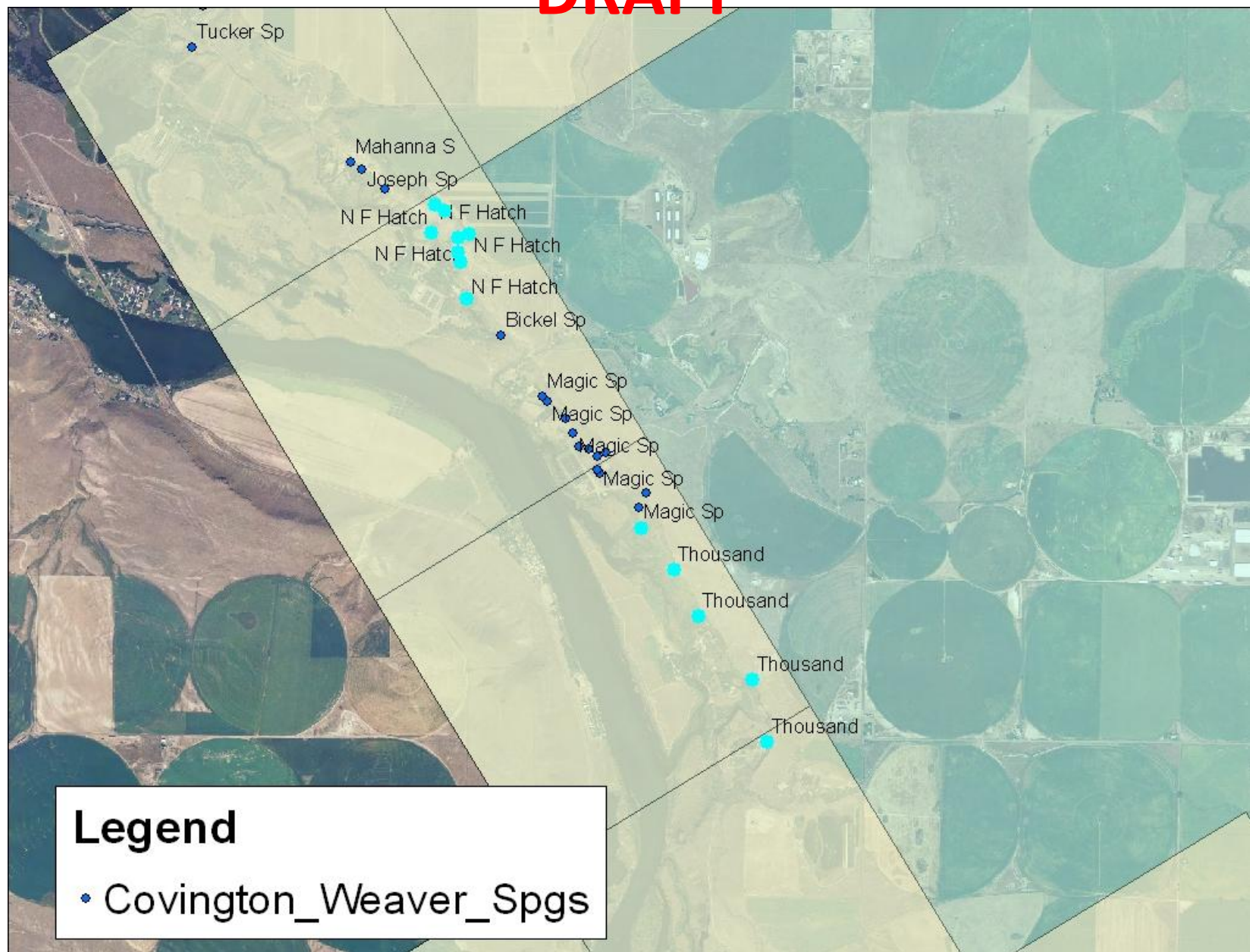


Figure 69. Magic Springs Complex.

DRAFT

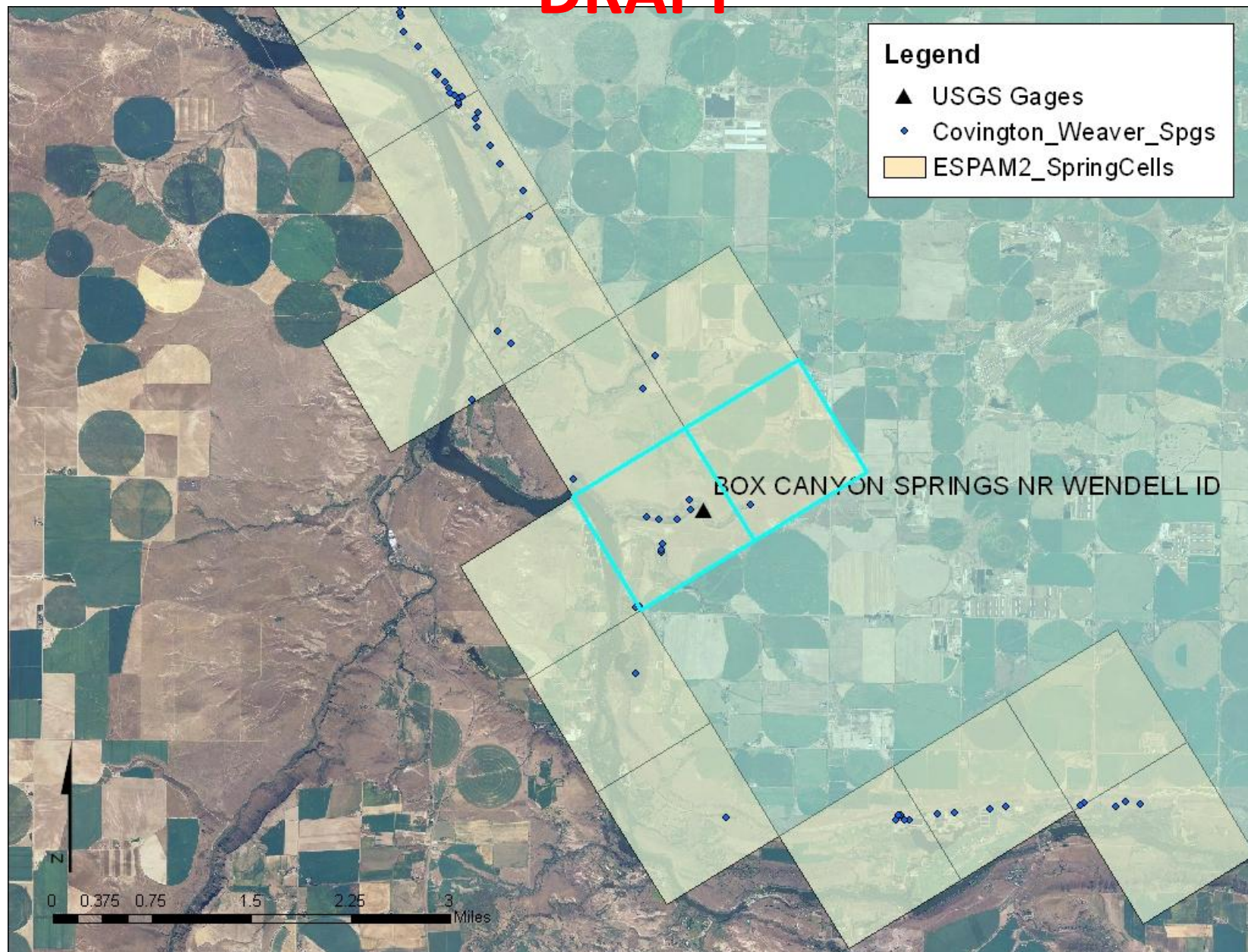


Figure 70. Box Canyon Springs location relative to the model drain cells.

DRAFT

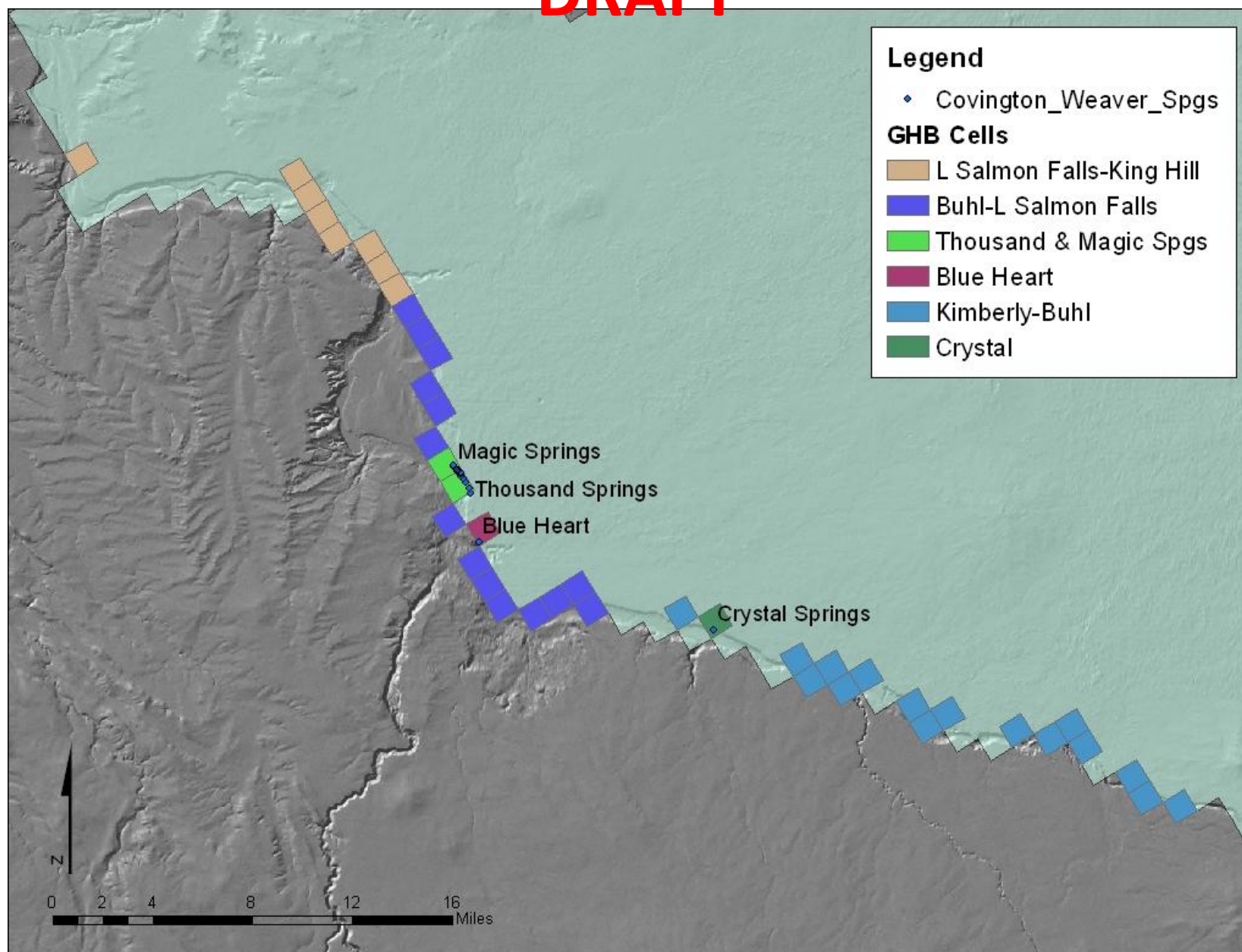


Figure 71. Location of General Head Boundary (GHB) targets in the Thousand Springs area.

DRAFT

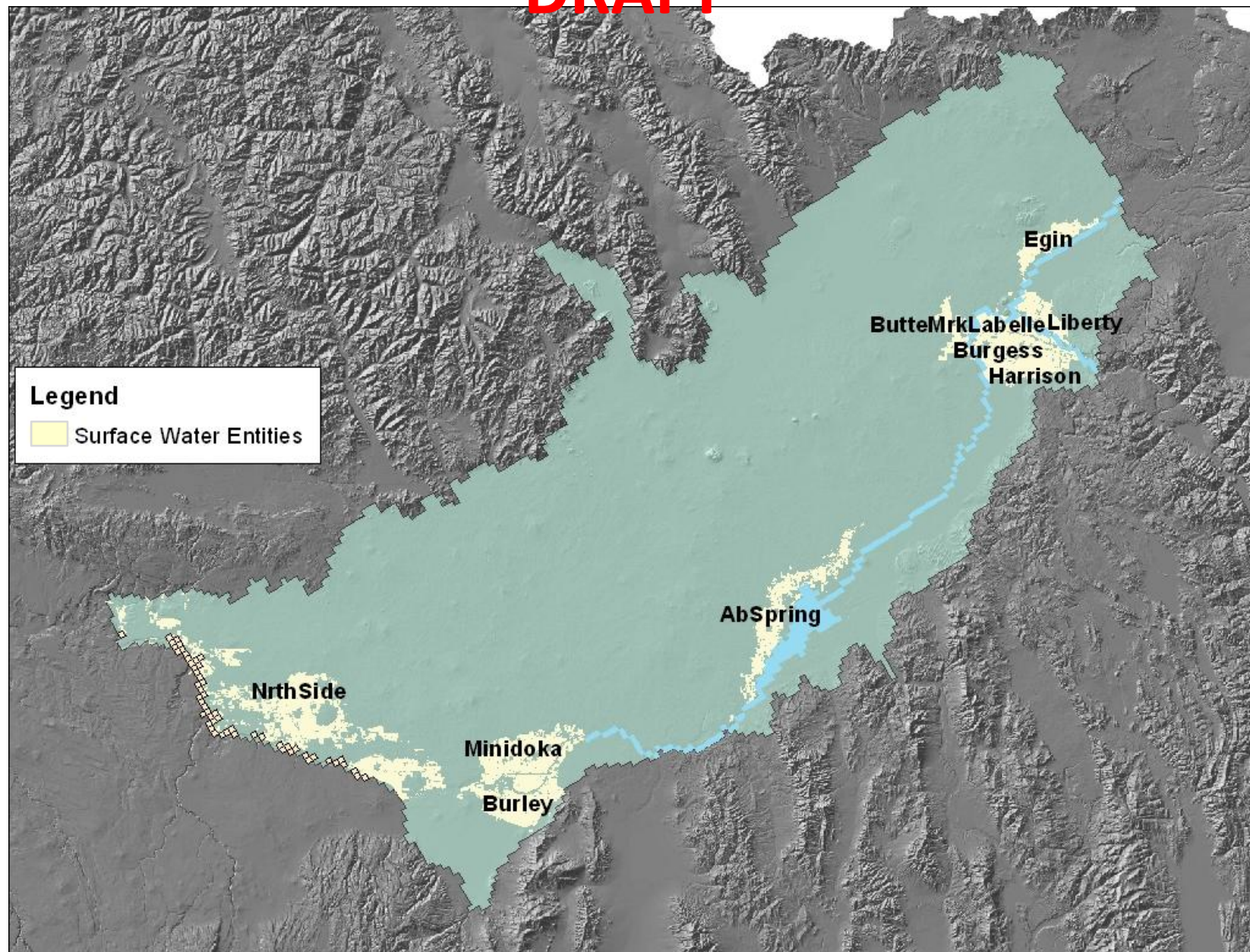


Figure 72. Location of entities with measured returns.

DRAFT

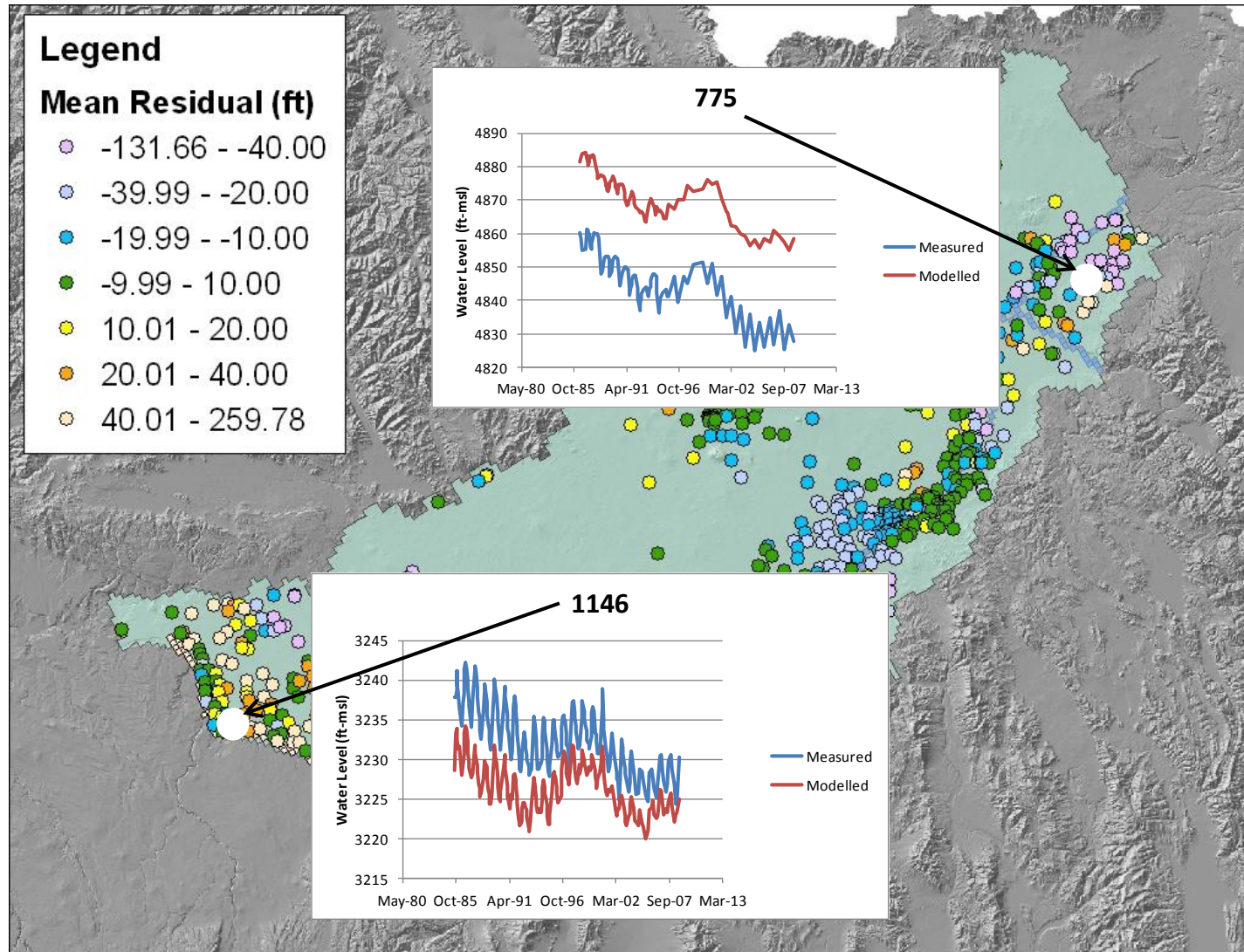


Figure 73. Simulated versus observed water levels for wells 775 and 1146.

DRAFT

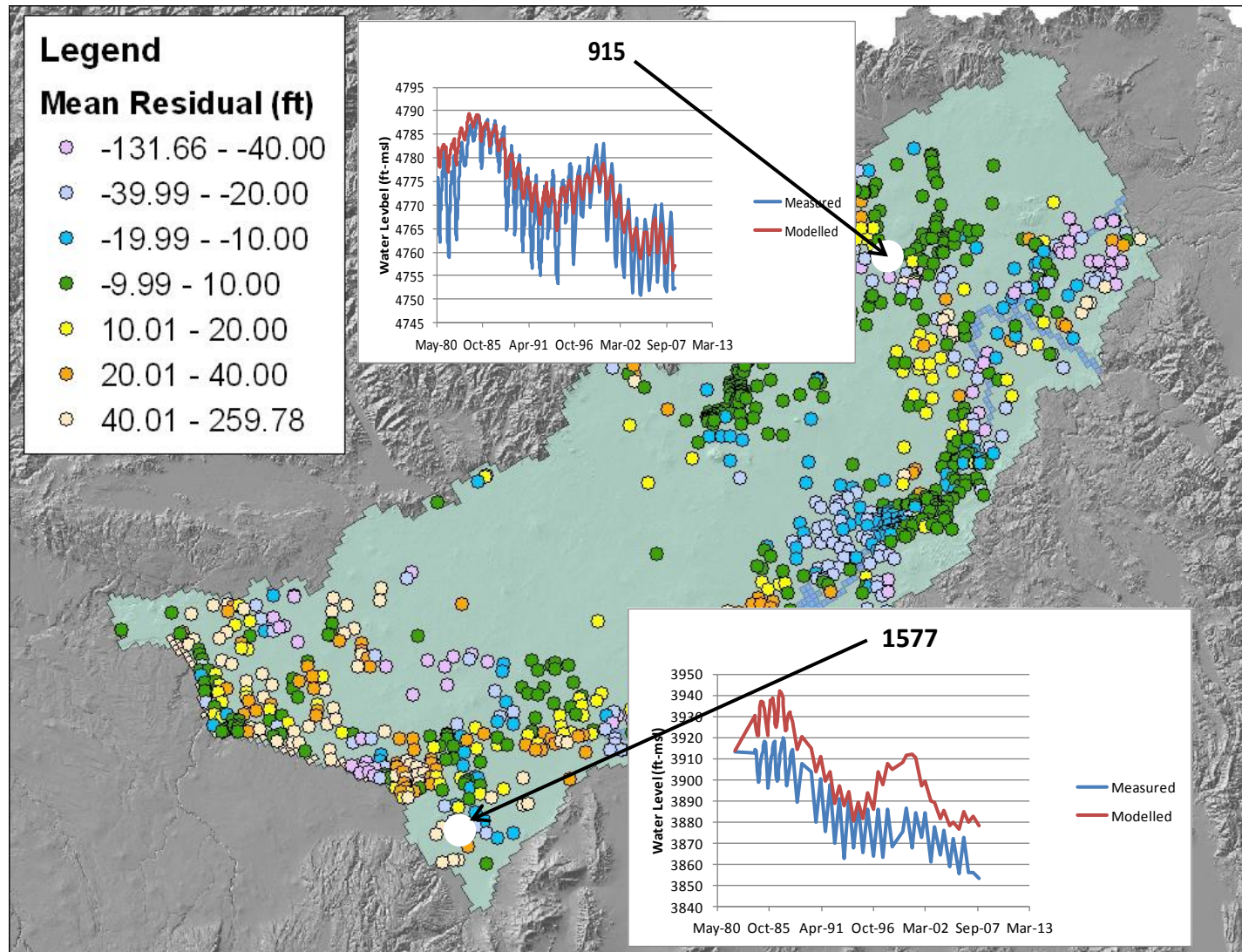


Figure 74. Simulated versus observed water levels for wells 915 and 1577.

DRAFT

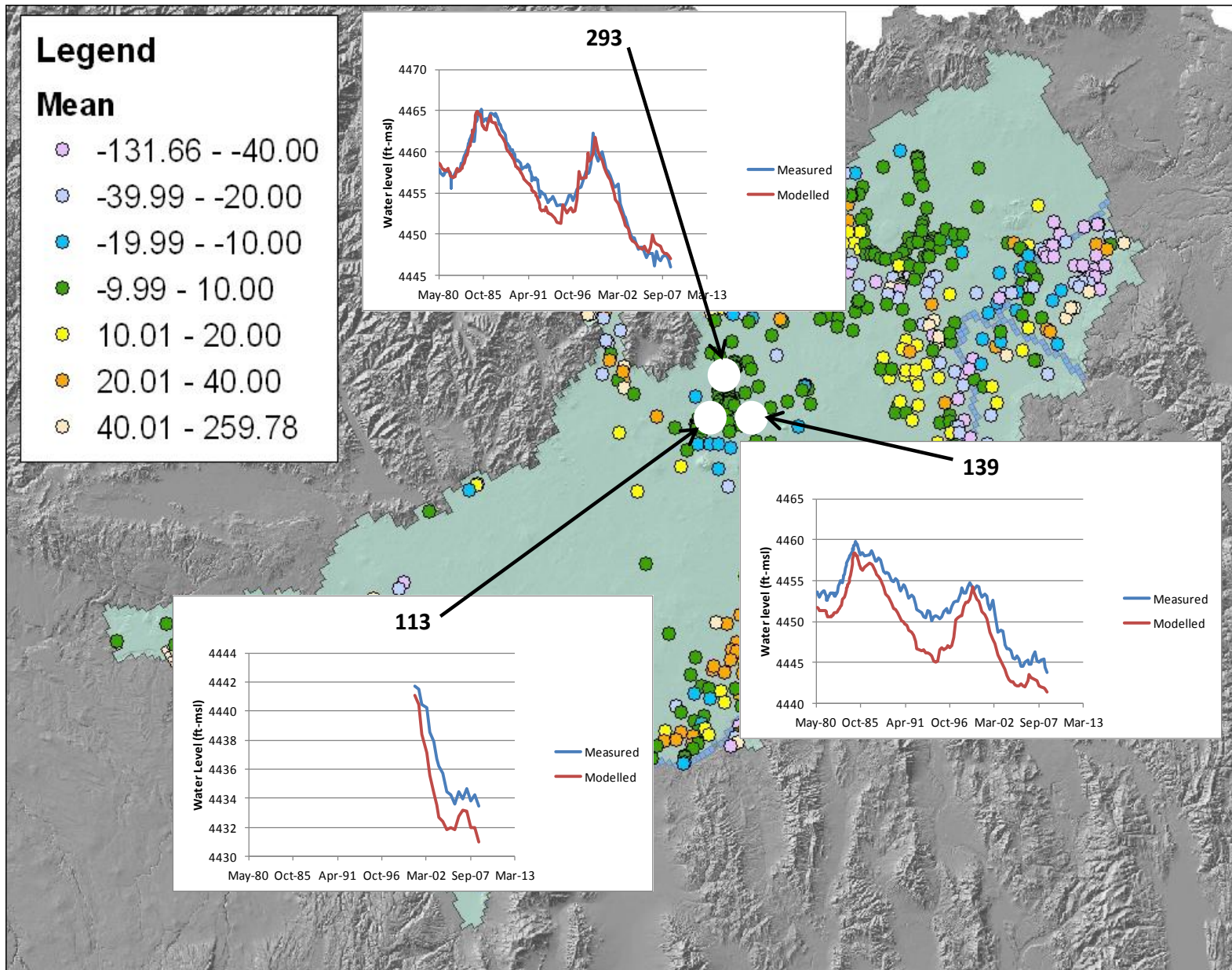


Figure 75. Simulated versus observed water levels for wells 113, 139, and 293.

DRAFT

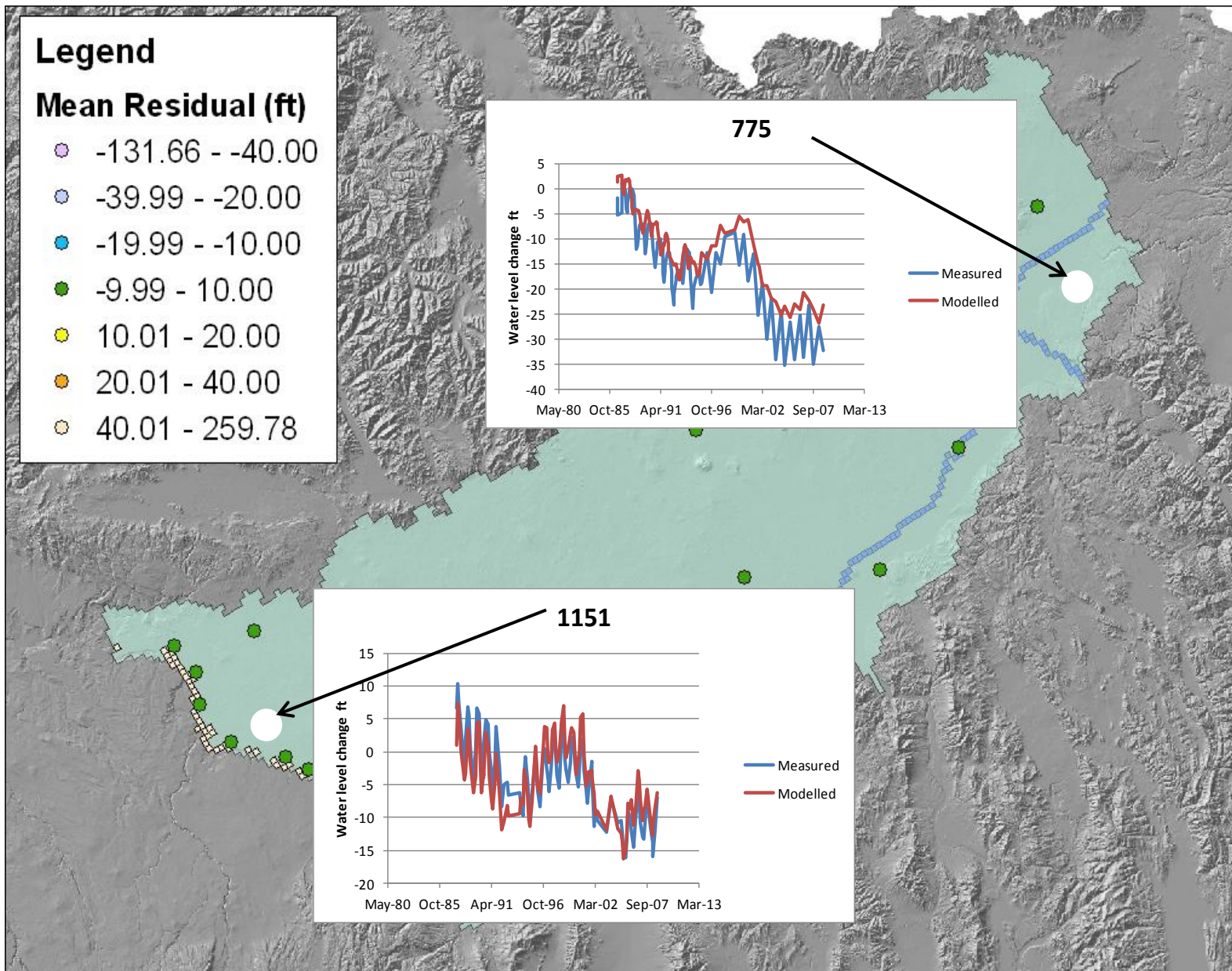


Figure 76. Simulated versus observed water level change for wells 775 and 1151.

DRAFT

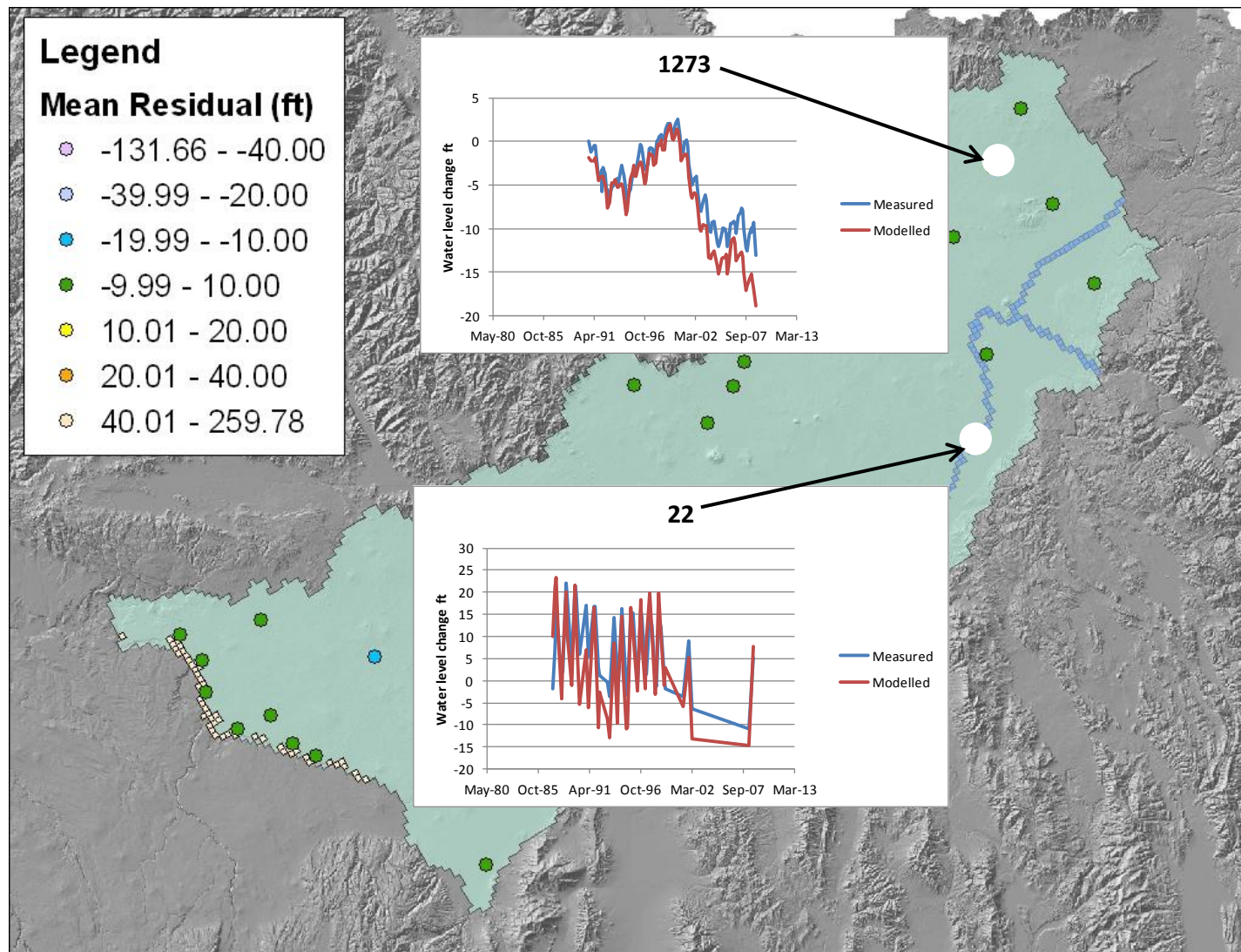


Figure 77. Simluated versus observed water level change for wells 22 and 1273.

DRAFT

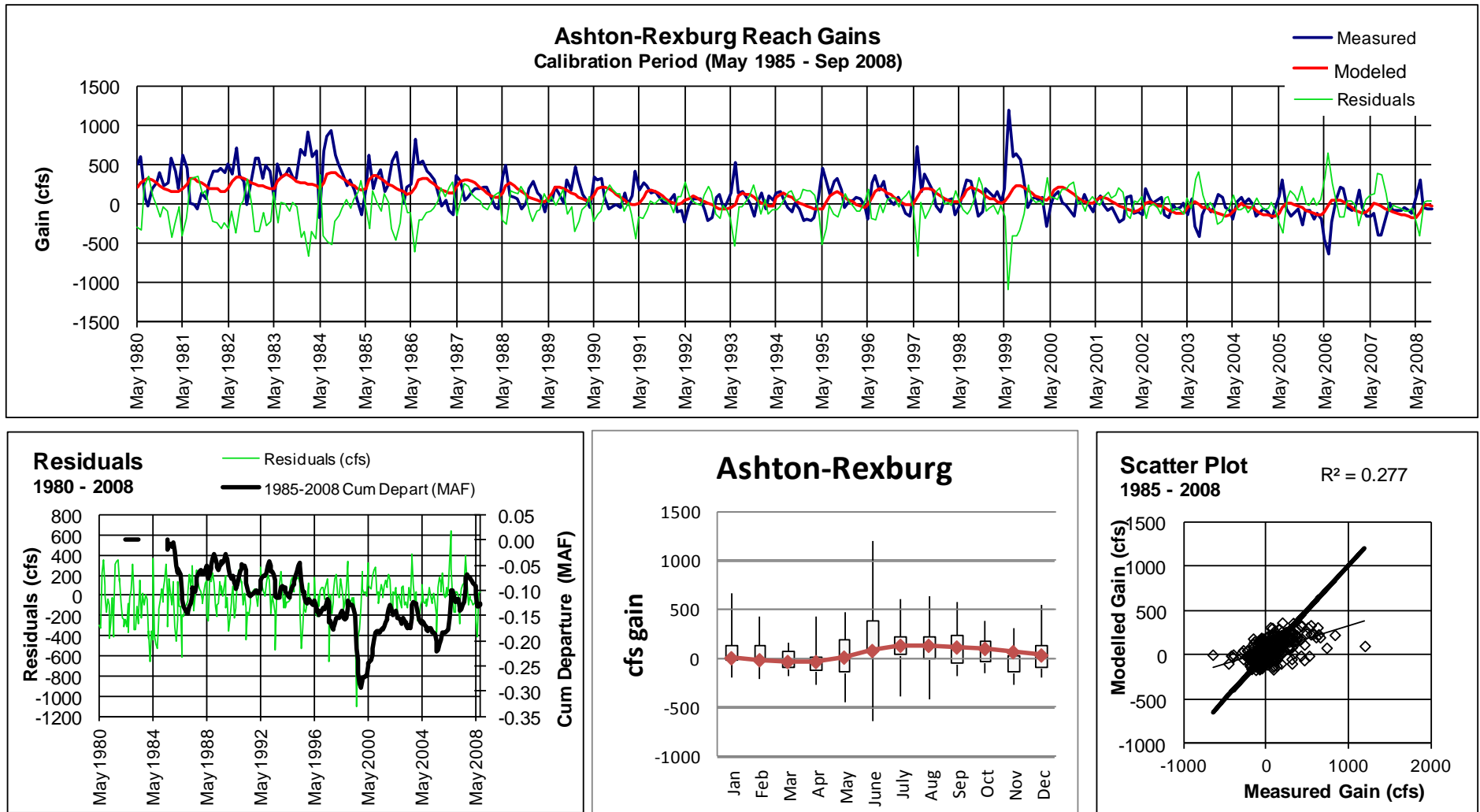


Figure 78. Reach gains in the Ashton-to-Rexburg reach. The top chart shows the measured gains, modeled gains, and residual over the calibration period. The lower chart figure shows the cumulative departures. The lower middle chart is a Box-and-Whisker plot of the gains. The lower right chart is a scatter plot of modeled gains against measured gains.

DRAFT

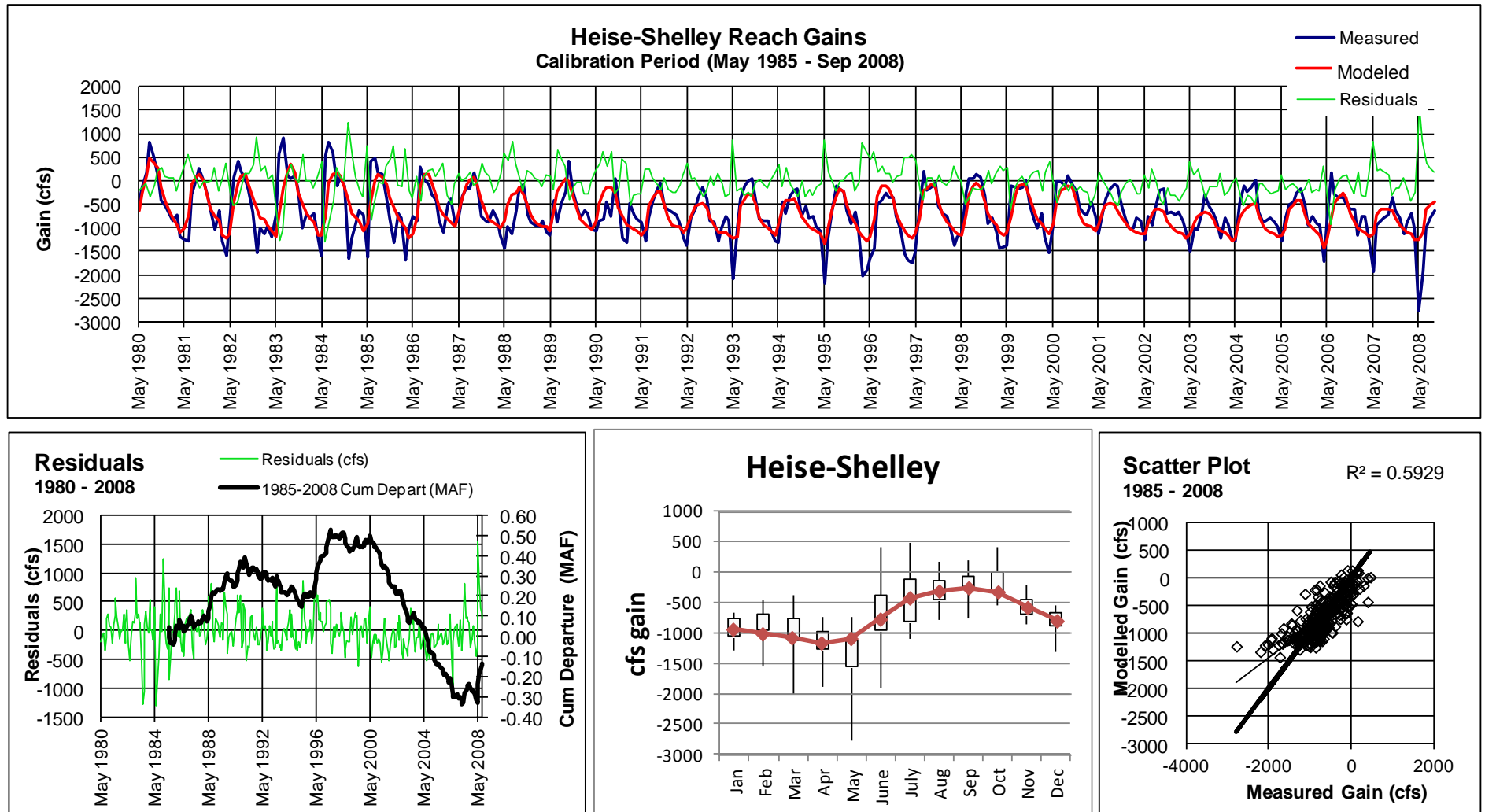


Figure 79. Reach gains in the Heise-to-Shelley reach. The top chart shows the measured gains, modeled gains, and residual over the calibration period. The lower chart figure shows the cumulative departures. The lower middle chart is a Box-and-Whisker plot of the gains. The lower right chart is a scatter plot of modeled gains against measured gains.

DRAFT

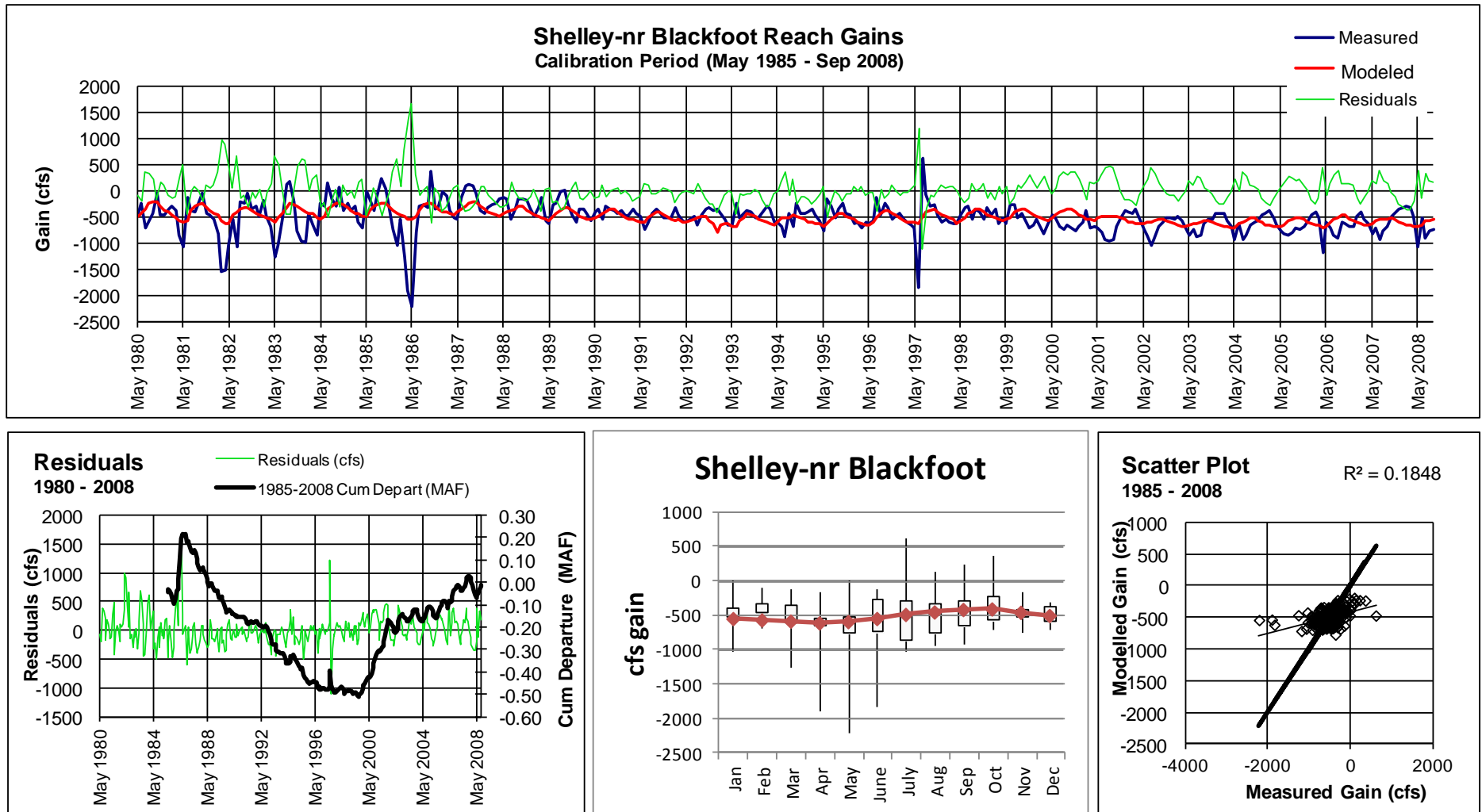


Figure 80. Reach gains in the Shelley-to-near Blackfoot reach. The top chart shows the measured gains, modeled gains, and residual over the calibration period. The lower chart figure shows the cumulative departures. The lower middle chart is a Box-and-Whisker plot of the gains. The lower right chart is a scatter plot of modeled gains against measured gains.

DRAFT

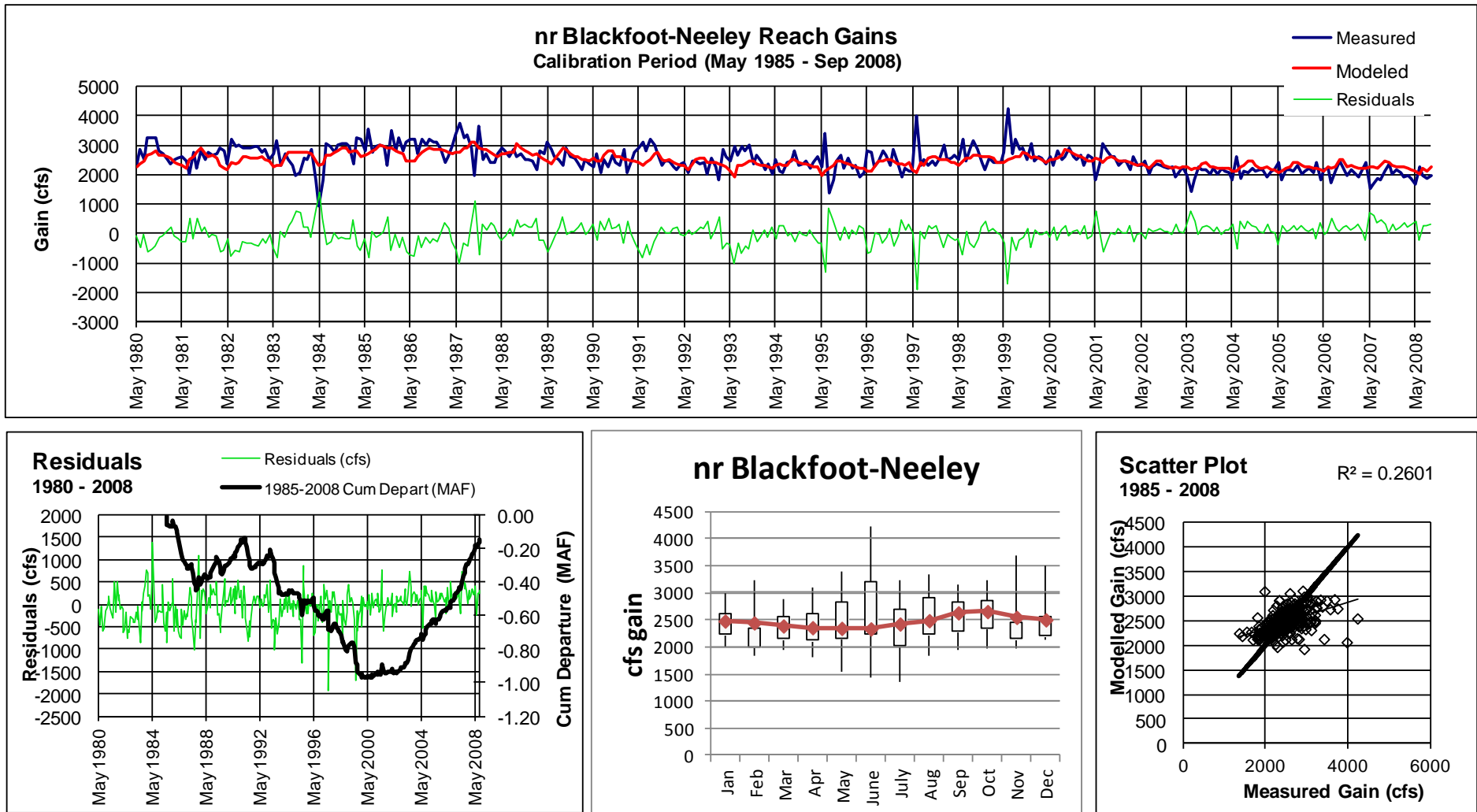


Figure 81. Reach gains in the near Blackfoot-to-Neeley reach. The top chart shows the measured gains, modeled gains, and residual over the calibration period. The lower chart figure shows the cumulative departures. The lower middle chart is a Box-and-Whisker plot of the gains. The lower right chart is a scatter plot of modeled gains against measured gains.

DRAFT

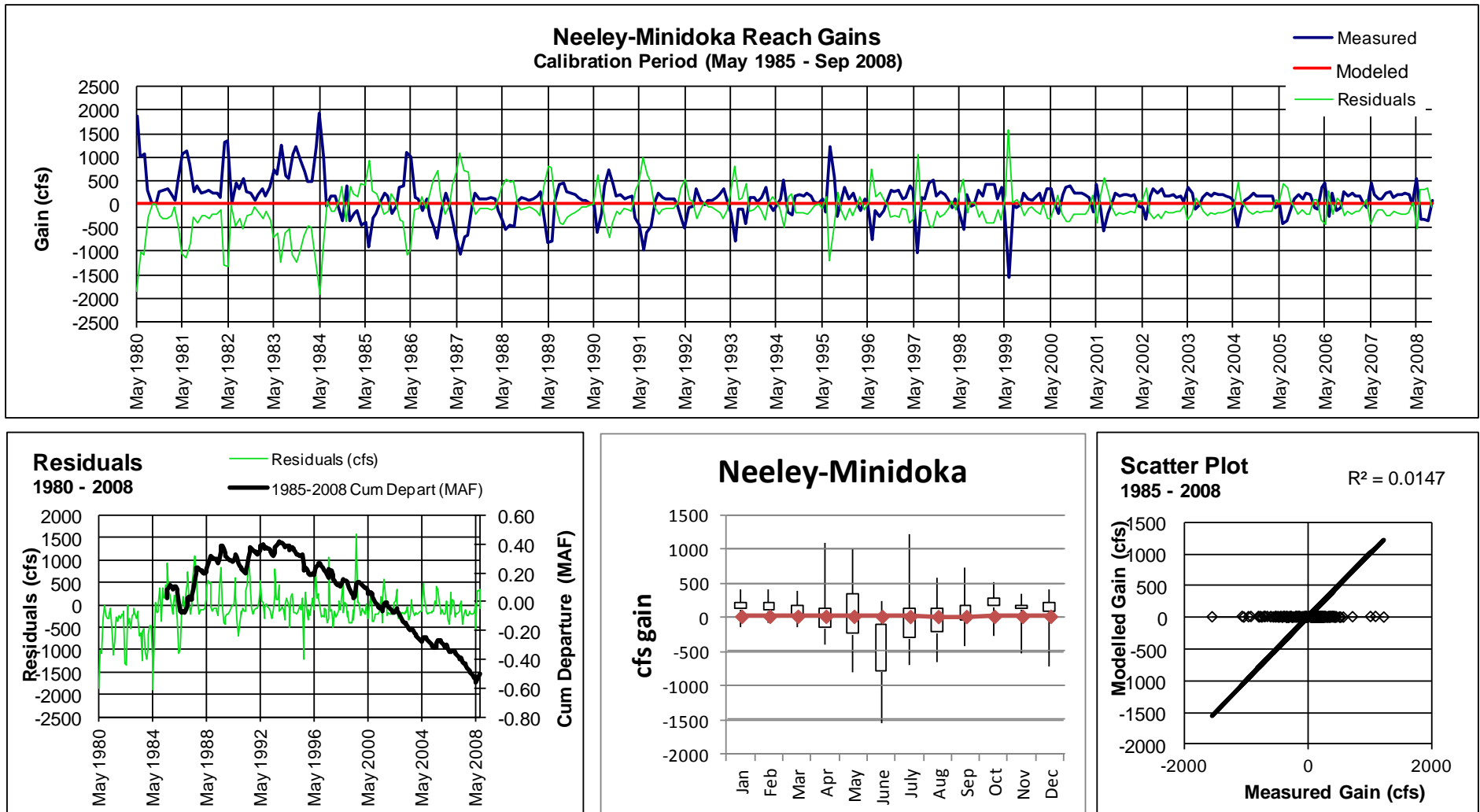


Figure 82. Reach gains in the Neeley-to-Minidoka reach. The top chart shows the measured gains, modeled gains, and residual over the calibration period. The lower chart figure shows the cumulative departures. The lower middle chart is a Box-and-Whisker plot of the gains. The lower right chart is a scatter plot of modeled gains against measured gains.

DRAFT

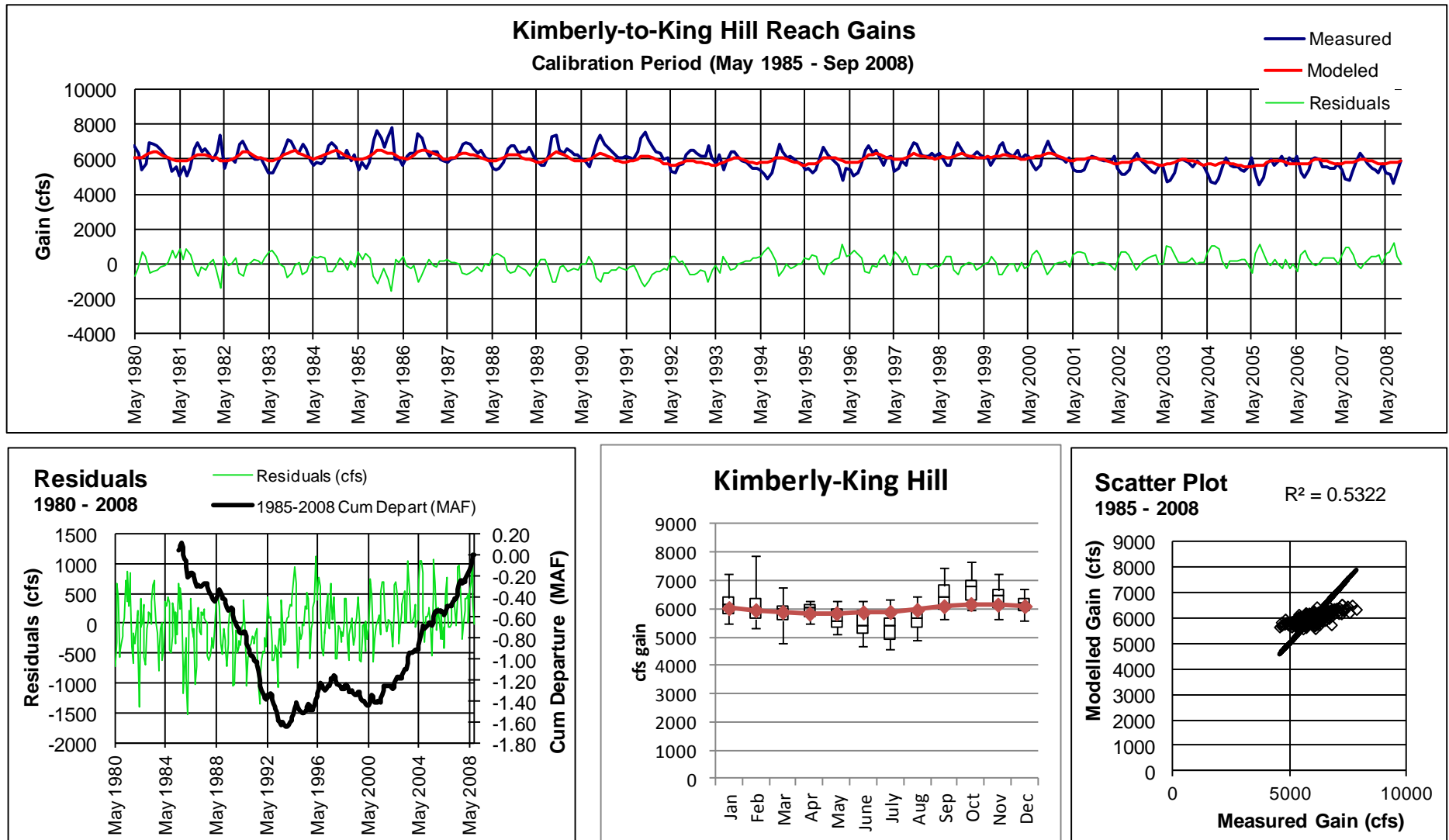


Figure 83. Reach gains in the Kimberly-to-King Hill reach. The top chart shows the measured gains, modeled gains, and residual over the calibration period. The lower chart figure shows the cumulative departures. The lower middle chart is a Box-and-Whisker plot of the gains. The lower right chart is a scatter plot of modeled gains against measured gains.

DRAFT

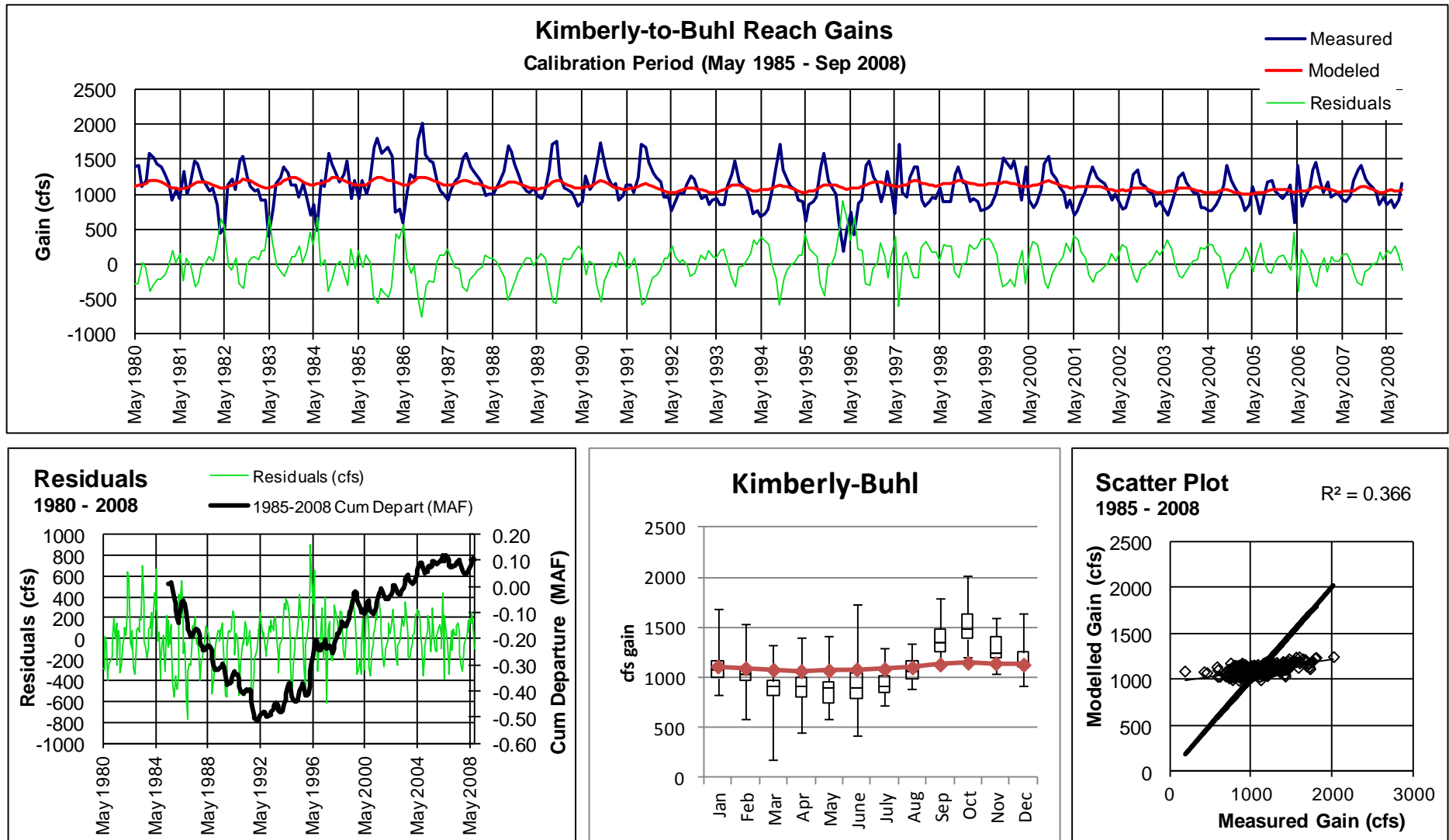


Figure 84. Reach gains in the Kimberly-to-Buhl reach. The top chart shows the measured gains, modeled gains, and residual over the calibration period. The lower chart figure shows the cumulative departures. The lower middle chart is a Box-and-Whisker plot of the gains. The lower right chart is a scatter plot of modeled gains against measured gains.

DRAFT

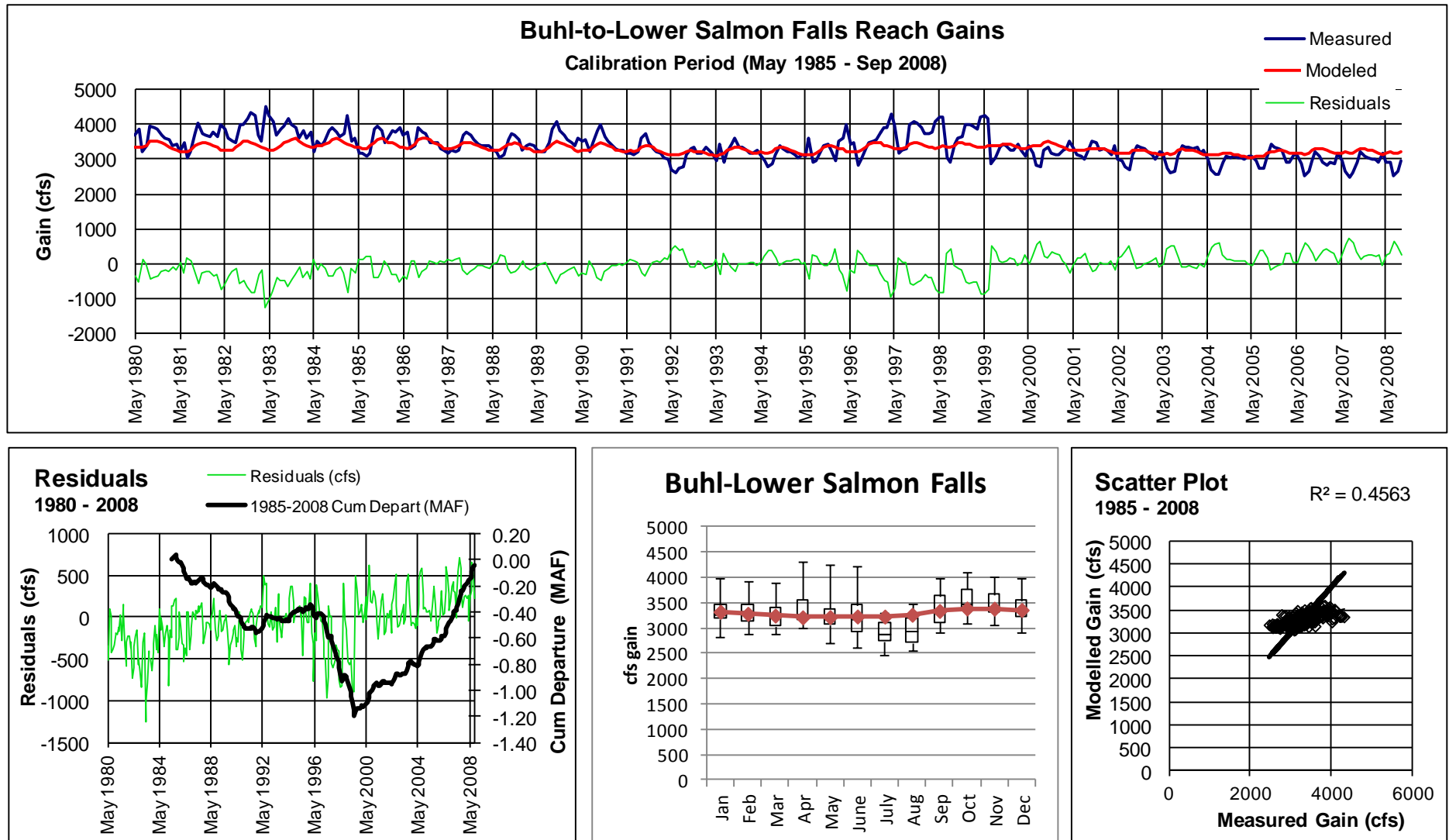


Figure 85. Reach gains in the Buhl-to-Lower Salmon Falls reach. The top chart shows the measured gains, modeled gains, and residual over the calibration period. The lower chart figure shows the cumulative departures. The lower middle chart is a Box-and-Whisker plot of the gains. The lower right chart is a scatter plot of modeled gains against measured gains.

DRAFT

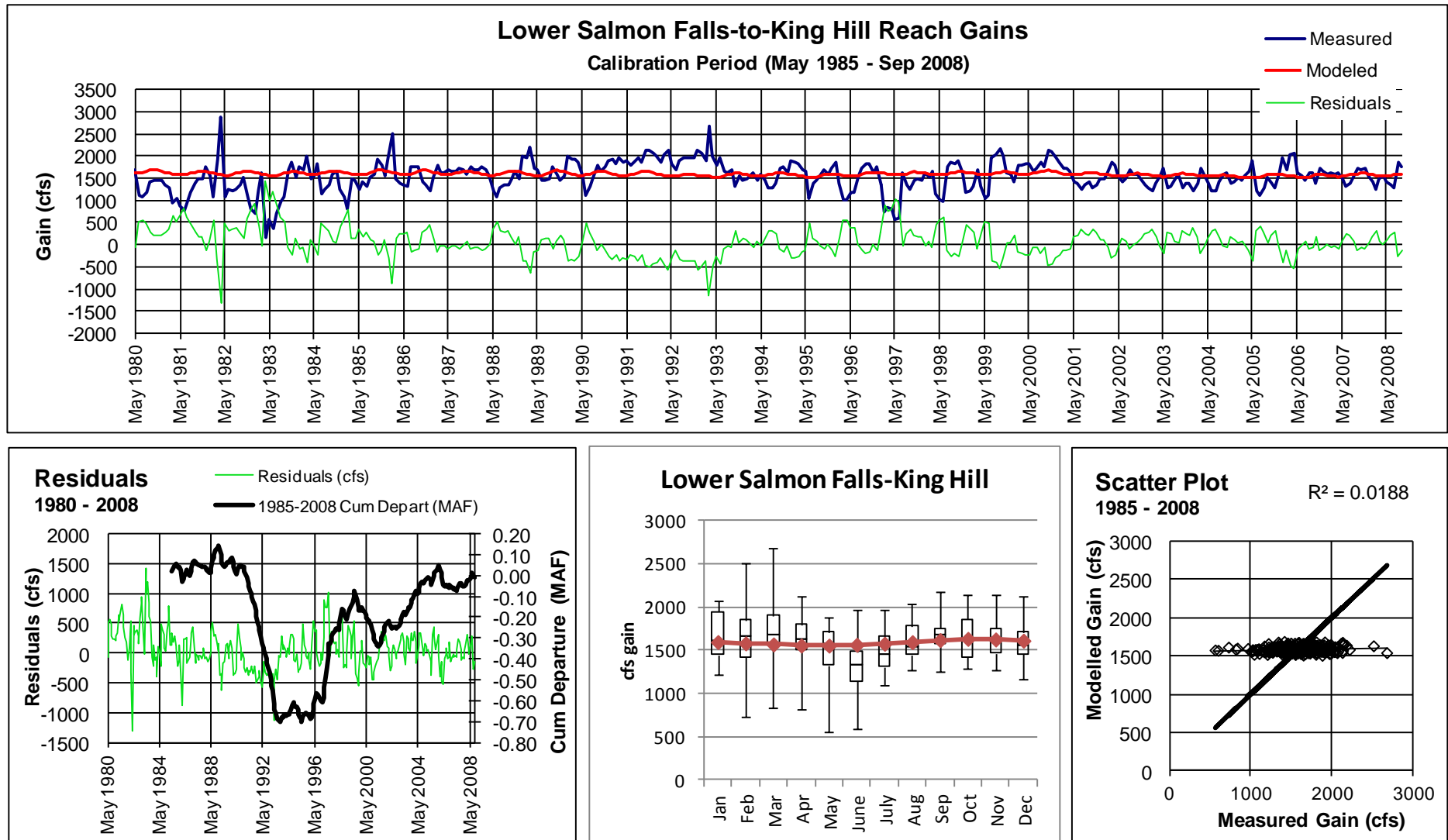


Figure 86. Reach gains in the Lower Salmon Falls-to-King Hill reach. The top chart shows the measured gains, modeled gains, and residual over the calibration period. The lower chart figure shows the cumulative departures. The lower middle chart is a Box-and-Whisker plot of the gains. The lower right chart is a scatter plot of modeled gains against measured gains.

DRAFT

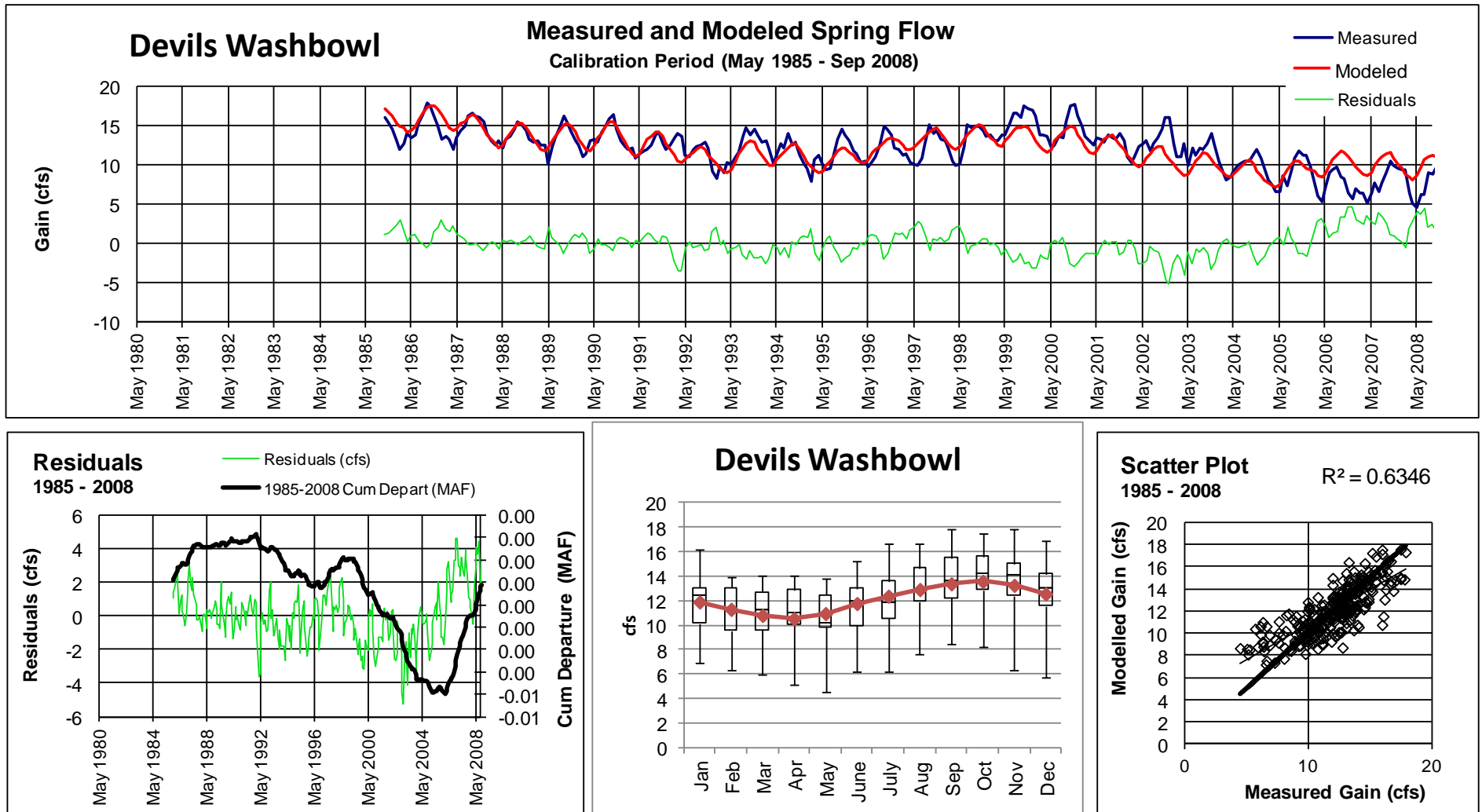


Figure 87. Spring flow for Devils Washbowl. The top chart shows the measured gains, modeled gains, and residual over the calibration period. The lower chart figure shows the cumulative departures. The lower middle chart is a Box-and-Whisker plot of the gains. The lower right chart is a scatter plot of modeled gains against measured gains.

DRAFT

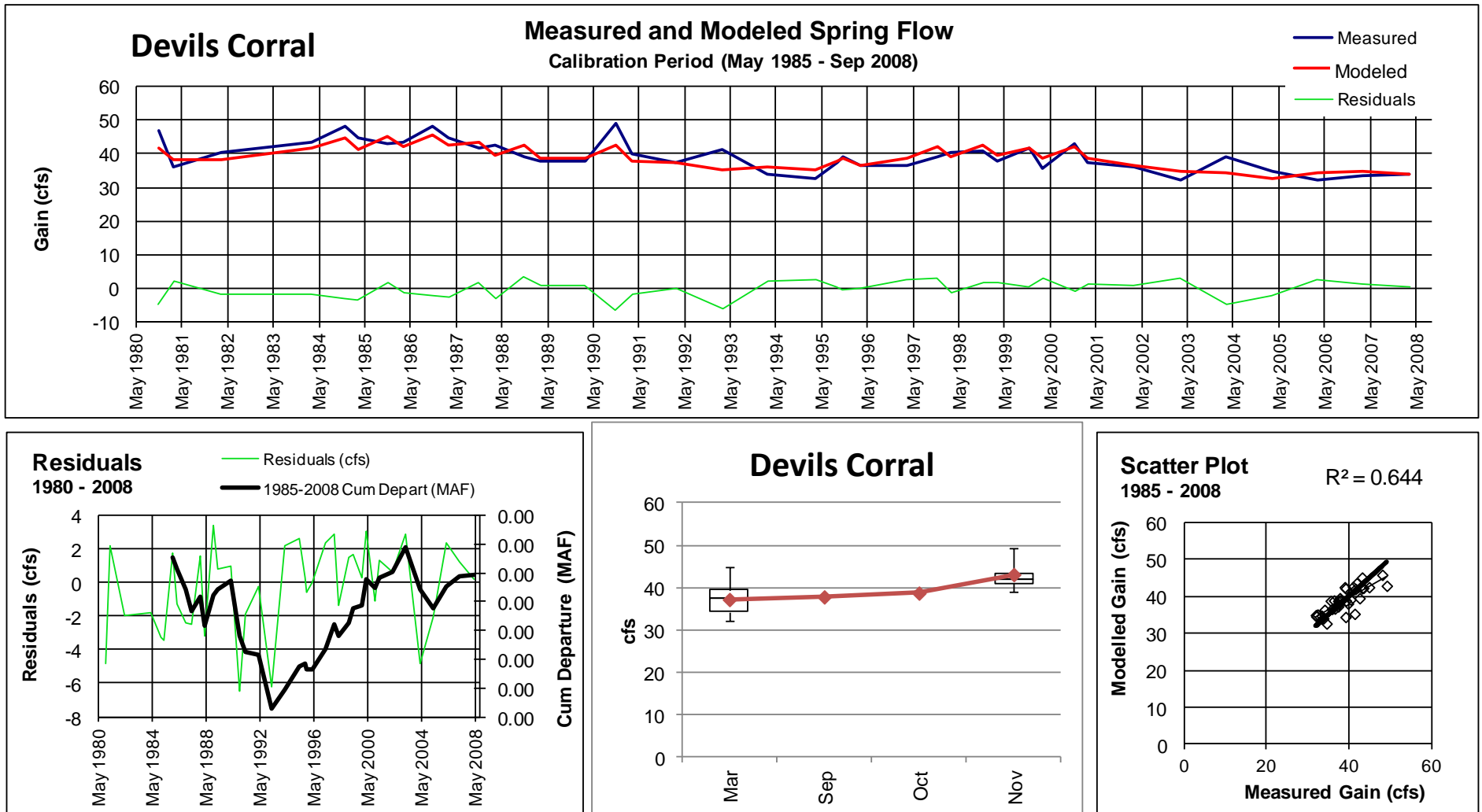


Figure 88. Spring flow for Devils Corral. The top chart shows the measured gains, modeled gains, and residual over the calibration period. The lower chart figure shows the cumulative departures. The lower middle chart is a Box-and-Whisker plot of the gains. The lower right chart is a scatter plot of modeled gains against measured gains.

DRAFT

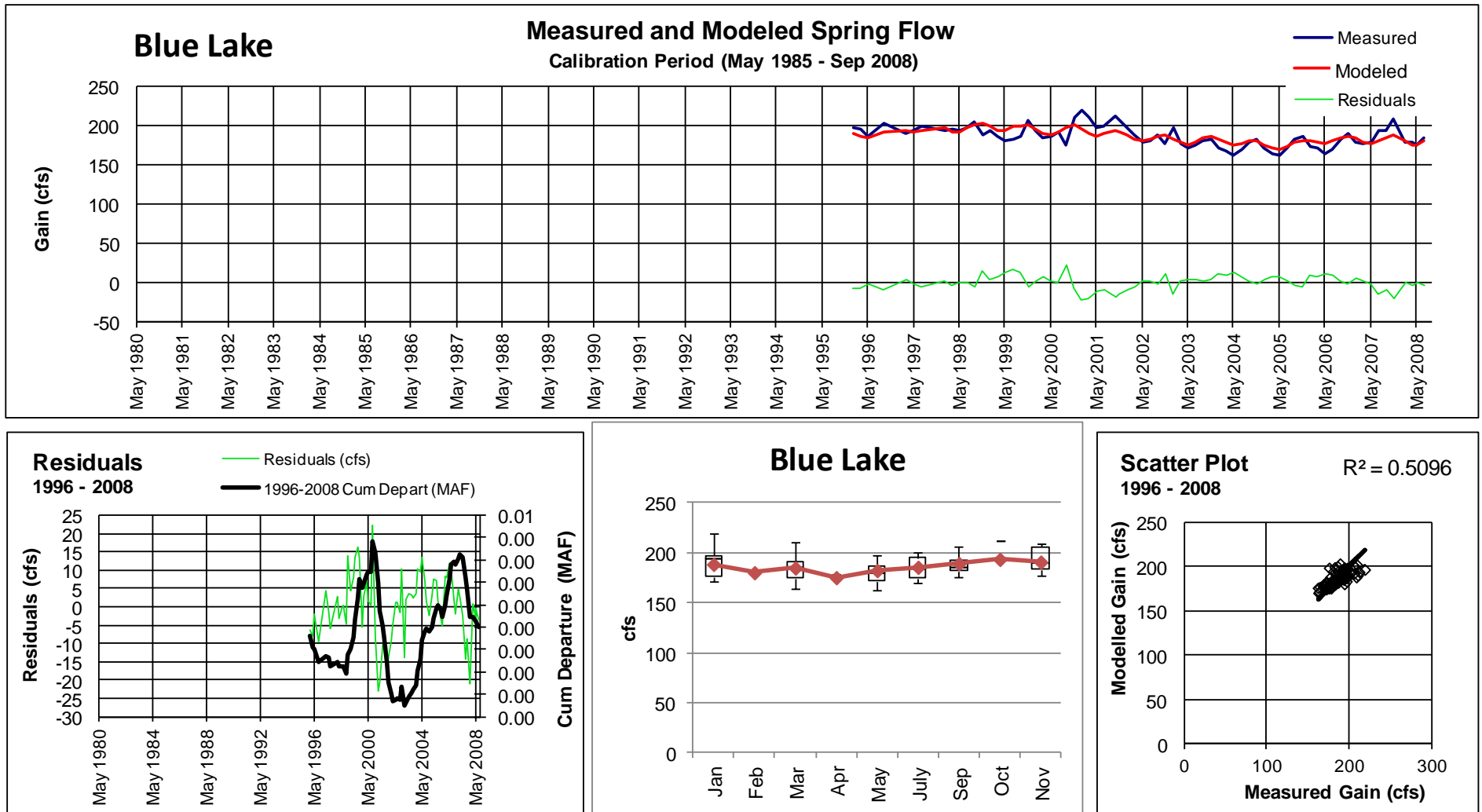


Figure 89. Spring flow for Blue Lake. The top chart shows the measured gains, modeled gains, and residual over the calibration period. The lower chart figure shows the cumulative departures. The lower middle chart is a Box-and-Whisker plot of the gains. The lower right chart is a scatter plot of modeled gains against measured gains.

DRAFT

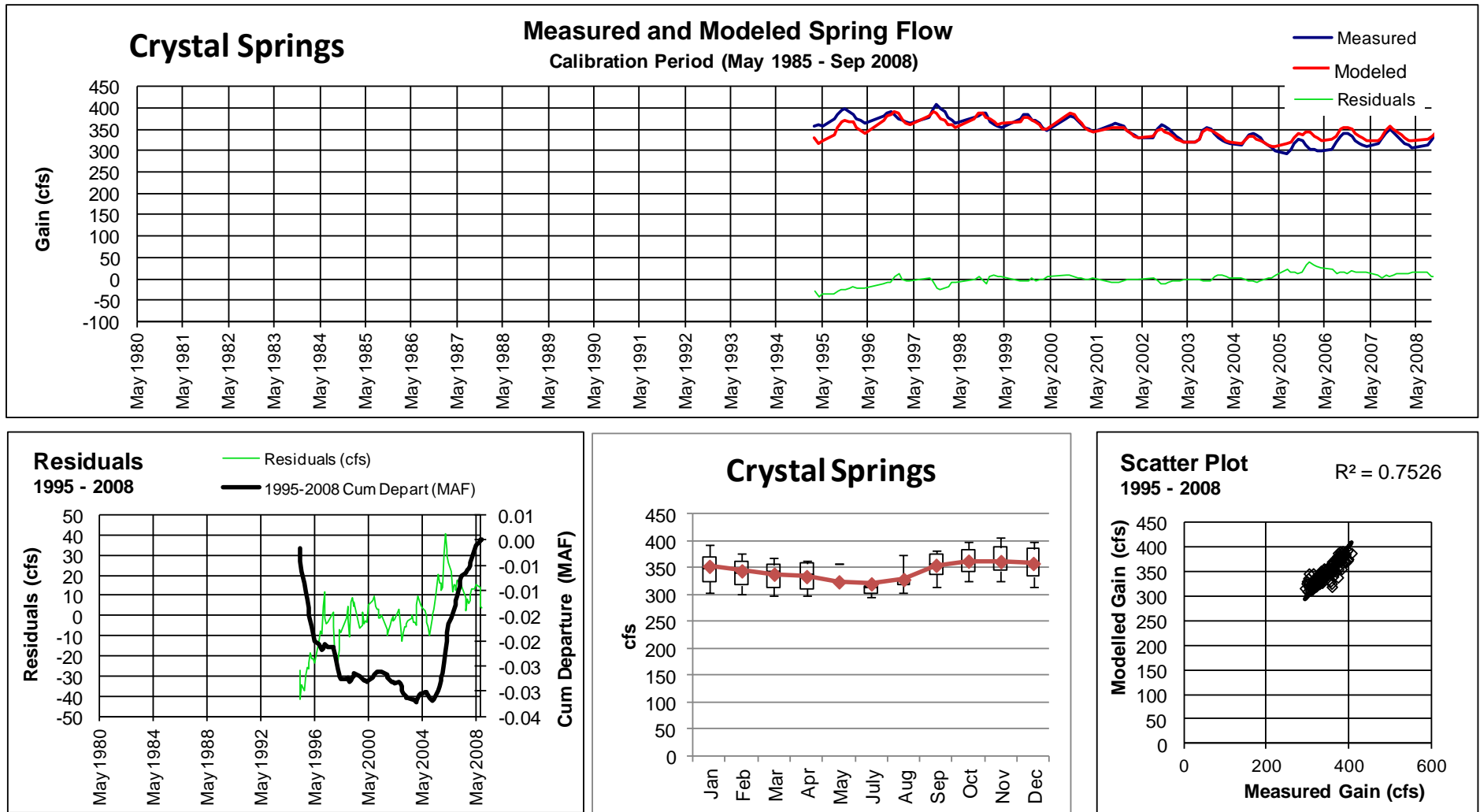


Figure 90. Spring flow for Crystal Springs. The top chart shows the measured gains, modeled gains, and residual over the calibration period. The lower chart figure shows the cumulative departures. The lower middle chart is a Box-and-Whisker plot of the gains. The lower right chart is a scatter plot of modeled gains against measured gains.

DRAFT

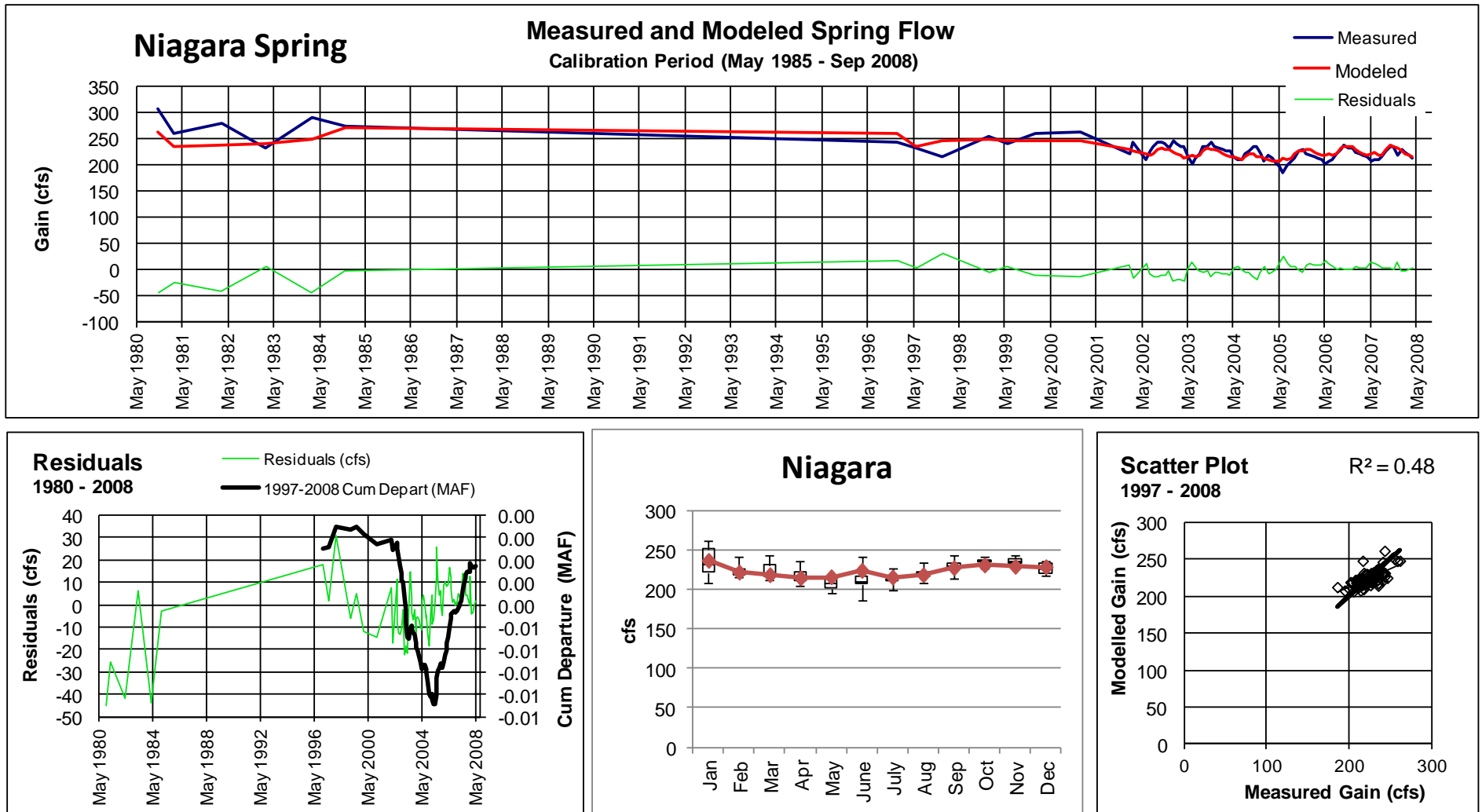


Figure 91. Spring flow for Niagara Spring. The top chart shows the measured gains, modeled gains, and residual over the calibration period. The lower chart figure shows the cumulative departures. The lower middle chart is a Box-and-Whisker plot of the gains. The lower right chart is a scatter plot of modeled gains against measured gains.

DRAFT

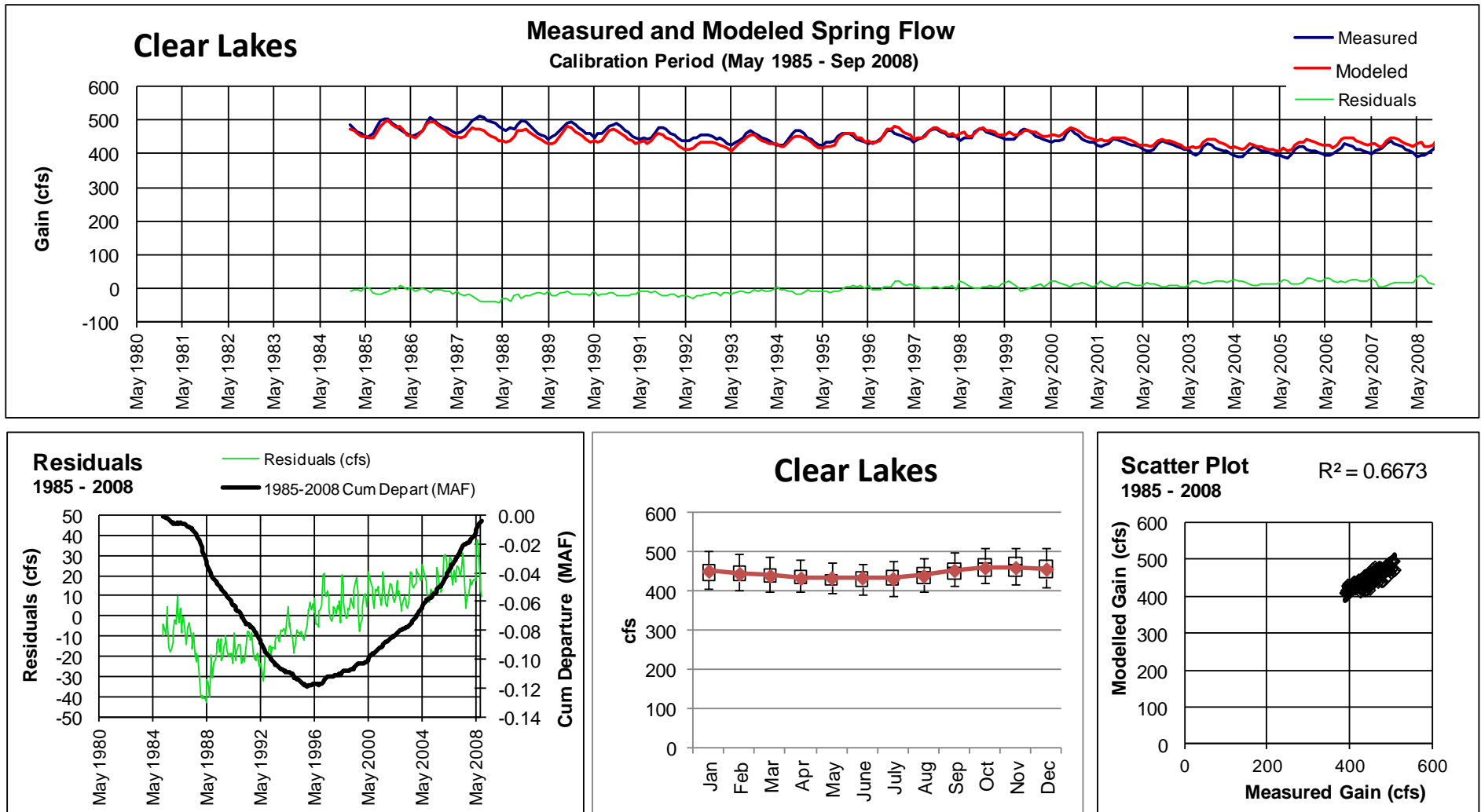


Figure 92. Spring flow for Clear Lakes Spring. The top chart shows the measured gains, modeled gains, and residual over the calibration period. The lower chart figure shows the cumulative departures. The lower middle chart is a Box-and-Whisker plot of the gains. The lower right chart is a scatter plot of modeled gains against measured gains.

DRAFT

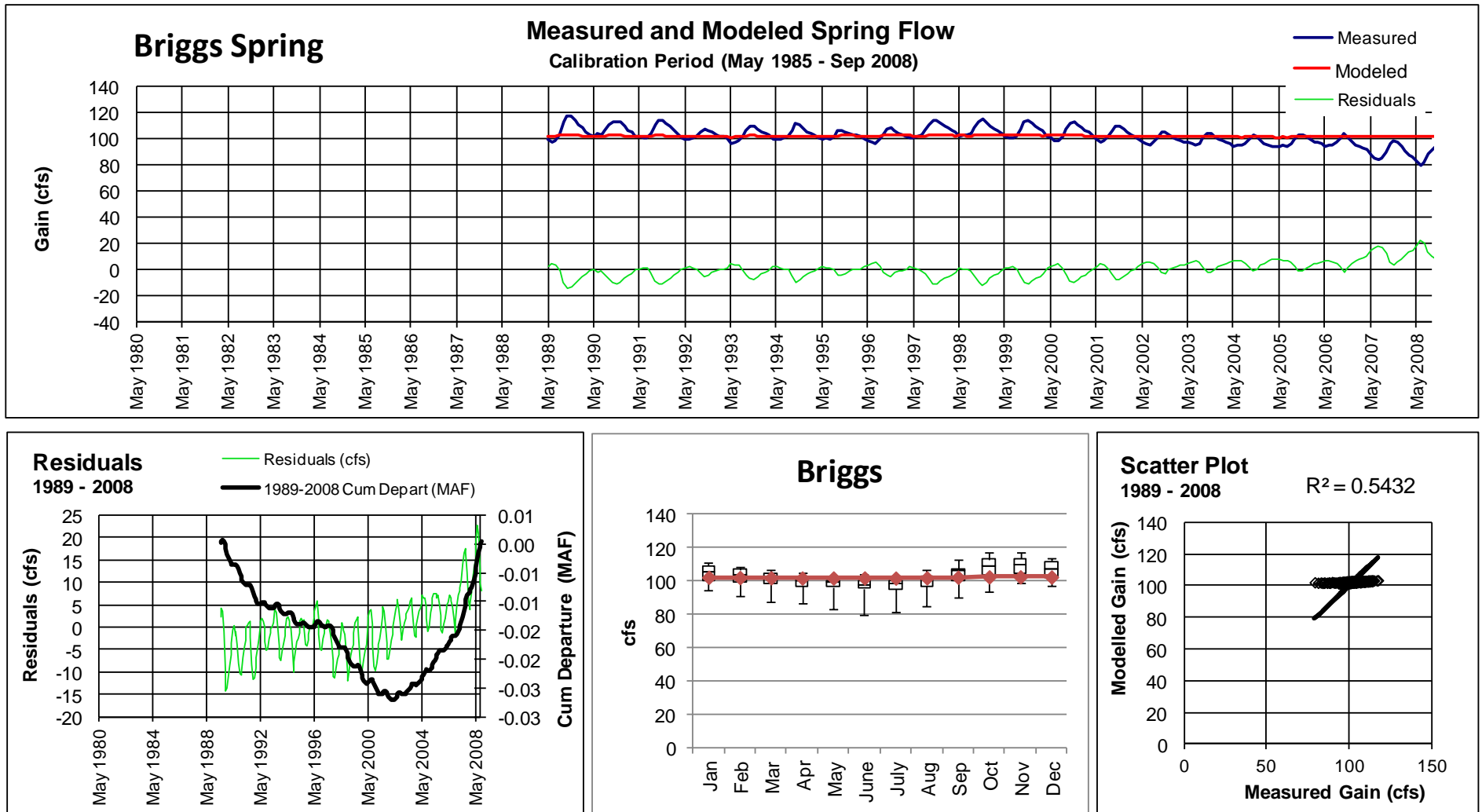


Figure 93. Spring flow for Briggs Spring. The top chart shows the measured gains, modeled gains, and residual over the calibration period. The lower chart figure shows the cumulative departures. The lower middle chart is a Box-and-Whisker plot of the gains. The lower right chart is a scatter plot of modeled gains against measured gains.

DRAFT

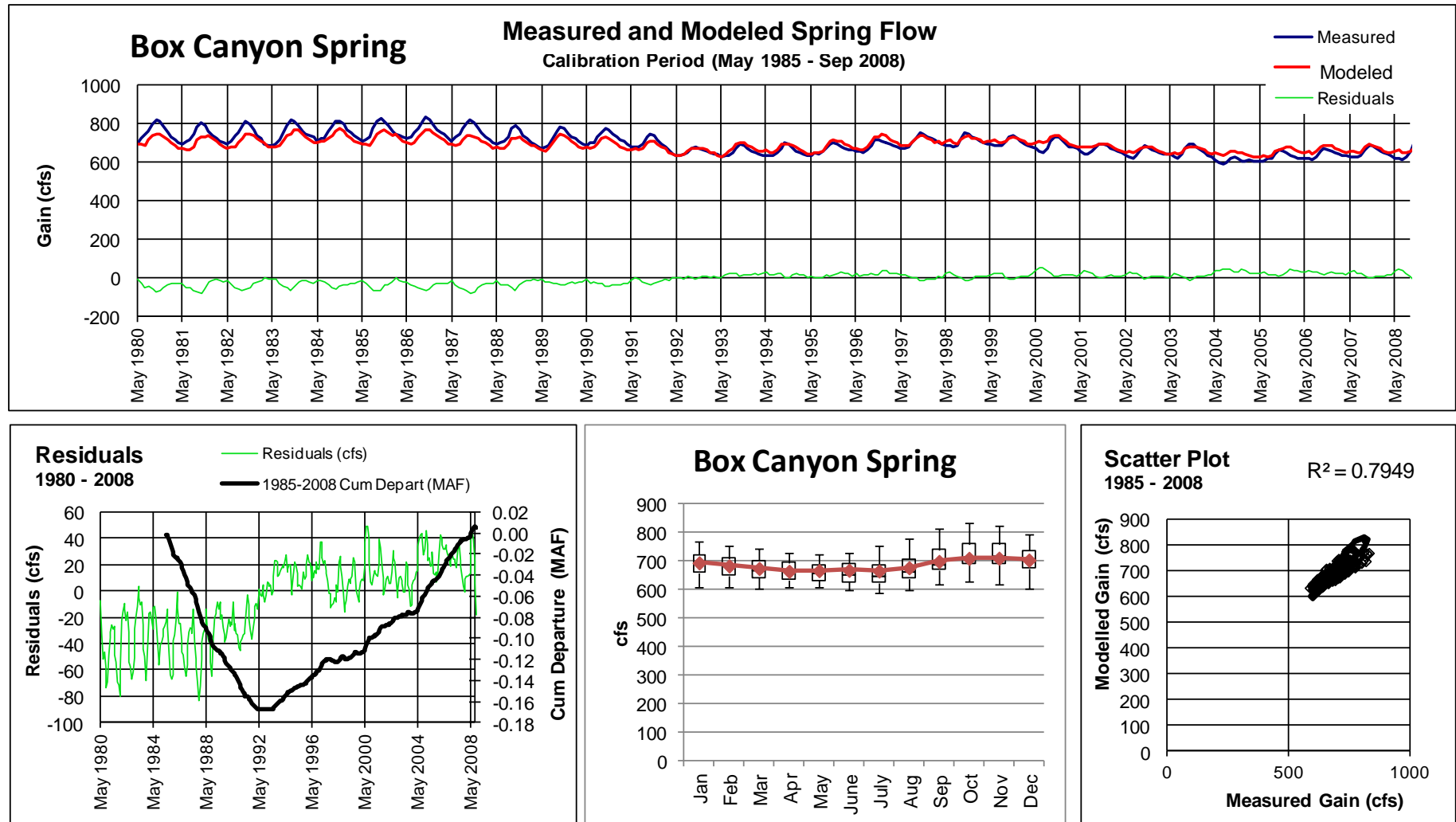


Figure 94. Spring flow for Box Canyon Spring. The top chart shows the measured gains, modeled gains, and residual over the calibration period. The lower chart figure shows the cumulative departures. The lower middle chart is a Box-and-Whisker plot of the gains. The lower right chart is a scatter plot of modeled gains against measured gains.

DRAFT

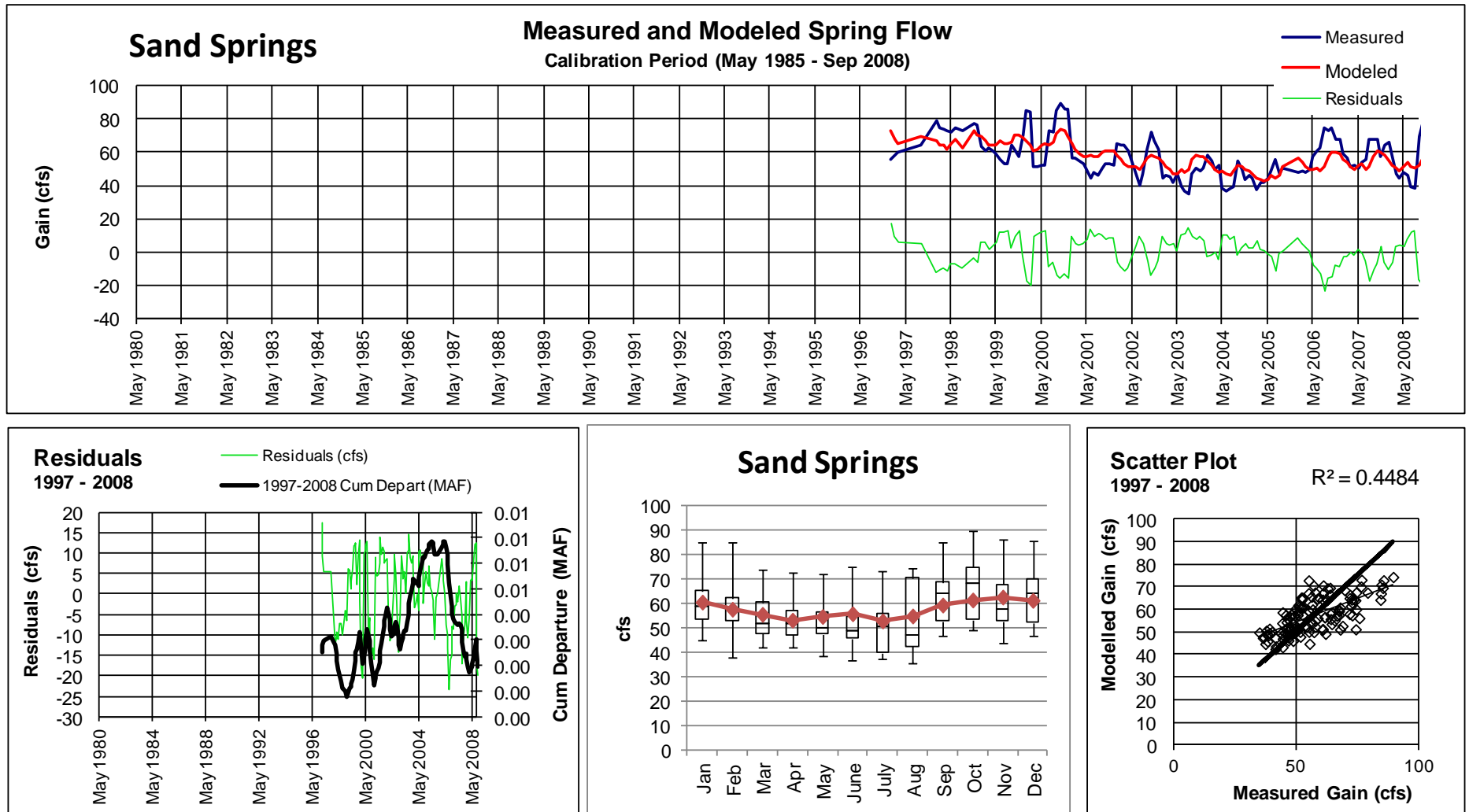


Figure 95. Spring flow for Sand Springs. The top chart shows the measured gains, modeled gains, and residual over the calibration period. The lower chart figure shows the cumulative departures. The lower middle chart is a Box-and-Whisker plot of the gains. The lower right chart is a scatter plot of modeled gains against measured gains.

DRAFT

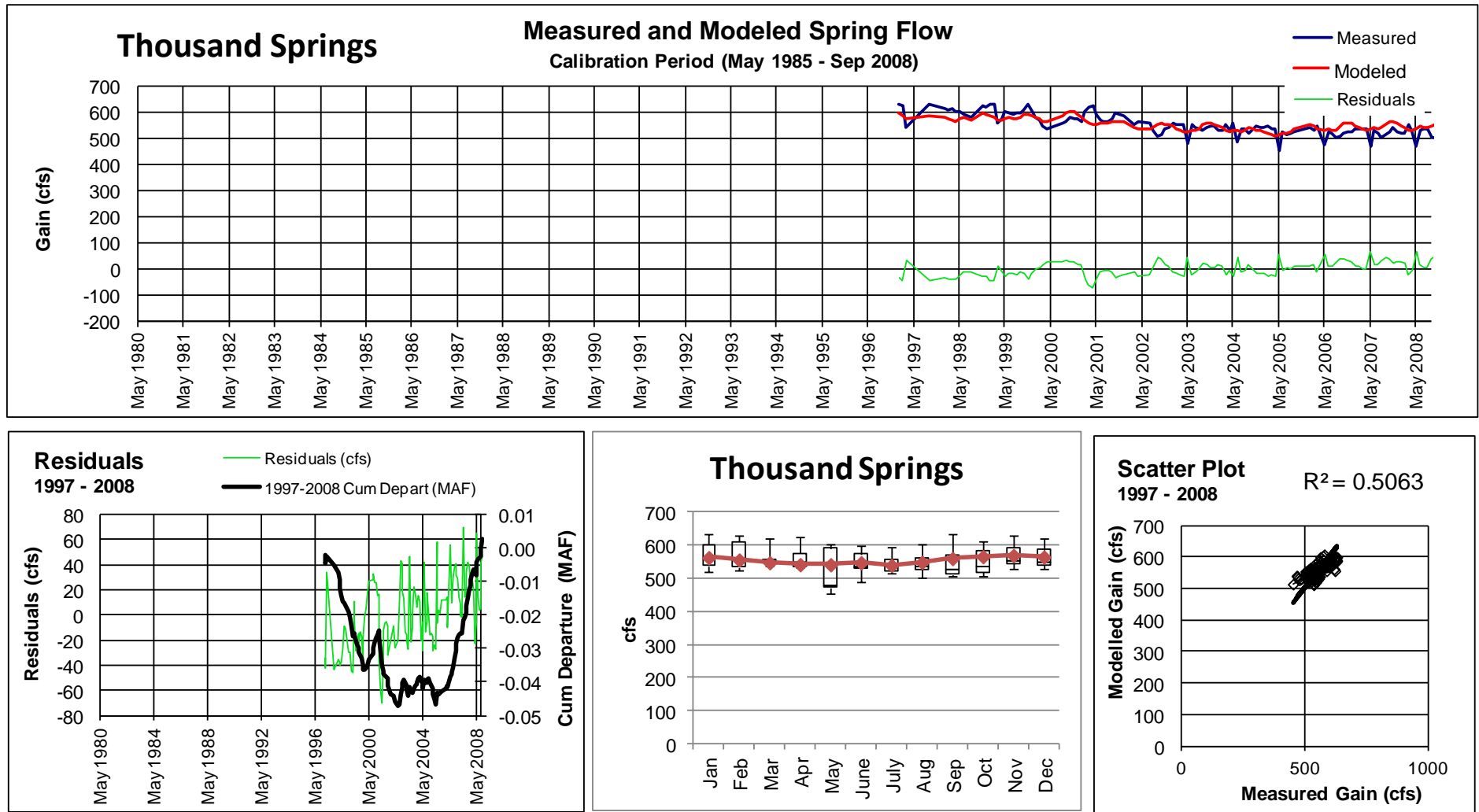


Figure 96. Spring flow for Thousand Springs. The top chart shows the measured gains, modeled gains, and residual over the calibration period. The lower chart figure shows the cumulative departures. The lower middle chart is a Box-and-Whisker plot of the gains. The lower right chart is a scatter plot of modeled gains against measured gains.

DRAFT

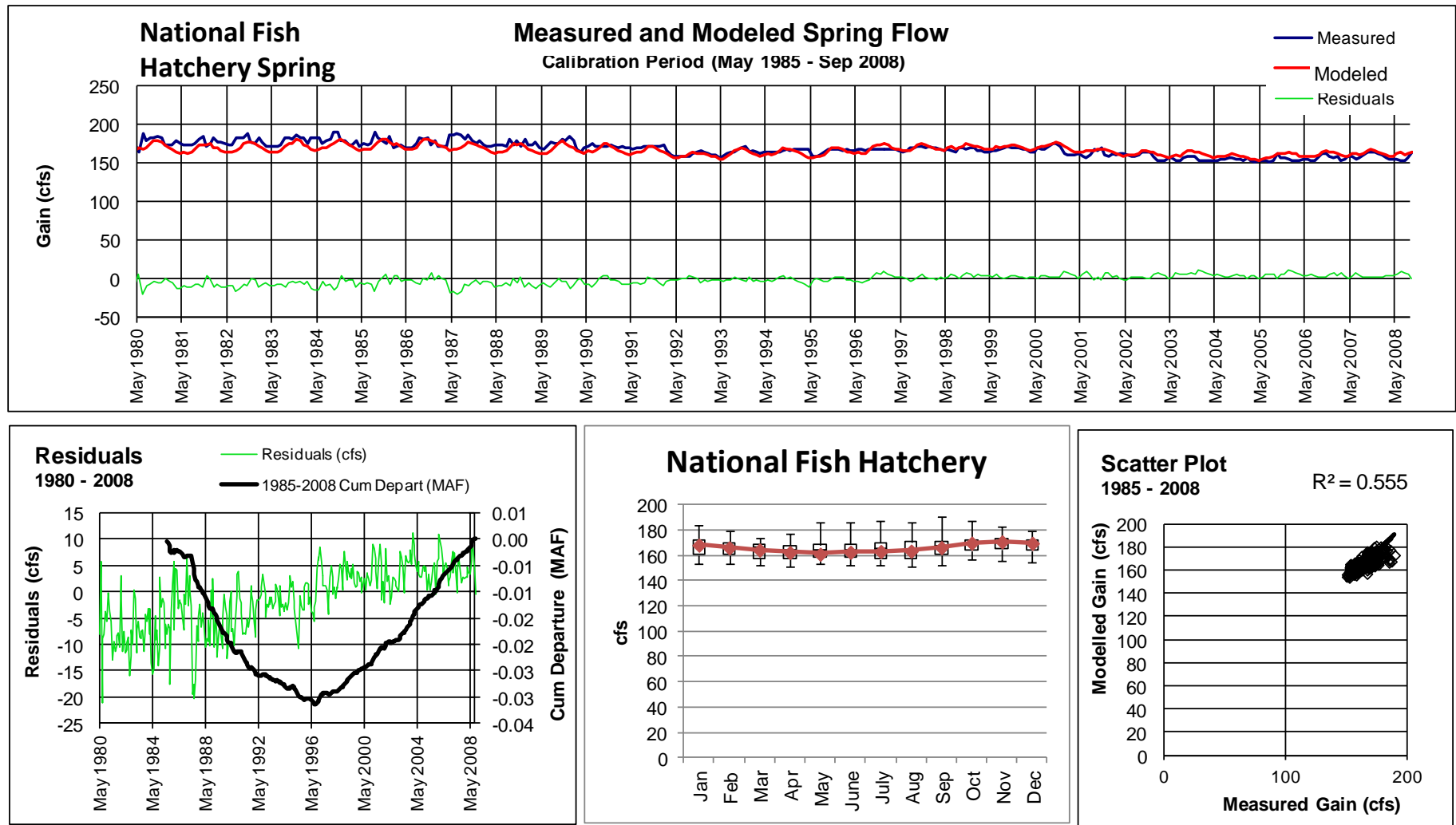


Figure 97. Spring flow for the National Fish Hatchery Spring. The top chart shows the measured gains, modeled gains, and residual over the calibration period. The lower chart figure shows the cumulative departures. The lower middle chart is a Box-and-Whisker plot of the gains. The lower right chart is a scatter plot of modeled gains against measured gains.

DRAFT

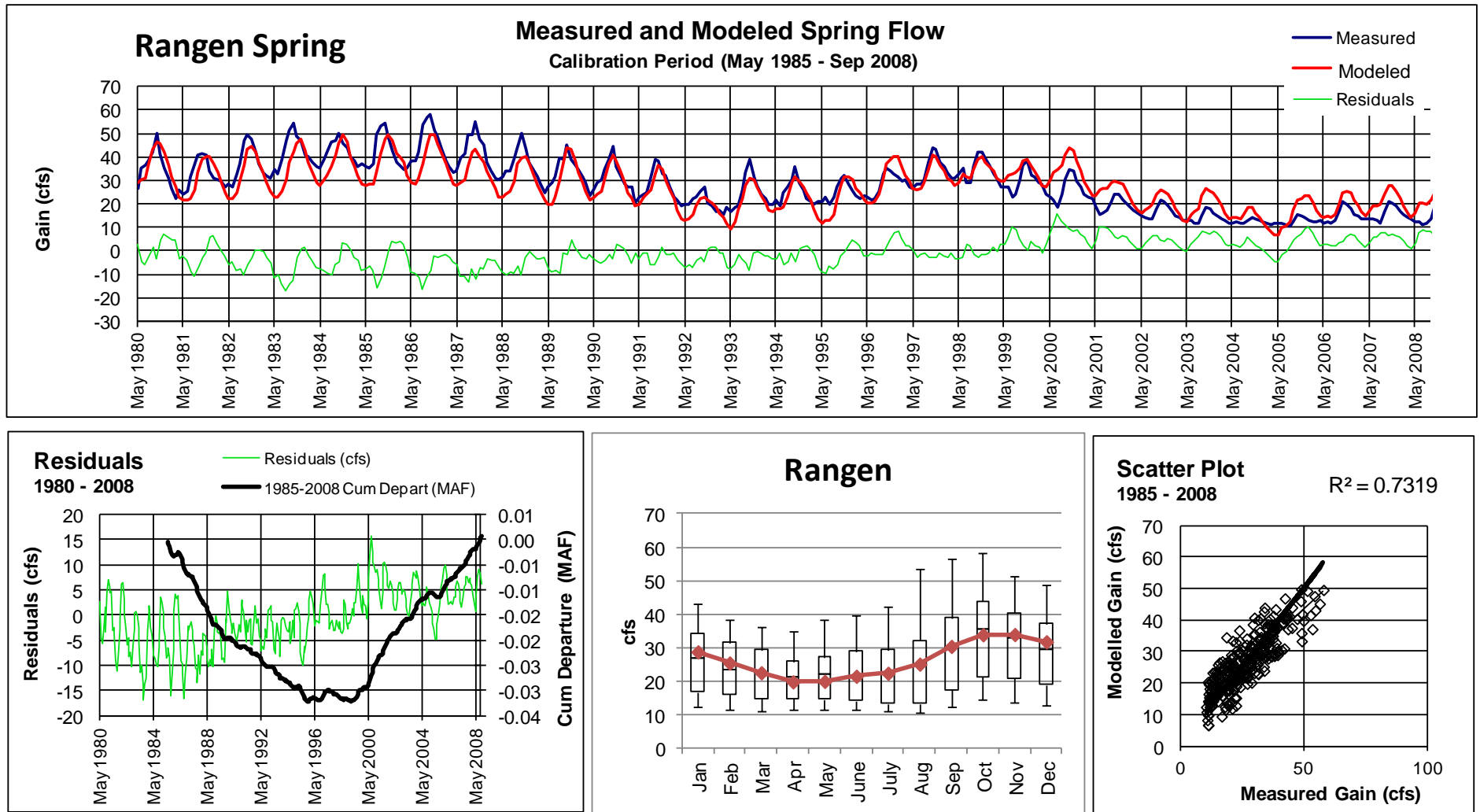


Figure 98. Spring flow for Rangen Spring. The top chart shows the measured gains, modeled gains, and residual over the calibration period. The lower chart figure shows the cumulative departures. The lower middle chart is a Box-and-Whisker plot of the gains. The lower right chart is a scatter plot of modeled gains against measured gains.

DRAFT

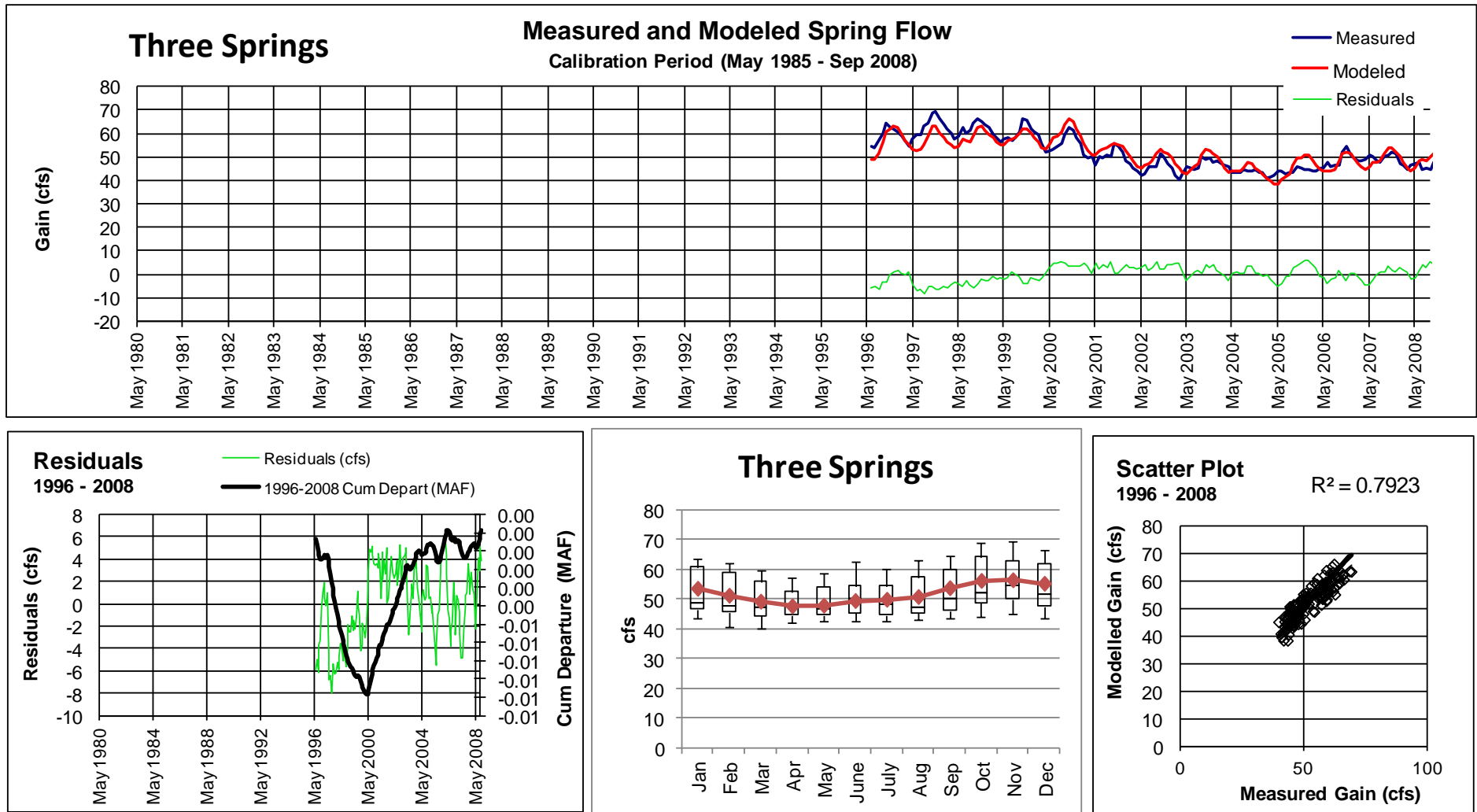


Figure 99. Spring flow for Three Springs. The top chart shows the measured gains, modeled gains, and residual over the calibration period. The lower chart figure shows the cumulative departures. The lower middle chart is a Box-and-Whisker plot of the gains. The lower right chart is a scatter plot of modeled gains against measured gains.

DRAFT

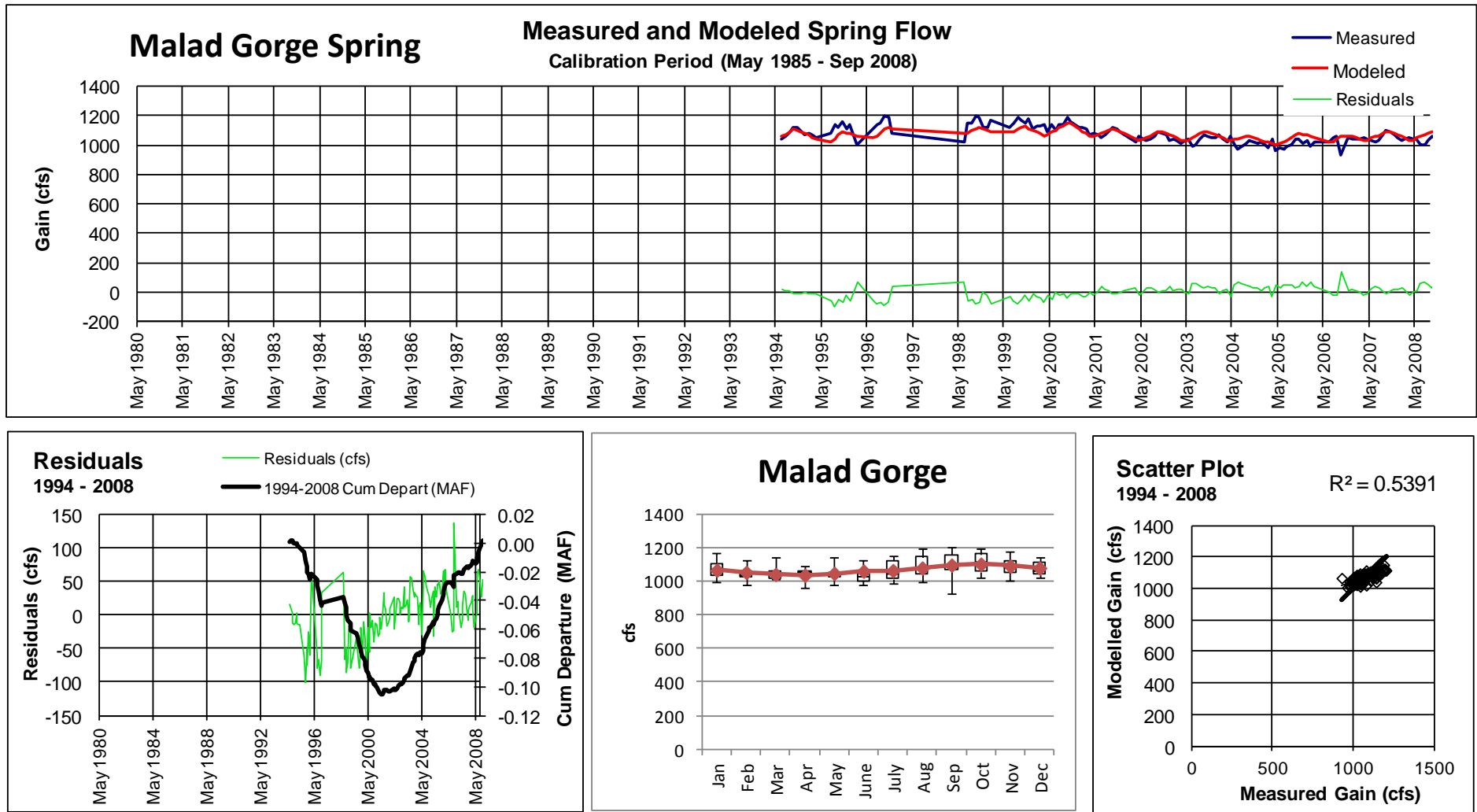


Figure 100. Spring flow for Malad Gorge Spring. The top chart shows the measured gains, modeled gains, and residual over the calibration period. The lower chart figure shows the cumulative departures. The lower middle chart is a Box-and-Whisker plot of the gains. The lower right chart is a scatter plot of modeled gains against measured gains.

DRAFT

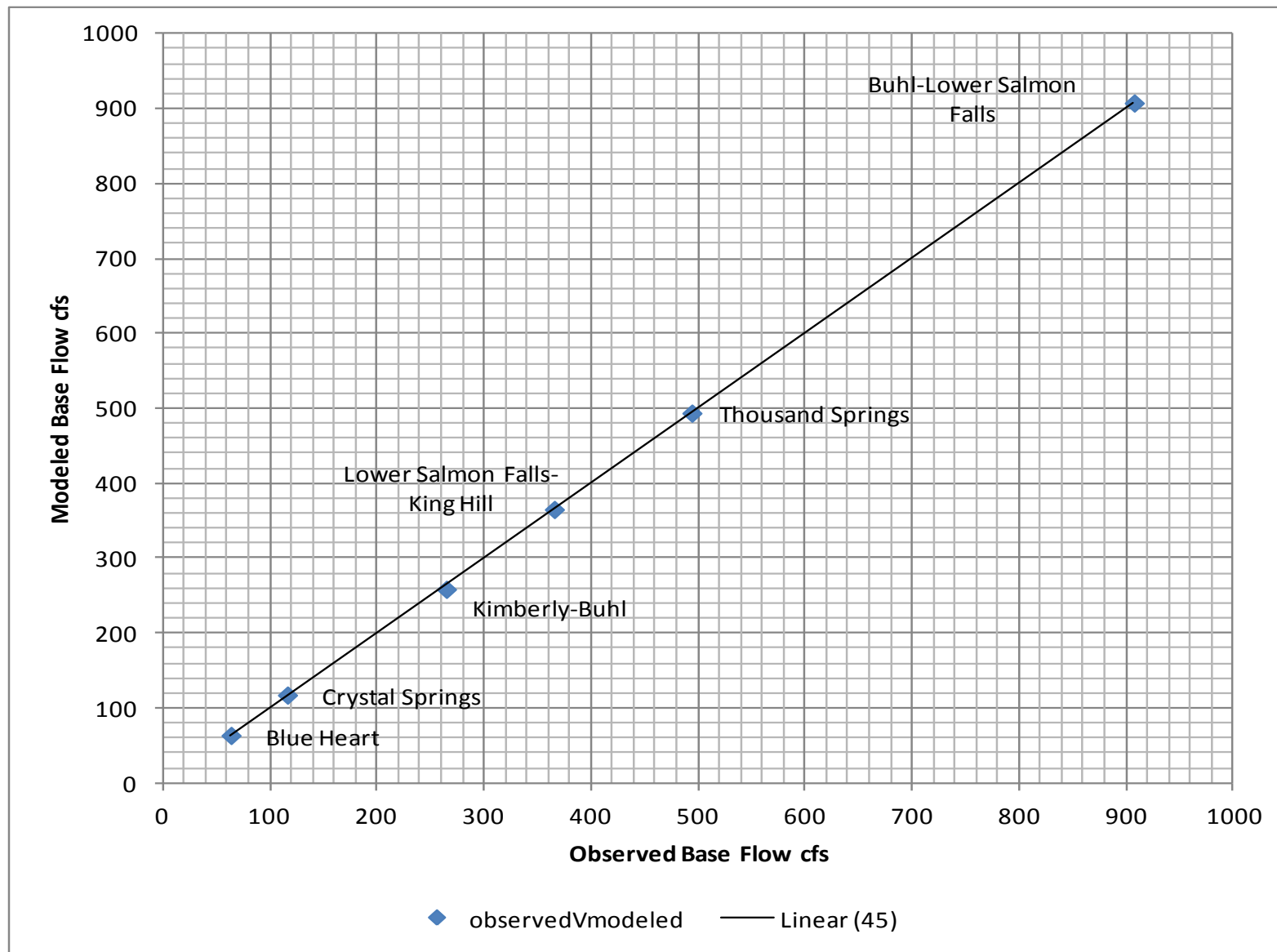


Figure 101. Plot of modeled base flow versus observed base flow for Kimberly-to-Buhl, Buhl-to-Lower Salmon Falls, Lower Salmon Falls reaches, and the local sites of Crystal Springs, Blue Heart Spring, and Thousand Springs.

DRAFT

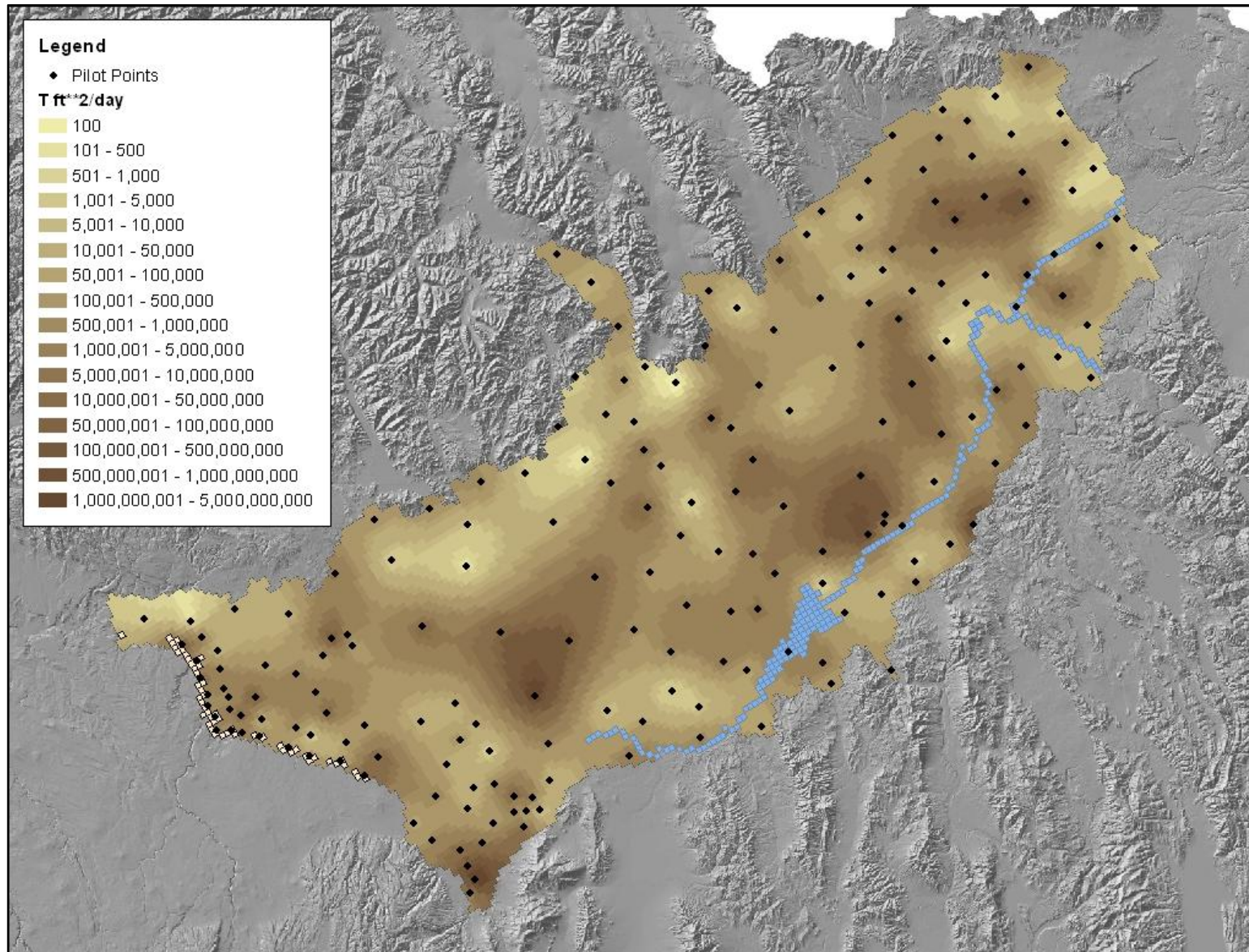


Figure 102. Map of the calibrated aquifer transmissivity (ft²/day) in the Enhanced Snake Plain Aquifer Model Version 2.1.

DRAFT

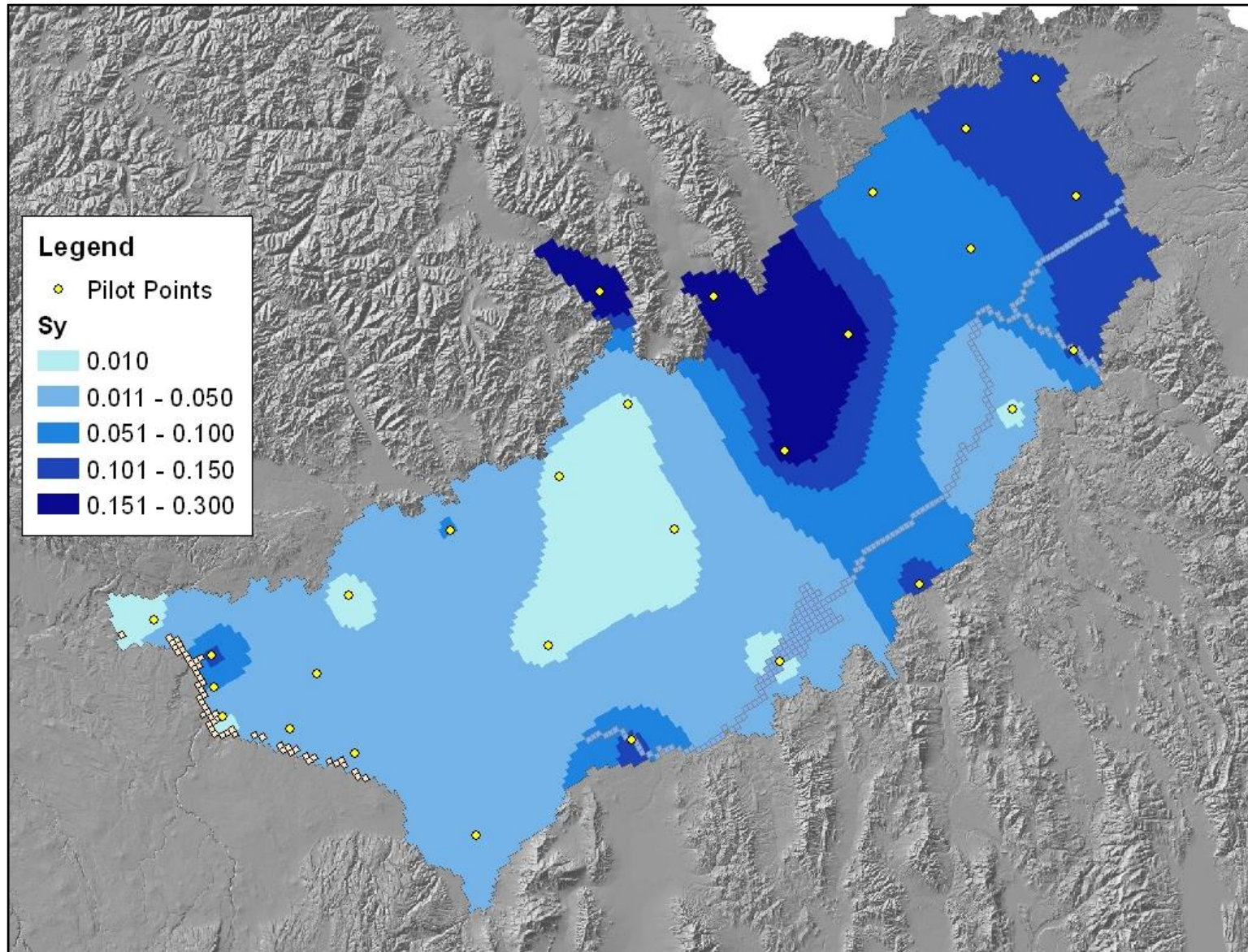


Figure 103. Map of the calibrated aquifer storage (S_v) and pilot points (yellow circles) used to adjust the values.

DRAFT

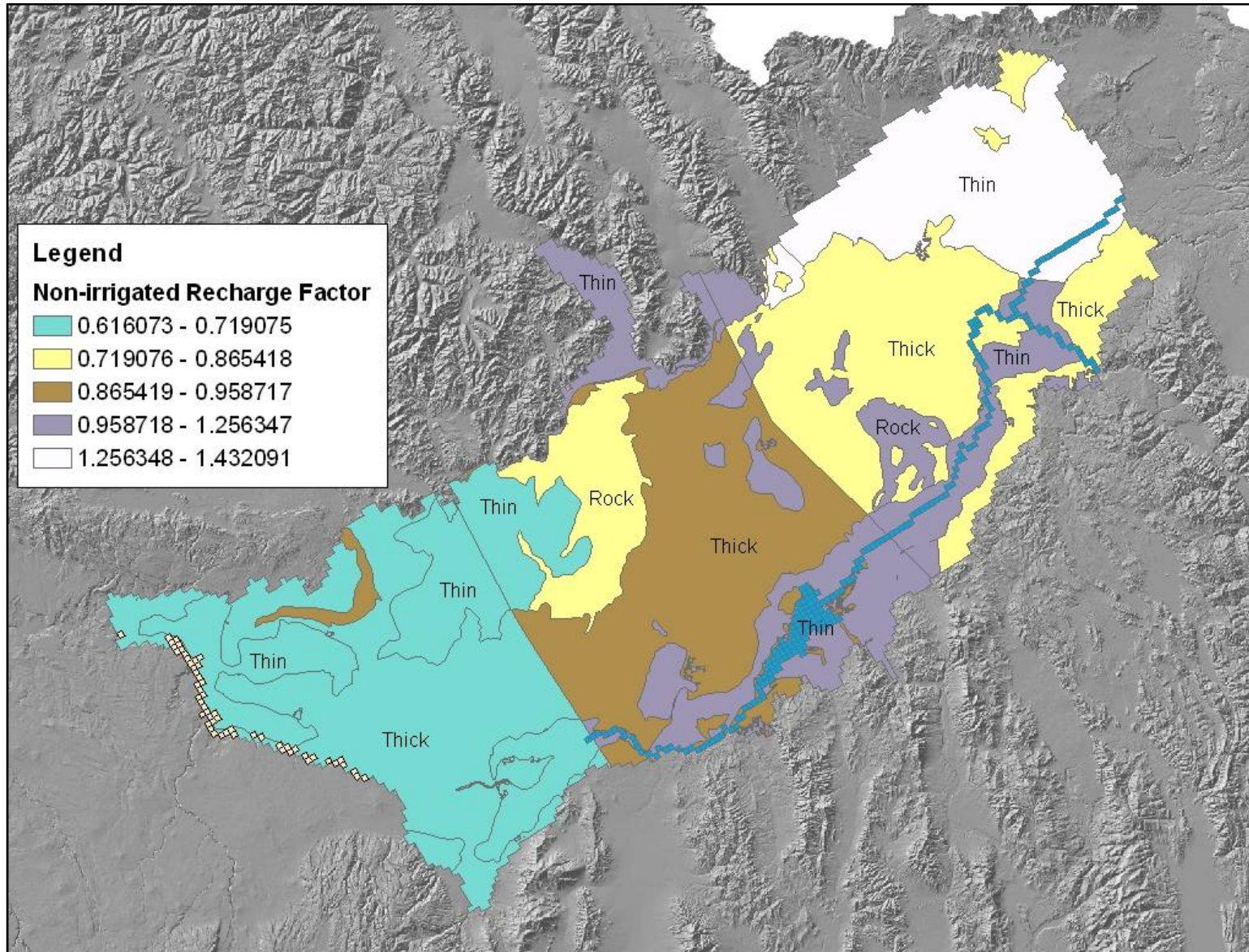


Figure 104. Calibrated non-irrigated recharge adjustment factors.

DRAFT

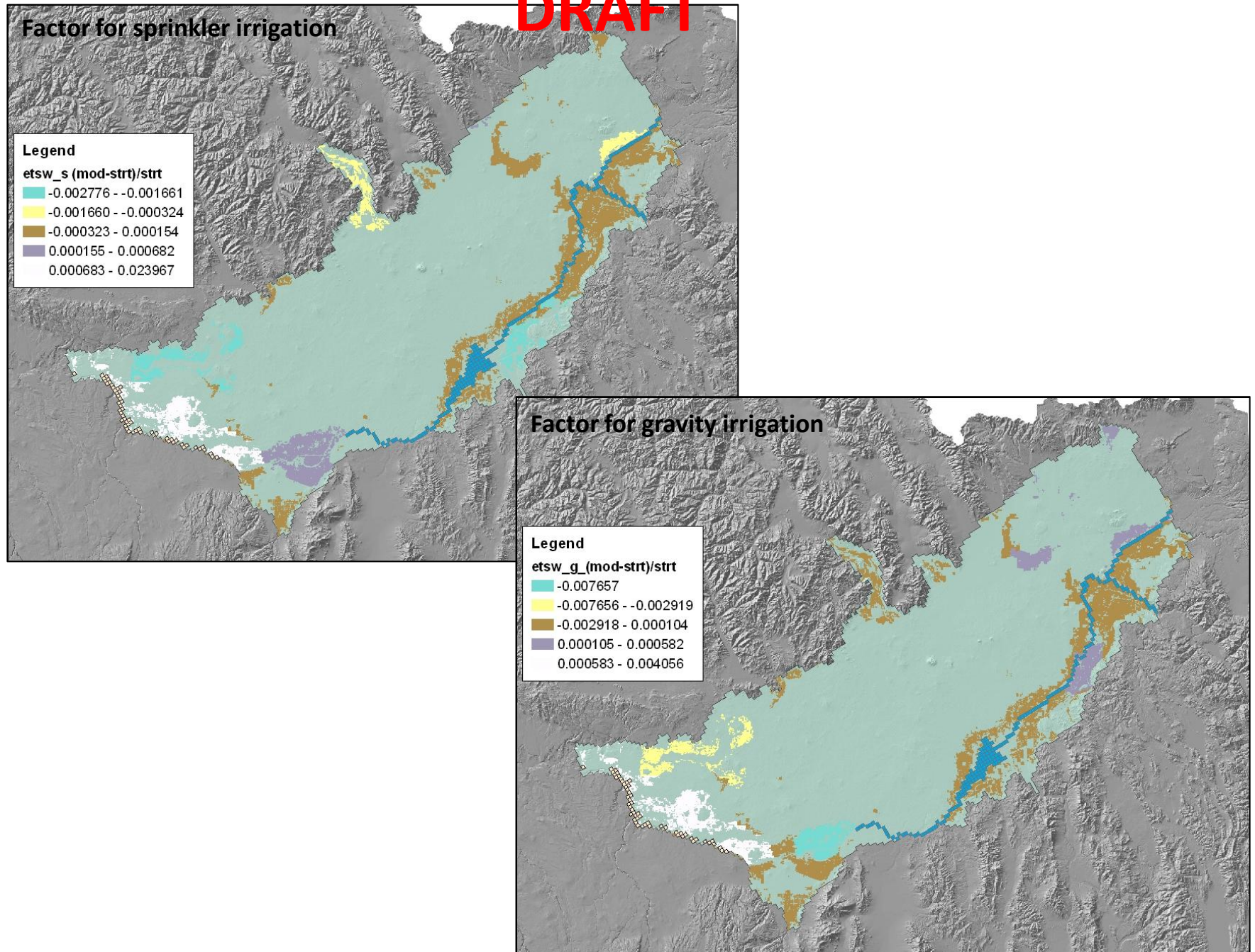


Figure 105. ET adjustment on surface-water irrigated lands.

DRAFT

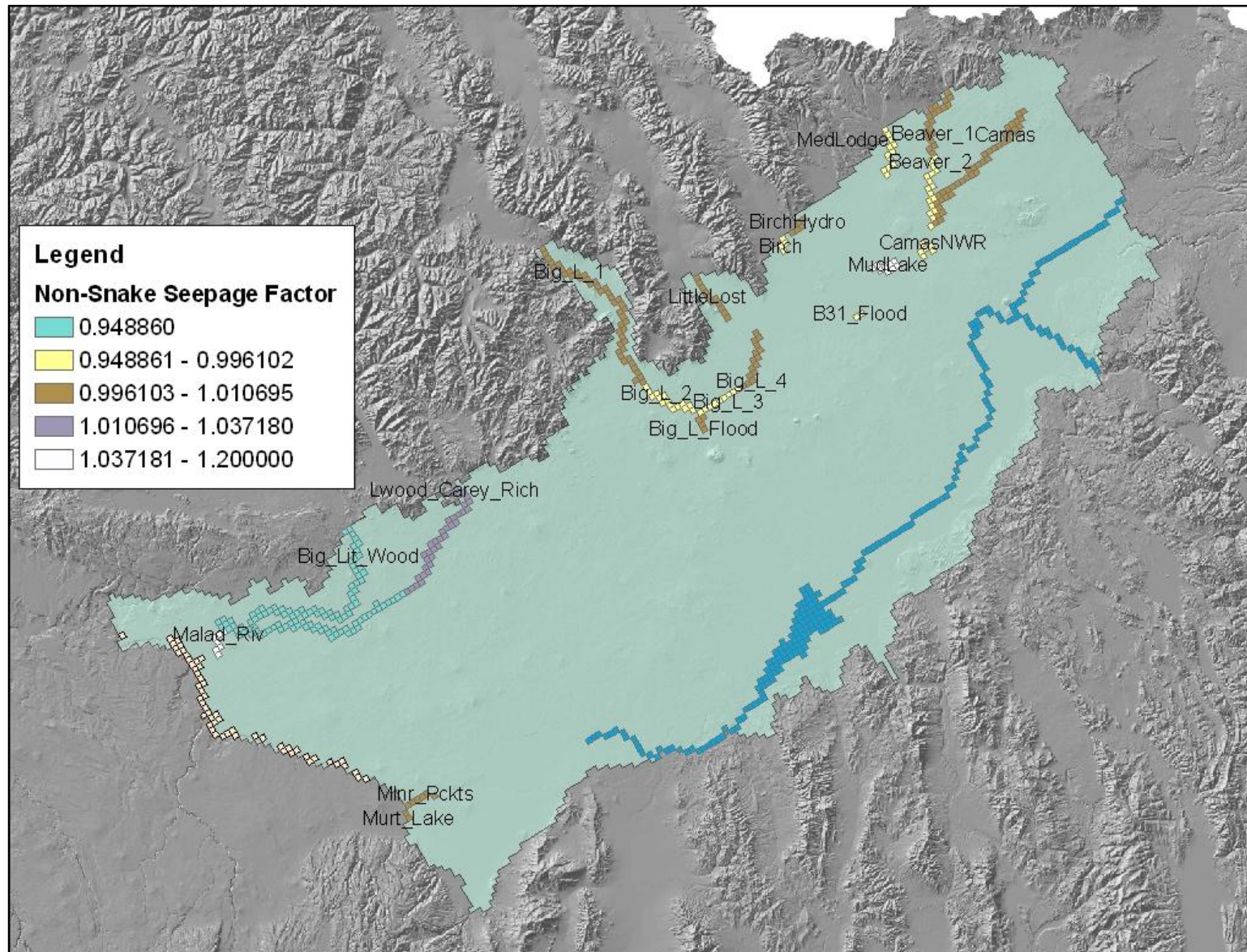


Figure 106. Adjustment factors for non-Snake River seepage sources.

DRAFT

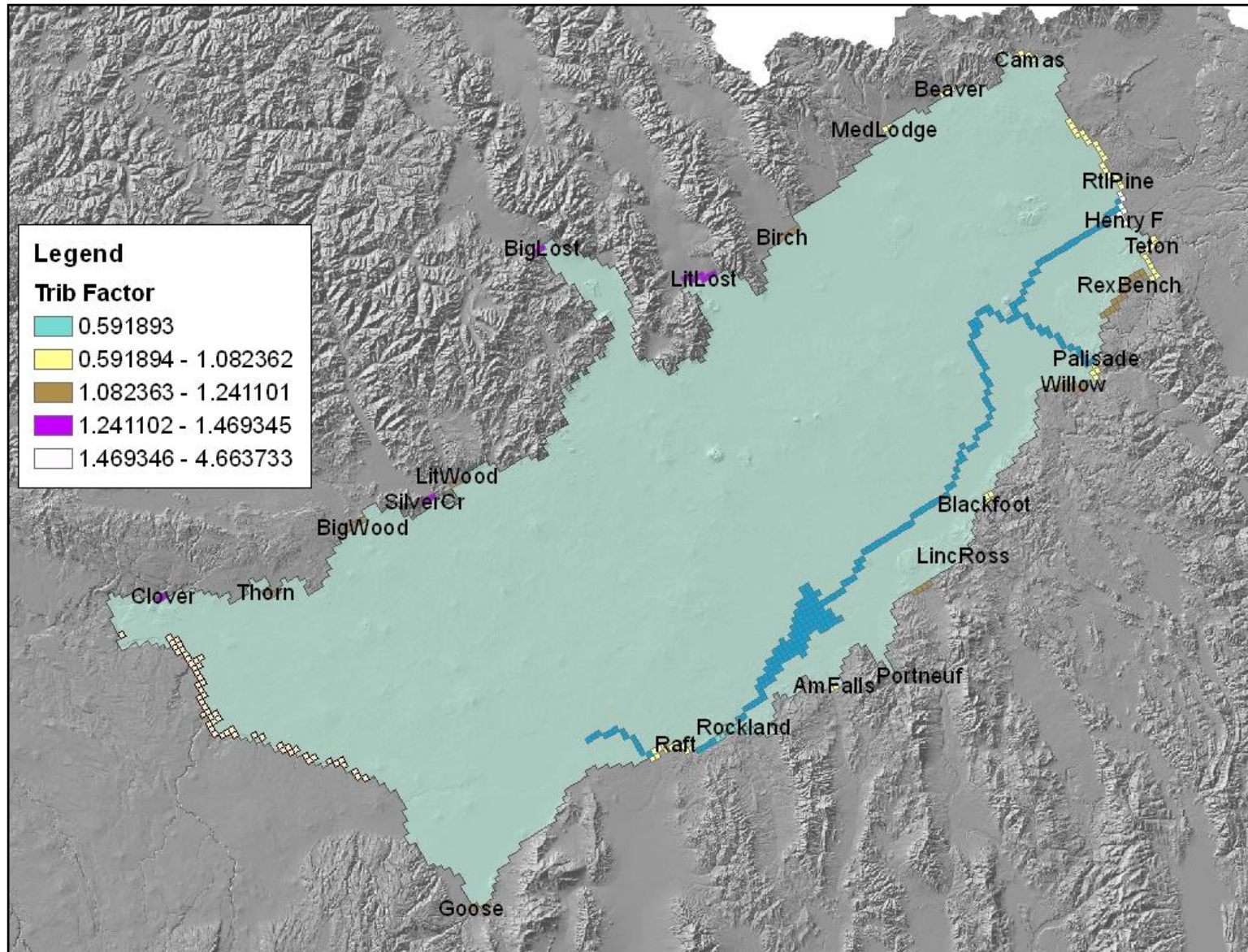


Figure 107. Adjustments factors for tributary underflow.

DRAFT

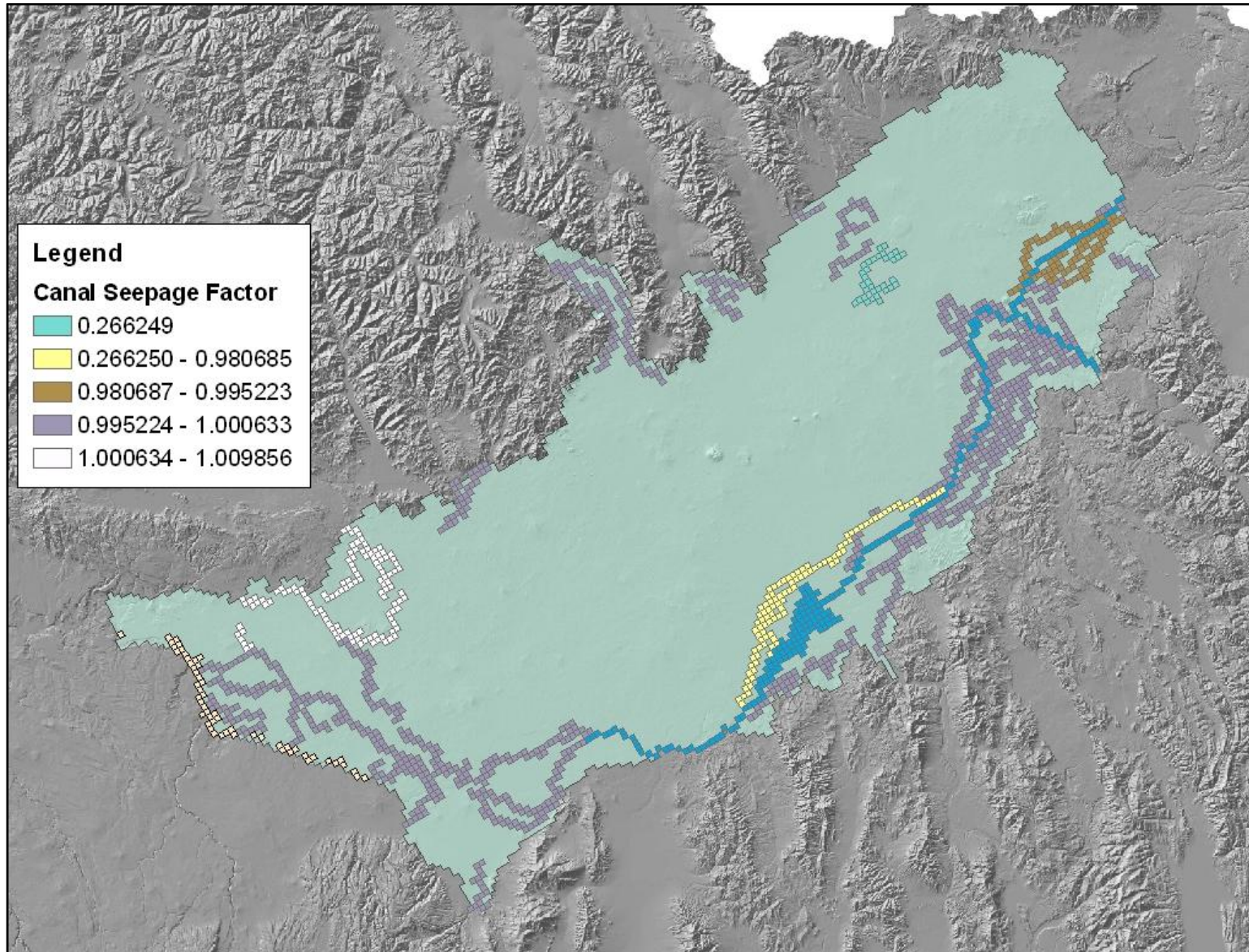


Figure 108. Adjustments factors for canal seepage.

DRAFT

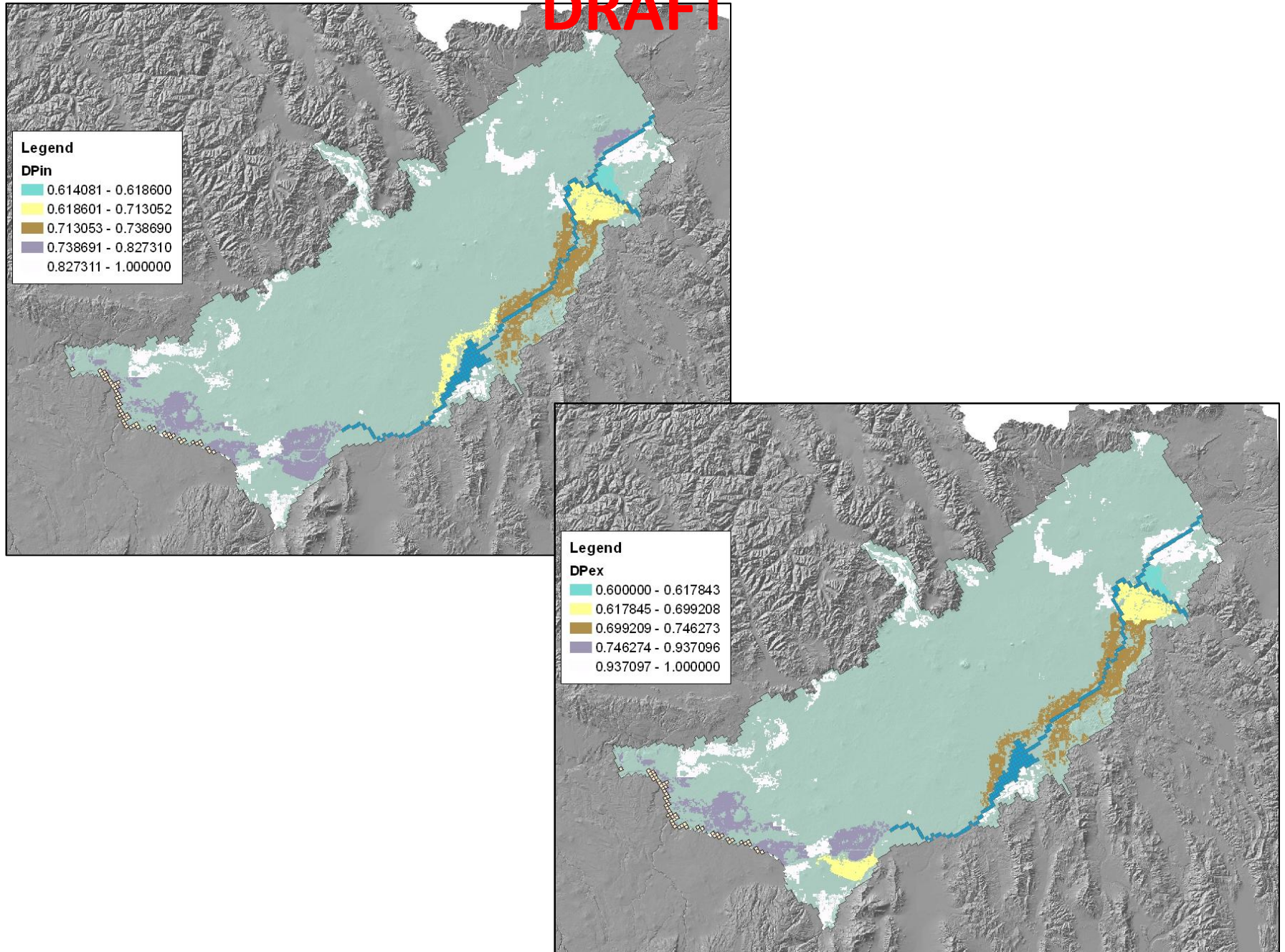


Figure 109. Distribution of the parameters DPin and DPex.

DRAFT

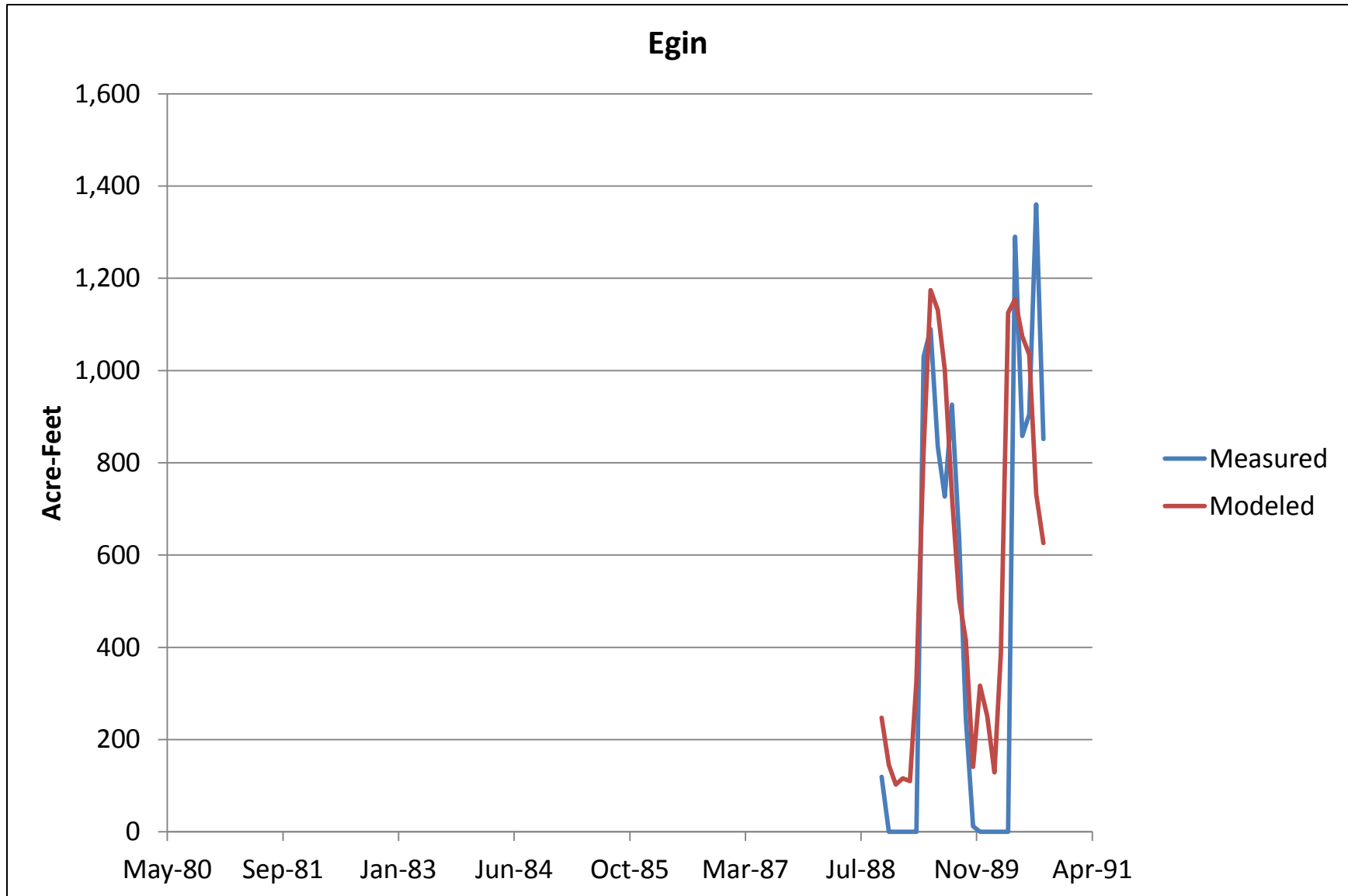


Figure 110. Measured and modeled return flows at Egin.

DRAFT

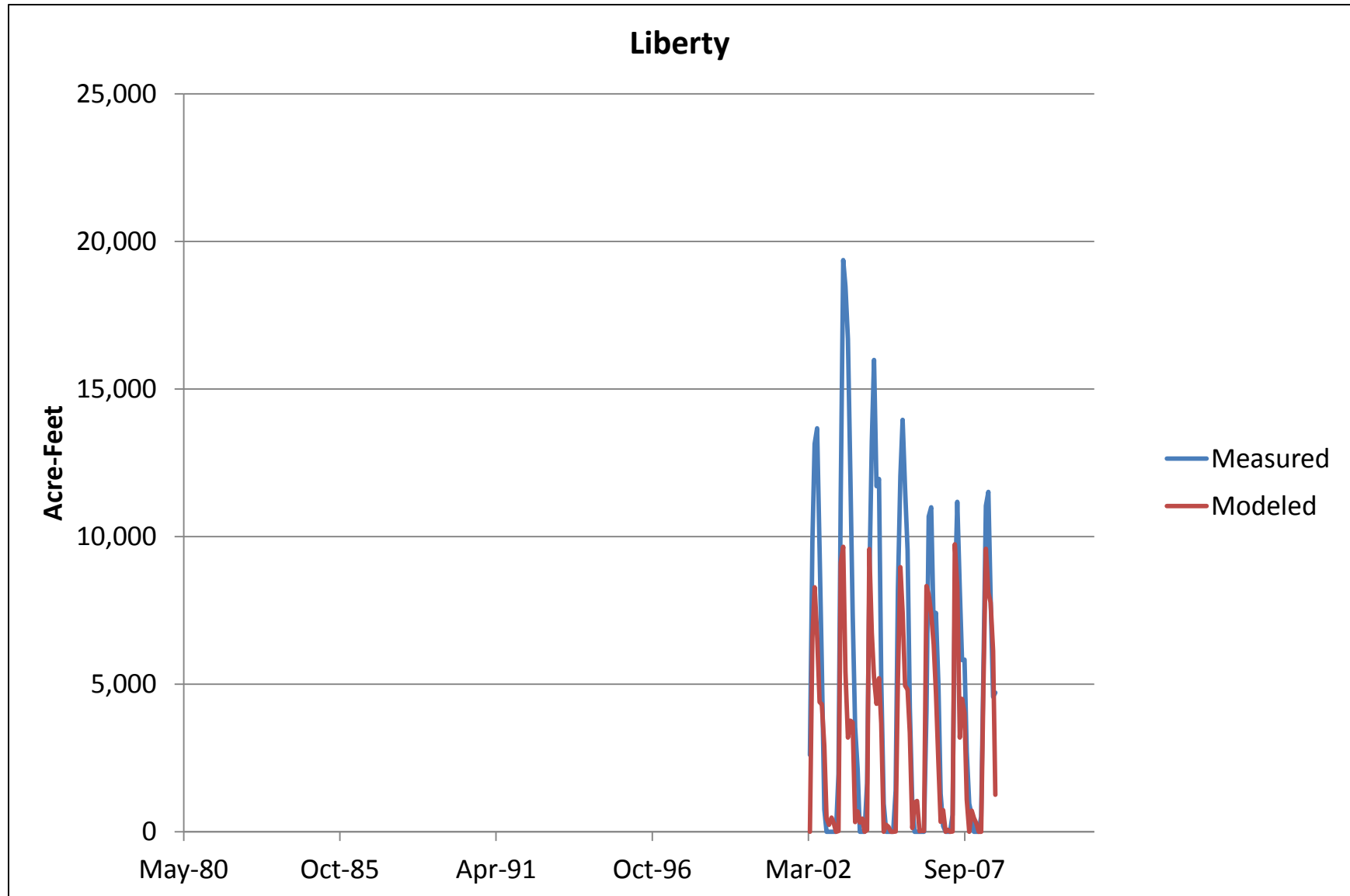


Figure 111. Measured and modeled return flows at Liberty.

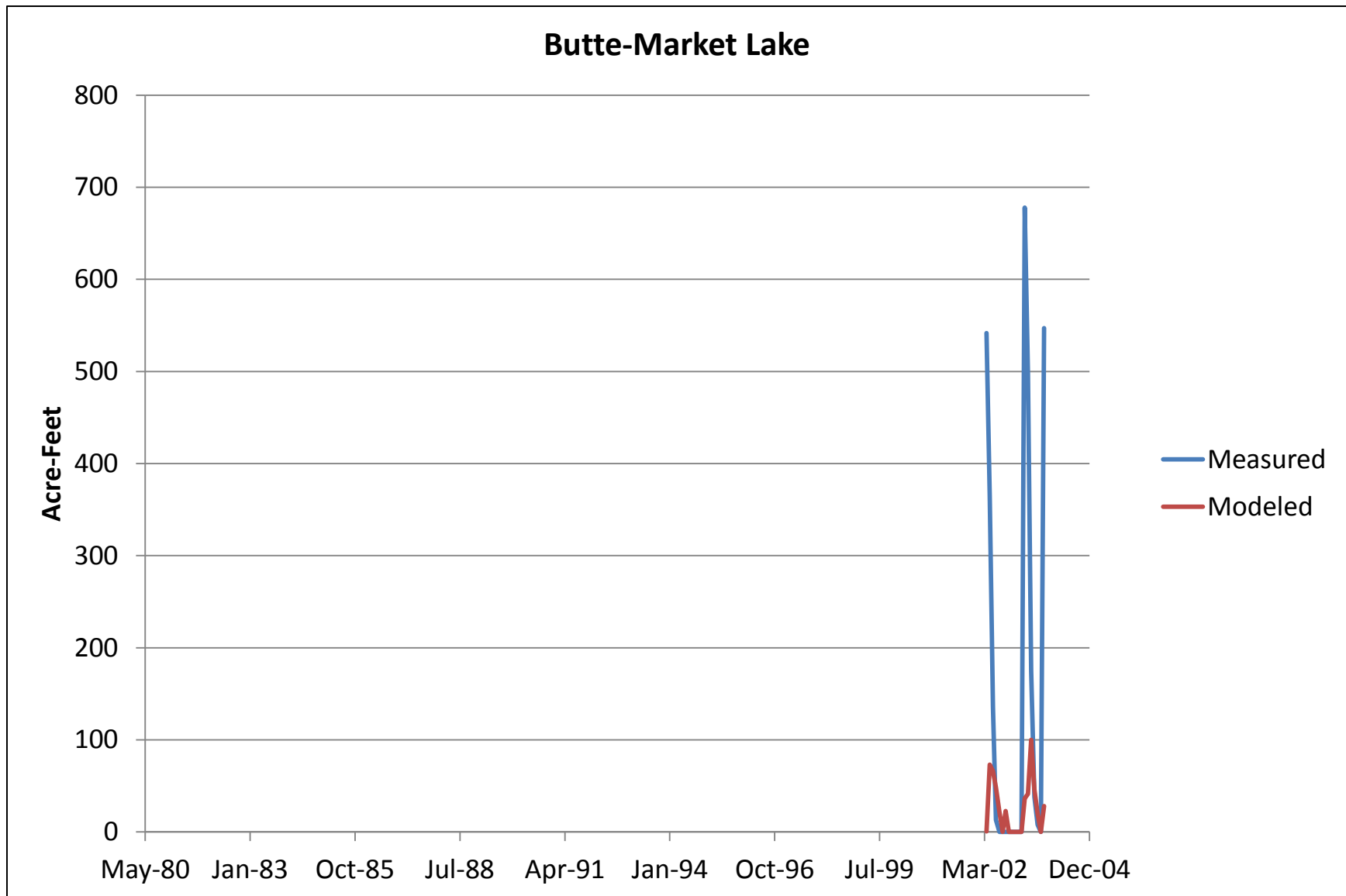


Figure 112. Measured and modeled return flows at Butte-Market Lake.

DRAFT

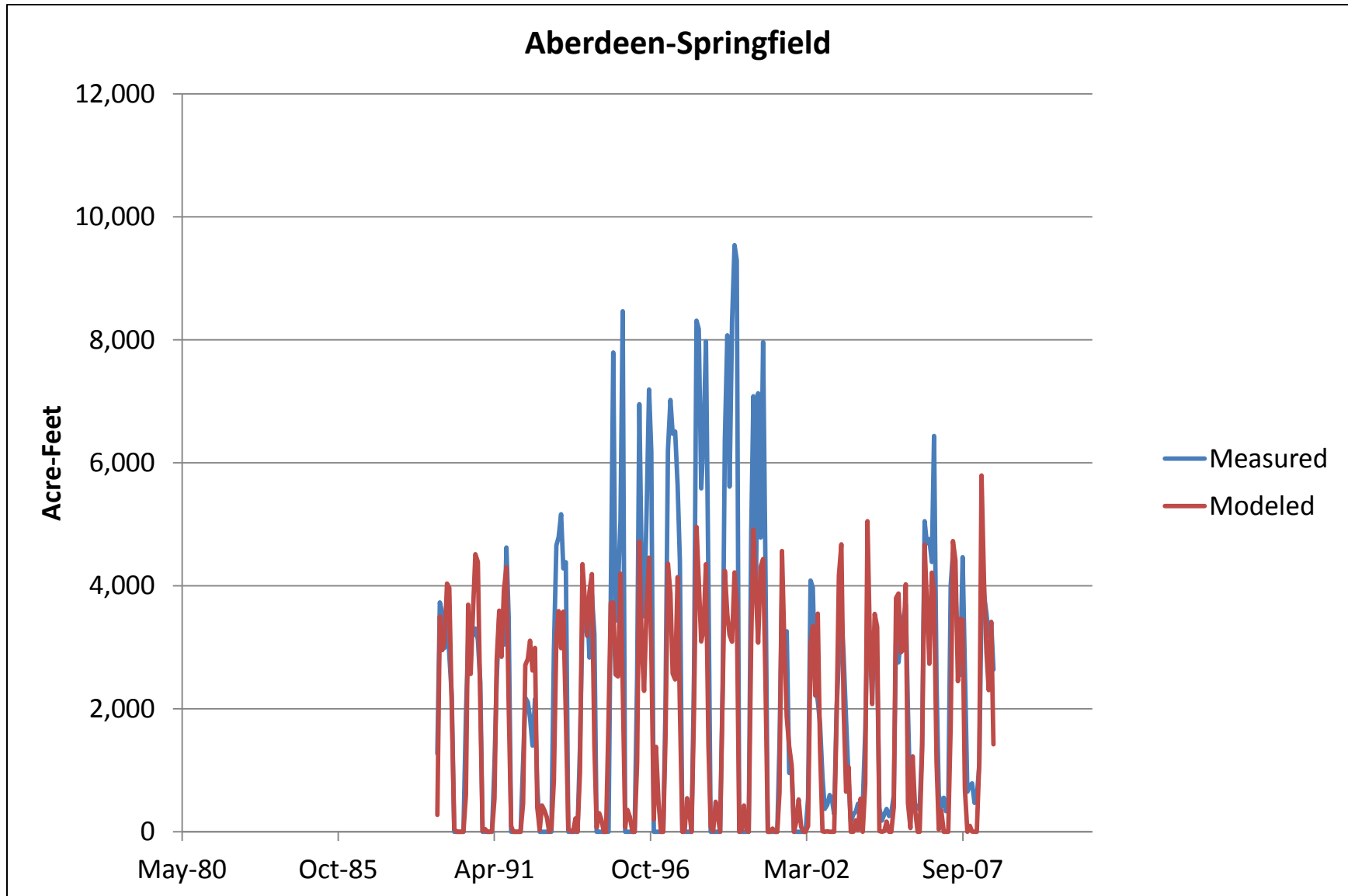


Figure 113. Measured and modeled return flows at Aberdeen-Springfield.

DRAFT

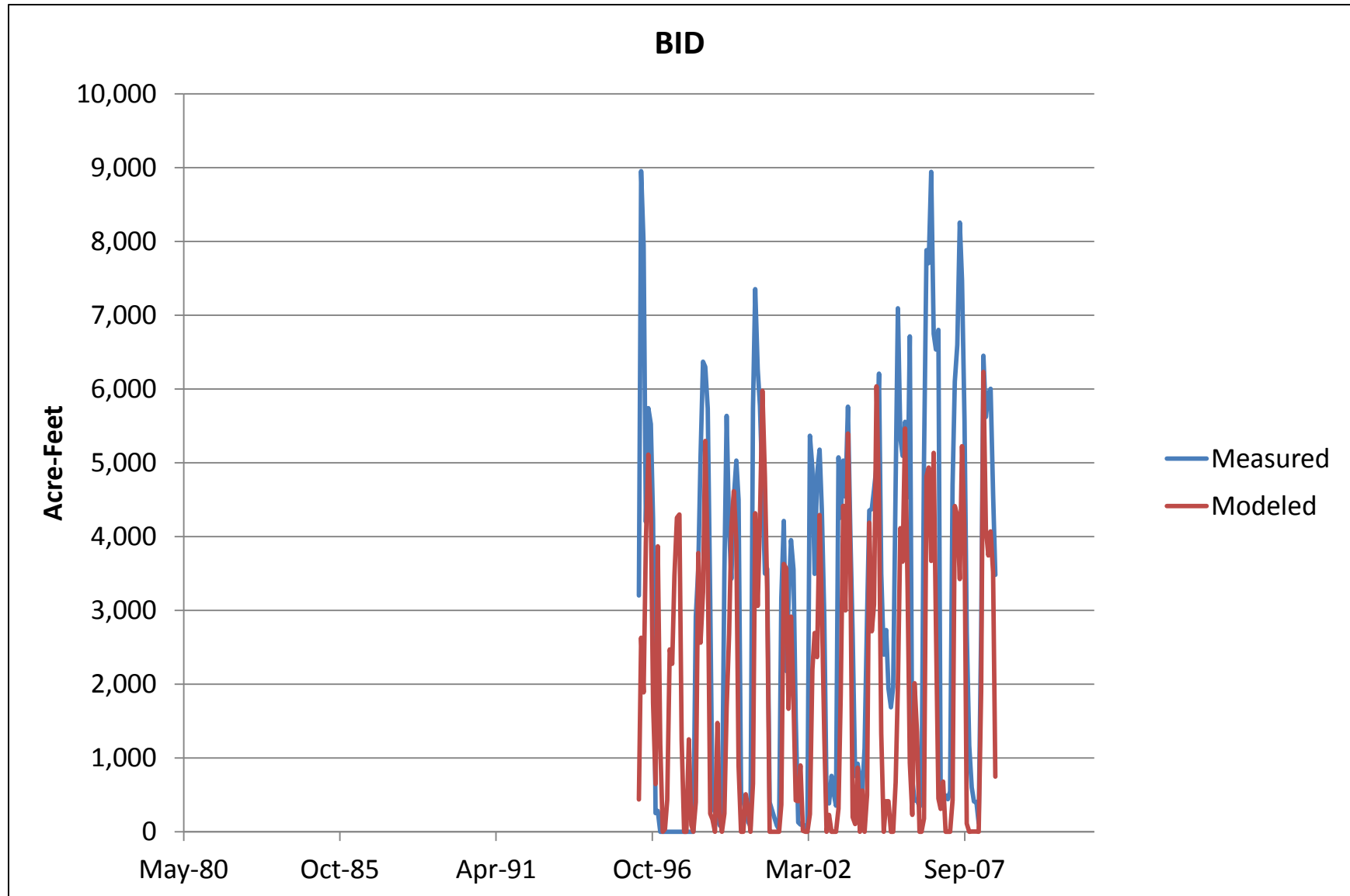


Figure 114. Measured and modeled return flows at Burley Irrigation District.

DRAFT

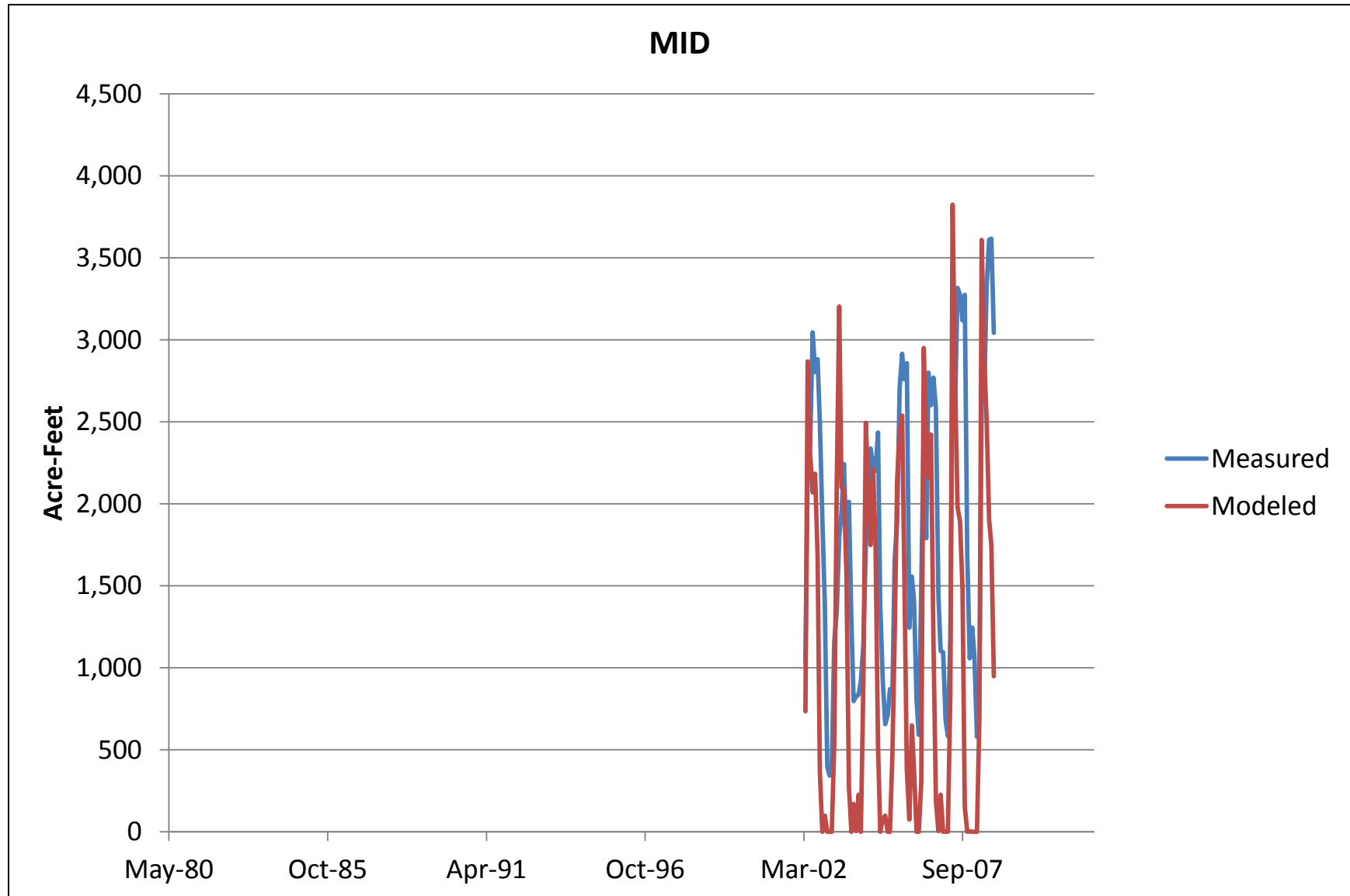


Figure 115. Measured and modeled return flows at Minidoka Irrigation District.

DRAFT

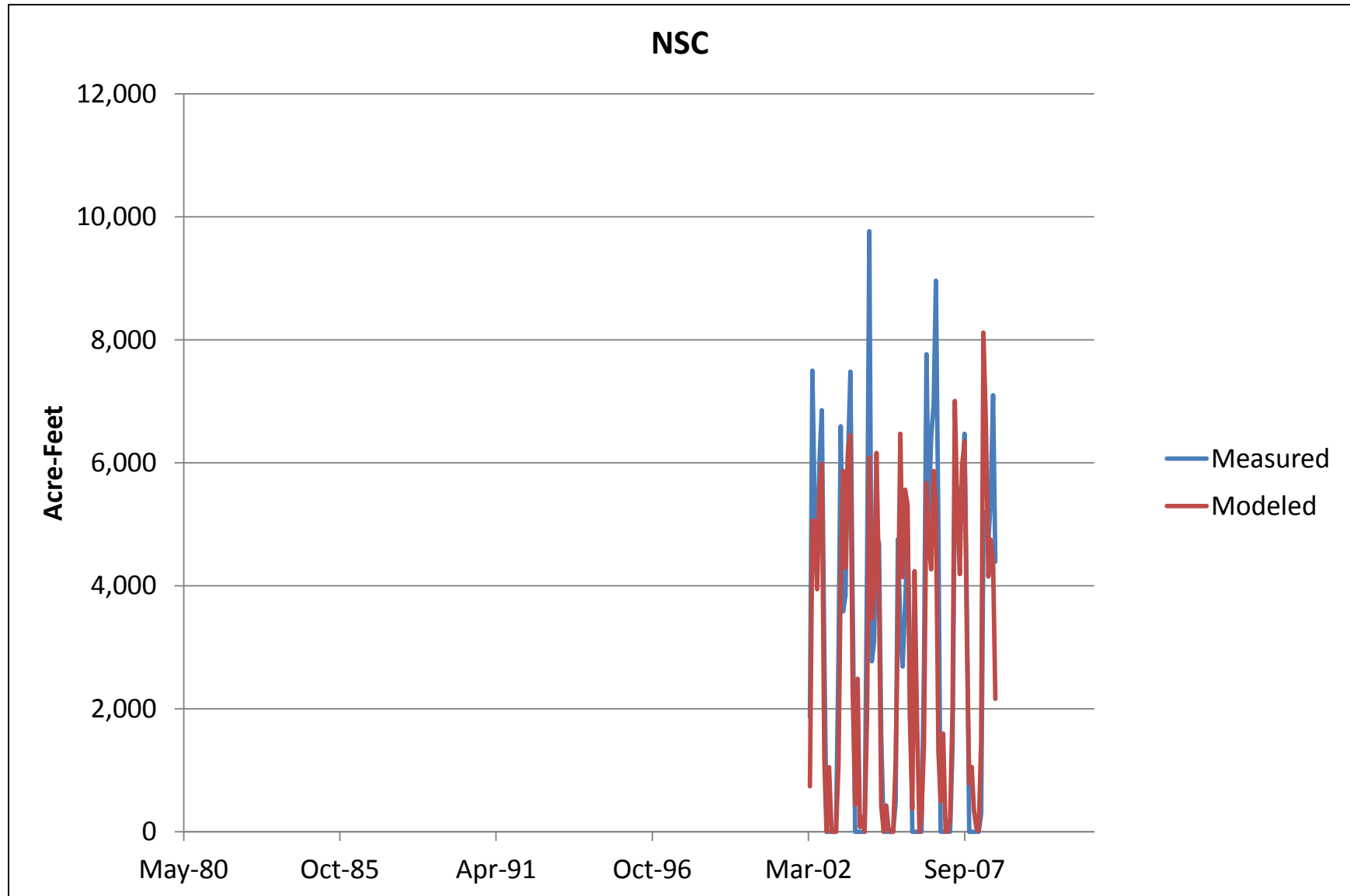


Figure 116. Measured and modeled return flows in the Northside Canal Company service area.

DRAFT

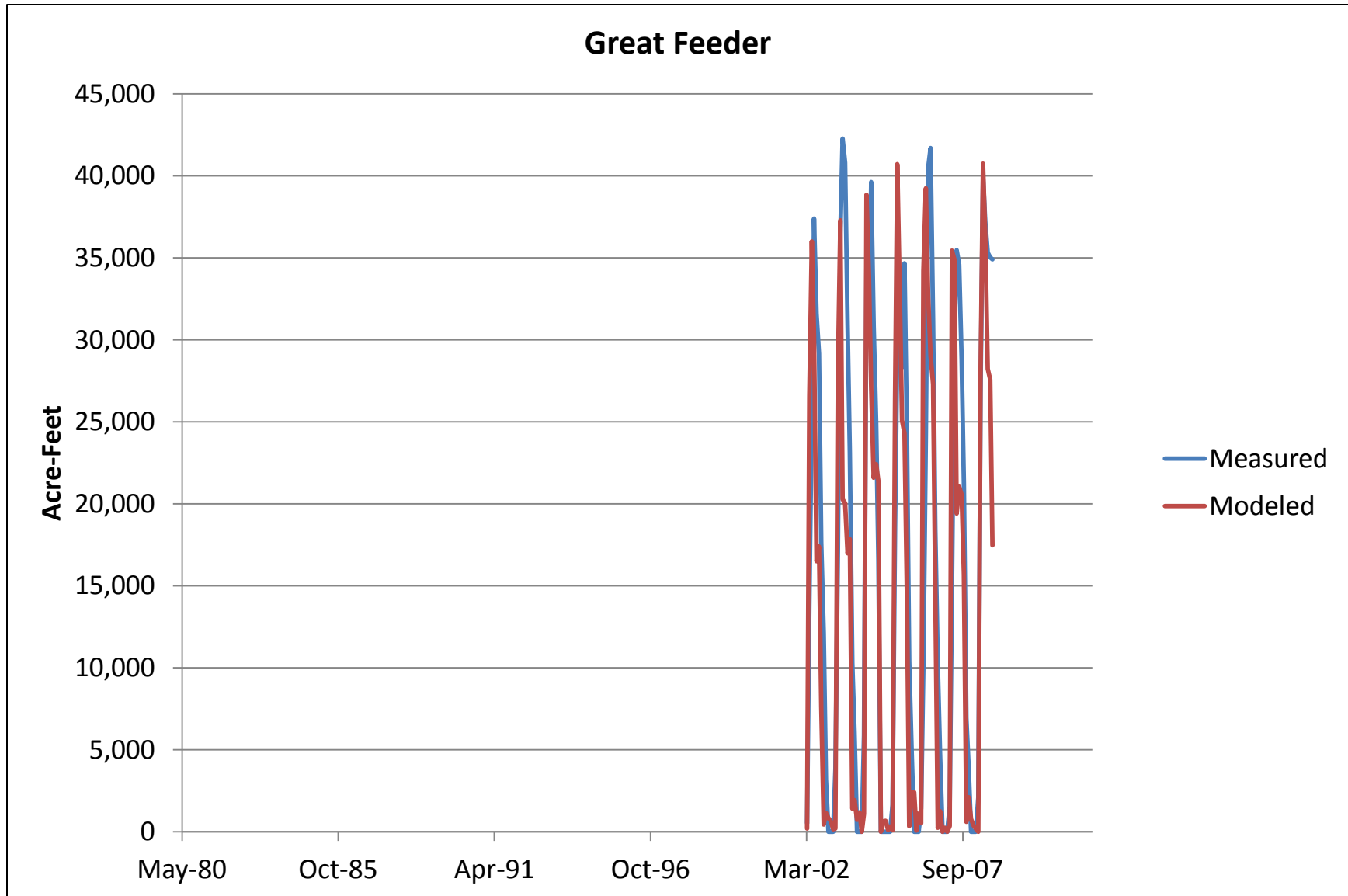


Figure 117. Measured and modeled return flows in the Great Feeder area.